MACROPOROUS POLY(HYDROXYETHYL-METHACRYLATE) BASED CRYOGELS FOR DEPLETION OF ALBUMIN FROM HUMAN SERUM

AYŞE MÜGE ANDAÇ

A0212387

Submitted to Institute for Graduate Studies
in Pure and Applied Sciences of
Hacettepe University as a partial fulfillment
to the requirements for the award of the degree of
DOCTOR OF PHILOSOPHY
in
CHEMISTRY

ANKARA
2009

İNSAN SERUMUNDAN ALBUMİN UZAKLAŞTIRILMASI İÇİN MAKROGÖZENEKLİ POLİ(HİDROKSİETİL-METAKRİLAT) KRİYOJELLER

AYŞE MÜGE ANDAÇ

ÖZ

Serum proteinleri hastalıklara özgü biyoişaretlerin (biomarker) tanımlanması için çok zengin bir kaynaktır. Bununla beraber, serum proteinlerinin eşit dağılım göstermemesi analizleri oldukça zorlaştırmaktır, çünkü yüksek yoğunlukta bulunan proteinler düşük yoğunlukta bulunanları maskelemektedir. Özellikle normal insan plazmasındaki toplam protein miktarının yaklaşık % 60'ını oluşturan albumin, serum, plazma, omurilik ve eklem sıvısıda yapılan proteom analizlerinde engel teşkil etmektedir. Yüksek yoğunluktaki serum proteinlerinin uzaklaştırılması, düşük yoğunluktaki hastalıklara özgü proteinlerin analizlerini kolaylaştırmaktadır. Son zamanlarda, kriyojeller kolay hazırlanabilmeleri, mükemmel akış özellikleri ve yüksek performansları nedeniyle biyomoleküllerin ayrılmasında yeni nesil sabit faz olarak kullanılmaktadırlar. Kriyojellerin gözenek yoğunluğu ve geniş gözeneklere sahip olması ve düşük akış direnci sağladığından, kan gibi viskoz ortamlarda çalışıldığında çok büyük kolaylık sağlamaktadır. PHEMA temelli makrogözenekli polimerik kriyojeller vücut sıvısı, hücre ve proteinleriyle biyouyumluluk göstermektedirler ve fizyolojik koşullarda oldukça kararlıdırlar. Bu tez çalışmasında, PHEMA temelli süpermakrogözenekli polimerik kriyojellere farklı ligandlar bağlanarak, insan serumdan seçici ve etkin olarak albumin uzaklaştırma performansları incelenmiştir.

Anahtar Sözcükler: Albumin uzaklaştırılması, Boya-ligand afinite kromatografisi, Moleküler baskılama, Kriyojeller.

Danışman: Prof. Dr. Adil DENİZLİ, Hacettepe Üniversitesi, Kimya Bölümü, Biyokimya Anabilim Dalı.

MACROPOROUS POLY(HYDROXYETHYL-METHACRYLATE) BASED CRYOGELS FOR DEPLETION OF ALBUMIN FROM HUMAN SERUM

AYŞE MÜGE ANDAÇ

ABSTRACT

Serum proteins may often serve as indicators of disease and is a rich source for biomarker discovery. However, the large dynamic range of proteins in serum makes the analysis very challenging because high abundant proteins tend to mask of those of lower abundance. Albumin, which comprises approximately 60% of the total protein milieu in normal human plasma, is particularly troubling for proteome analysis which uses serum, plasma, cerebrospinal fluid or synovial fluid samples. Depletion of abundant serum proteins will help in the discovery and detection of less abundant proteins that may prove to be informative disease markers. Recently, cryogel materials are considered as a novel generation of stationary phases in the separation science because of their easy preparations, excellent flow properties and high performances compared to conventional beads for the separation of biomolecules. Porous cryogels are a very good alternative to protein separation with many advantages. Several potential advantages of cryogels are large pores, short diffusion path, low pressure drop and very short residence time for both adsorption and elution. PHEMA based macroporous cryogel was selected as the basic component because of its inertness, mechanical strength, chemical and biological stability and biocompatibility. In this thesis, PHEMA based cryogels with different ligands were prepared for investigation of selective and efficient depletion of HSA from human serum.

Keywords: Albumin depletion, Dye-ligand affinity chromatography, Molecular imprinting, Cryogels.

Advisor: Prof. Adil DENİZLİ, Hacettepe University, Department of Chemistry, Biochemistry Division.

ACKNOWLEDGEMENTS

It is a pleasure to thank the many people who made this thesis possible.

It is difficult to overstate my gratitude to my Ph. D. supervisor, Prof. Adil Denizli. With his enthusiasm, his inspiration, and his great efforts to explain things clearly and simply, he provided not only this thesis but also life to be fun for me. I am very greatly indebted to him for his valuable guidance, professional advice, constructive criticism and suggestion during my research. I feel myself lucky for studying with such an accomplished scientist.

I would like to express my special graditute to Assoc. Prof. Handan Yavuz for providing encouragement, sound advice, good teaching, good company, and lots of good ideas throughout my thesis period. I would have been lost without her light.

I would like to express my graditute to my colleagues and my friends, Dr. Mehmet Odabaşı (Aksasay University), Dr. Sinan Akgöl (Ege University), Dr. Bora Garipcan (he is in army now), Dr. Serpil Özkara (İnönü University), Dr. Lokman Uzun (Hacettepe University) for their emotional support and sincereness.

I would like to also express my graditute to Prof. Süleyman Patır (Hacettepe University), Prof. Rıdvan Say (Anadolu University), Prof. Güleren Alsancak (Süleyman Demirel University), Assoc. Prof. Igor Yu Galaev (Lund University), Prof. Serap Şenel (Hacettepe University), Prof. Emir Baki Denkbaş (Hacettepe University) for their valuable guidance during my research.

Special thanks to my best friends Funda Altın, Gözde Baydemir, Handan Yavuz, Melike Karataş and Bahar Ergün for helping me get through the difficult times, and for all the emotional support, comradery, entertainment, and caring they provided. I would also like to emphasize my graditute to my dear friend Gözde Baydemir for inspiration and for assisting me in the process of writing this thesis.

I wish to thank my friends, Müfrettin Sarı, Ahmet Hamdi Demirçelik, Bahar Ergün, Erkut Yılmaz, Deniz Türkmen, Gülsu Şener, Işık Perçin, Nilay Bereli, Fatma Yılmaz, Ali Derazshamshir, Veyis Karakoç, Engin Bayram, İlker Koç, Erdoğan Özgür, Emel Tamahkâr, Sevgi Aslıyüce, Yeşeren Saylan, Canan Armutçu, Gizem Ertürk, Ilgım Göktürk, Hatice Bektaş, Cemil Aydoğan, Alper Türkoğlu, Kıvılcım Çaktü, Ayşenur Sağlam, Dursun

Ali Köse, Ebru Çubuk Demiralay, for their help in laboratory, for their collaborating, assisting, and providing me a pleasant atmosphere to work in.

I am greatly indebted to my dear brother Cenk Andaç, for being with me at all time, for his valuable guidance, and for support on AMBER calculations. Without him, this thesis would not have been as colorful as this.

I am very grateful to my dear husband Erdinç Özdil, for his patience during my thesis and for supporting a lovely atmosphere at home.

Lastly, and most importantly, I wish to thank my mother, Asiye Erdoğan and my father, Prof. Faruk Andaç. They bore me, raised me, supported me, taught me and loved me. To them I dedicate this thesis.

This thesis would not have been as good as it is now without support and assistance of the people I acknowledged here. So, I feel obliged to say thank all of you one more time.

INDEX

FIGURE LEGENDS

TABLE LEGENDS

1. INTRODUCTION

Proteomics is the study of proteins and their interactions in a cell. With the completion of the Human Genome Project, the emphasis is shifting to the protein compliment of the human organism. Because proteome reflects more accurately on the dynamic state of a cell, tissue, or organism, much is expected from proteomics to yield better disease markers for diagnosis and therapy monitoring.

The advent of proteomics technologies for global detection and quantitation of proteins creates new opportunities and challenges for those seeking to gain greater understanding of diseases. High-throughput proteomics technologies combining with advanced bioinformatics are extensively used to identify molecular signatures of diseases based on protein pathways and signaling cascades. Mass spectrometry plays a vital role in proteomics and has become an indispensable tool for molecular and cellular biology (Cho, 2007).

Serum proteins may often serve as indicators of disease and is a rich source for biomarker discovery. However, the large dynamic range of proteins in serum makes the analysis very challenging because high abundant proteins tend to mask of those of lower abundance (Björhall, 2005). Albumin, which comprises approximately 60% of the total protein milieu in normal human plasma, is particularly troubling for proteome analysis which uses serum, plasma, cerebrospinal fluid or synovial fluid samples (Rothemund, 2003). When large amounts of protein are loaded to facilitate detection of less abundant forms in 2-DE, resolution can be comprised due to expansive albumin spots that overlap proteins of lower abundance, masking their presence and producing smears and precipitates (Badock, 2001; Herbert, 2000). Further, those proteins in a sample mixture that have p*I* values close to that of albumin may be co-precipitated, resulting in protein loss (Herbert, 2000). Depletion of abundant serum proteins will help in the discovery and detection of less abundant proteins that may prove to be informative disease markers (Steel, 2003).

A variety of depletion methods for specific removal of high abundant proteins from body fluids have been developed. Several major strategies are available concerning the mechanisms of removal of HSA and IgG. In the case of HSA, depletion can be achieved by either dye-ligands such as the widely recognized Cibacron Blue F3GA and derivatives thereof (Gianazza, 1982), or specific antibodies (Wang, 2003). A dye affinity resin for removal of HSA has the advantage of high loading capacity as compared to an antibody based system but has been shown to lack of specificity (Denizli, 2001; Ahmed, 2003). Other methods reported include a proprietary polypeptide affinity matrix that removes albumin together with IgG, but is now apparently unavailable (Lollo, 1999), and a method based on the size separation in a centrifugal filtration device that was, perhaps predictably, unsuccessful (Georgiou, 2001).

Cibacron Blue F3GA (CB) is a monochlorotriazine dye which contains three acidic sulfonate groups and four basic primary and secondary amino groups, which bind with considerable specificity and significant affinity to nucleotide dependent enzymes and to a series of other proteins (Kopperschlager, 1982). After fixation to appropriate insoluble supports, CB has been used as ligand in affinity chromatography to isolate and remove albumin from human plasma. Dye immobilization requires an inert, hydrophilic support, which possesses chemically modifiable groups. Most frequently used matrices are the naturally occurring polysaccharide polymers: dextran, agarose and cellulose. However, these materials can undergo biological degradation. Synthetic polymers like poly(hydroxyethylmethacrylate) (PHEMA) are very resistant towards microbial degradation. Arica *et al*. and Denizli *et al*. have demonstrated an increase of albumin adsorption onto PHEMA surface after CB immobilization (Arica, 1998; Denizli, 1998). CB immobilization was carried out in alkaline solution to induce the covalent binding between the hydroxyl groups of the polymer and the triazine ring of the CB, since the amino coupled CB shows very low binding to albumin (Leatherbarrowand, 1980).

Conventional packed-bed columns possess some inherent limitations such as the slow diffusional mass transfer and the large void volume between the beads (McCoy, 1996). Although some new stationary phases such as the non-porous

polymeric beads (Denizli, 2000) and perfusion chromatography packing are designed to resolve these problems, these limitations cannot be overcome in essence (Özkara, 2003). Recently, cryogel materials are considered as a novel generation of stationary phases in the separation science because of their easy preparations, excellent flow properties and high performances compared to conventional beads for the separation of biomolecules (Lozinsky, 2003; Arvidsson, 2003; Lozinsky, 2002; Arvidsson, 2002; Babaç, 2006). Porous cryogels are a very good alternative to protein separation with many advantages. Several potential advantages of cryogels are large pores, short diffusion path, low pressure drop and very short residence time for both adsorption and elution.

Molecularly imprinted polymers (MIPs) are polymers prepared in presence of a template that serves as a mould for the formation of template-complementary binding sites (Mosbach, 1994; Sellergren, 2001a,b). Thus, MIPs can be created to recognize a large variety of target molecules often with affinity and selectivity comparable to those exhibited by poly- or monoclonal antibodies. MIPs are less expensive and quicker to prepare than biological receptors. Additionally, they are capable of withstanding much harsher conditions than antibodies, such as high temperature, pressure, extreme pH, and organic solvents. These properties have made them extremely attractive for solving problems in the fields of preparative chemical separations (Sellergren, 2001a,b), solid phase extraction (Lanza and Sellergren, 2001; Andersson and Schweitz, 2003) and sensing (Chianella, 2003; Haupt and Mosbach, 2000), or for the removal of specific molecular targets from food (Whitcombe, 1997; Ramstrom, 2001). MIPs have been prepared using polypeptides (Kempe, 1995; Andersson, 1995; Minoura and Rachkov, 2000), bacteria (Dickert and Hayden, 2002), low molecular mass compounds (Katz and Davis, 2000; Chianella, 2003) and proteins (Burow and Minoura, 1996; Bossi, 2001; Guo, 2004) as templates. In the case of proteins, however, only modest success has been obtained due to the specific properties of these templates. First, all proteins are water-soluble compounds that are not always compatible with mainstream MIP technologies, which relies on the use of organic solvents for the polymer preparation. Second, proteins have a large amount of functional groups available for the interaction with functional monomers. Third, proteins have a flexible structure and conformation, which can be easily affected by changes in

temperature or the nature of the solvent. Thus, from a thermodynamic and practical standpoint, it is difficult to develop successful imprints for such molecules. In the last 10 years, some new approaches have been proposed, which use both covalent and non-covalent methods (Wulff, 1993; Mosbach and Ramstrom, 1996). The immobilization of the protein template on a supporting surface (Shi, 1999; Yilmaz, 2000; Shiomi, 2005) provides a number of advantages, i.e. it allows the imprinting of templates independently of their solubility in the polymerization mix, it minimizes protein aggregation and it creates more homogeneous binding sites.

Basically, poly(hydroxyethyl methacrylate) (PHEMA) based cryogel was prepared for selective and efficient depletion of HSA from human serum. PHEMA was selected as the basic component because of its inertness, mechanical strength, chemical and biological stability and biocompatibility (Denizli, 2003). All these advantages of HEMA were combined with the interconnected open macroporous network of pores existing in so called cryogel. Spongy morphology and macroporous structure of cryogel allows movement of molecules of varying sizes, particularly body fluids, through the gels both by diffusion and convection (Lozinsky, 2002; Noppe, 2007). An advantage of cryogels is that they have large, highly interconnected pores which provide cryogels with low back pressures. However, large pores result in much lower surface area compared to other chromatographic supports (Baydemir, 2009). This turned in resulted small amounts of ligands available for binding and low adsorption capacity when using cryogels in affinity separations (Arvidsson, 2003).

In the present thesis, we attempted to prepare 3 different affinity columns for the recognition of human serum albumin (HSA). The first one was CB attached PHEMA cryogel. CB was covalently attached to the PHEMA cryogel via the nucleophilic substitution reaction between the chloride of their triazine ring and the hydroxyl groups of the PHEMA under alkaline conditions to produce PHEMA-CB cryogel column. The second one was based on the non-covalent imprinting of HSA in complex with newly synthesized functional monomer (MAPA) to produce HSA-imprinted PHEMAPA cryogel column.

Here, it was also reported the development and application of HSA-surface imprinted PGMA beads embedded PHEMA composite cryogel system for the depletion of HSA from human serum. PGMA beads embedded composite cryogels aim to combine the advantages of both small particles and convective media without bringing along the disadvantages of a high pressure drop and low binding capacity. By this purpose, the protein template is immobilised at the surface of the PGMA beads, with an approach modified from Tan et al., in which surface imprinting was achieved by minidispersion polymerization **(Tan, 2008).** The cryogels thus obtained were characterized, the binding capacity for HSA, the binding kinetics, the specificity of the HSA binding and the recovery of bound protein.

Finally, the application of all affinity columns that prepared with different methods to a real biological fluid, human serum, in which HSA is the most abundant protein (ca. 60% of the total proteins) was investigated (Andersson and Anderson, 2002; Tirumalai, 2003). The high quantity of HSA in serum is considered as a drawback, since it seriously hampers the detection of low abundant proteins, which are often marker of diseases. It has been demonstrated that if serum is selectively depleted of HSA, it would facilitate the analysis of such low abundant proteins. Albumin removal has been achieved through adsorption to immobilized dyes (Ahmed, 2003), immunoaffinity extraction (Wang, 2003) or affinity capture by immobilized phage-derived peptides (Sato, 2002), but to date there have been no reports concerning the use of molecularly imprinted polymers. In the present case, we attempt the use of a synthetic receptor, the imprinted cryogels, for the specific removal of HSA from serum.

2. GENERAL INFORMATION

2.1. Proteomics Technologies and Challenges

Proteomics is the protein equivalent of genomics and has captured the imagination of biomolecular scientists worldwide. It encompasses a broad range of technologies aimed at determining the identity and quantity of expressed proteins in cells, their three dimensional structure and interaction partners. In the postgenomic era, proteomics is a rapidly growing field of research that is becoming increasingly important. For example, it is extensively applied to the study of proteins involved in carcinogenesis, as well as to discover biomarkers for clinical use (Cho, 2007).

Disease markers are widely used for screening, diagnosis, staging, prognosis, monitoring response to treatment, and detection of recurrent diseases. As protein-protein interactions are the key to signal transduction to many regulatory events, a systematic classification of protein-protein interfaces is a valuable resource for understanding the principles of molecular recognition and for modeling protein complexes (Kim, 2006). The question of how one protein regulates the activity of another by binding to it requires an integration of structural, functional, and dynamic information. In the last decade, there have been many improvements in protein separation techniques, including two-dimensional polyacrylamide gel electrophoresis (2-D PAGE), liquid chromatography (LC), isotope-coded affinity tag (ICAT) labeling, and so on. Much progress has also been recently achieved in the analysis of proteins from tryptic digests using mass spectrometry (MS) and database searching. The newest generation of MS, combined with good separation techniques, is capable of providing rapid and confident protein identifications at the low femtomole level (Mc Cormack, 1997; Bogan and Agnes, 2004; Cho and Cheng, 2007; Cho 2007).

2.1.1. From Genomics to Proteomics

With the completion of the Human Genome Project, the emphasis is shifting to the protein compliment of the human organism. This has given rise to the science of

proteomics, the study of all the proteins produced by cell and organism, which involves the identification of proteins in the body and the determination of their roles in physiological and pathophysiological functions. As sequencing of the entire genomes ofmany prokaryotes and eukaryotes has been completed, there is a revival of interest in proteomics.

The term “proteome” refers to all the proteins expressed by a genome. While a genome remains unchanged to a large extent, the proteins in any particular cell change dramatically as genes are turned on or off in response to the environment. Since it is proteins that are directly involved in both normal and disease-associated biochemical processes, a more complete understanding of disease may be gained by looking directly into the proteins within a diseased cell or tissue. As a reflection of the dynamic nature of the proteome, some researchers use the term “functional proteome” to describe all the proteins produced by a specific cell in a single time frame. Whilst humans are estimated to have 30,000 to 40,000 genes potentially encoding 40,000 different proteins, alternative RNA splicing and post-translational modification (PTM) may increase this number up to 2,000,000 proteins or protein fragments (Kosak and Groudine, 2004). As a consequence, the proteome is far more complex than the genome.

Genomics has provided a vast amount of information linking gene activity with disease, but it does not predict PTM that most proteins undergo. Although DNA/RNA is easier to work with, there are limitations to the information that can be derived from DNA/RNA analysis. There are a number of reasons why gene sequence information and the pattern of gene activity in a cell do not provide a complete and accurate profile of a protein’s abundance or its final structure and state of activity. After synthesis on ribosomes, proteins are cut to eliminate initiation, transit, and signal sequences, as well as simple chemical groups or complex molecules that are attached. The gene transcript can be spliced in different ways prior to translation into protein. Following translation, most proteins are chemically changed through PTM, mainly through the addition of carbohydrate and phosphate groups. Such modification plays a vital role in modulating the function of many proteins but is not directly coded by genes. The PTMs are numerous (more than 300 types have been documented), static, and dynamic,

including phosphorylation, glycosylation, acetylation, deamidation, palmitoylation, sulfation, and so on. As a consequence, the information from a single gene can encode as many as 50 different protein species. Therefore, DNA sequence analysis does not predict the active form of a protein and RNA quantitation does not always reflect the corresponding protein levels. Multiple proteins can be obtained from each gene when PTM and mRNA splicing are taken into account. DNA/RNA analysis cannot predict the amount of a gene product, including the type and amount of PTM when a gene is translated, or the events involving multiple genes such as aging, stres responses, drug responses, and pathological transformations. Beyond the genomic level, it is clear to see why genomic information often does not provide an accurate profile of protein abundance, structure, and activity.

Actually, genomics and proteomics are complementary fields, with proteomics extending the functional analysis. It is believed that through genomics and proteomics, new disease markers and drug targets can be identified, which will ultimately help design products to prevent, diagnose, and treat diseases. The future of medicine and biotechnology will be impacted greatly by genomics and proteomics, but there is much needed to be done to realize the potential benefits.

2.1.2. Serum and Plasma Proteomics

There is a saying, “Eyes are the windows to the soul”. In much the same vein, blood, since it flows through the entire body, can be considered the window to the physical condition of the patient. Virtually everyone who has been to visit their doctor has given blood that is tested to detect any present disease conditions and determine the functional state of the body’s organs. A variety of different characteristics of blood are often measured depending on the physical condition of the patient (Figure 2.1). The fact that blood is comprised of several different types of cells and compounds such as salts and proteins makes blood tests very useful diagnostic tools. For example, the physician may request a white blood cell count if an infection is suspected or a Basic Metabolit Profile (i.e., measurement of sodium, potassium, chloride, calcium, bicarbonate, blood urea nitrogen, creatinine, and glucose levels) may be needed to determine the present state of renal

function (Engle, 1983). Depending on the required test, blood can be separated into different components. A simple blood smear can be prepared on a microscope slide to examine and count red and white blood cells, as well as platelets. The liquid portion of blood is referred to as plasma. When blood is permitted to clot after it has been drawn from the patient, the blood cells and some of the proteins precipitate. Centrifugation of this sample is used to separate these solids, leaving behind the serum portion of blood (Issaq, 2007).

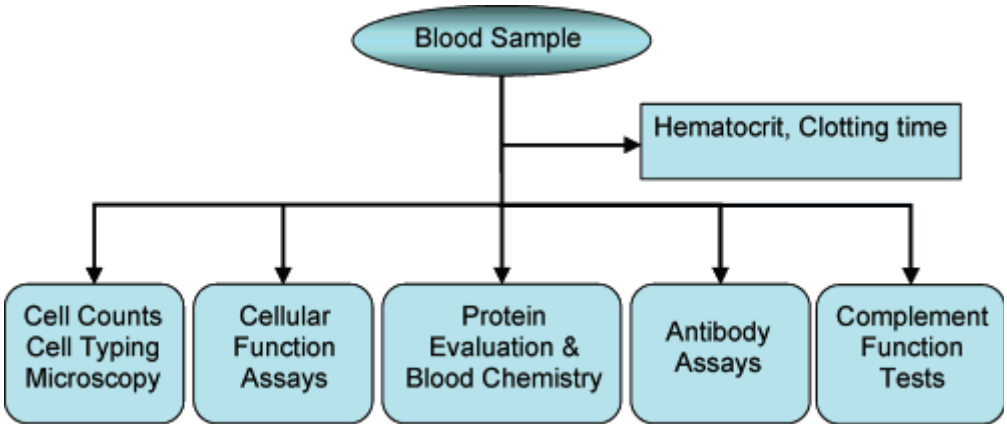

Figure 2.1. Blood is an extremely valuable fluid for monitoring the well-being of the patient. A variety of different tests are conducted on a blood sample to assist the physician in diagnosing the patient's physical condition.

While numerous diagnostic tests for diseases ranging from cancer to diabetes are presently conducted using blood samples, the general consensus is that the archive of information within this biofluid has only begun to be understood. It is this hope that has driven the efforts to develop technologies necessary to mine this information within blood. These developments have impacted not only the instrumentation used to acquire the data but also how the samples are prepared and how the data is analyzed before and after data acquisition, respectively.

2.1.3. Why Study the Proteome of Blood?

The human body possesses over 60000 miles of veins, arteries, and capillaries. Approximately five liters of blood travels continuously through the body by way of

the circulation system. Blood carries oxygen and nutrients to cells and transports carbon dioxide and waste products excreted from cells. It is estimated that no cell is more than four cell units removed from the circulation system. No other biofluid has intimacy with the body like blood has, and therefore, it is not surprising that it possesses such a richness of information concerning the overall pathophysiology of the patient. Unlike specific cell types, however, blood does not contain its own genome. Its genome can be considered as a compilation of the organism's foundational genome along with all of the variations (i.e., mutations, single nucleotide polymorphisms, gene duplications, etc.) that are found in particular cells. Since it lacks a specific genome, blood does not have its own transcriptome. Rather, it can potentially contain any portion of a transcript that is transcribed within any cell in the body. Likewise, the proteome of blood can potentially contain portions of any protein found within any cell. A recent study comparing N-linked glycopeptides within cultured cells, solid tissues, and plasma, and other studies that have characterized the serum proteome have clearly substantiated this hypothesis (Zhang, 2007; Adkins, 2002; Chan, 2004).

2.1.4. What's the Difference between Serum and Plasma?

There has been an overwhelming interest in trying to decipher valuable information from the proteome content of blood. To be clear, it is not actually blood that is directly analyzed in most proteomic studies; rather, it is the plasma or serum portion of blood. As briefly mentioned above, plasma is the liquid portion of *unclotted* blood that is left behind after all the various cell types are removed. To prepare plasma, blood is withdrawn from the patient using venipuncture in the presence of an anticoagulant and the sample is centrifuged to remove cellular elements. The most commonly used anticoagulants include heparin, ethylenediamine tetraacetic acid (EDTA), or sodium citrate. Heparin prevents coagulation by activating anti-thrombin while both EDTA and sodium citrate prevent coagulation by chelating calcium ions. It is also possible to draw blood through a resin that removes calcium, thereby preventing the coagulation. Serum is prepared by collecting plasma in the absence of any coagulant. Under these conditions, a fibrin clot forms. This clot is then removed using centrifugation, leaving behind serum.

The process of coagulation makes serum qualitatively different from plasma. The removal of a large portion of the fibrinogen content of plasma in the form of the fibrin clot results in serum having a protein concentration lower than that of plasma. This difference, however, is only on the order of 3–4% (Lum and Gambino, 1974). Other proteins are also removed by specific or nonspecific interactions within the fibrin clot. Conventional thinking would surmise that many coagulation factors are also removed in the preparation of serum. Actually, factors IX, X, XI, and VII/VIIa are found within serum (Spence, 2002). While the primary effect of the coagulation process is the removal of the fibrin clot, platelets, erythrocytes, and leukocytes secrete and increase certain proteins in serum during the same process. One study showed that the levels of platelet-secreted vascular endothelial growth factor (VEGF) are 230 ± 63 and 38 ± 8 pg/mL in the serum and plasma of normal individuals, respectively. In studies of patients suffering from thrombocytosis, in which their platelet count is substantially increased compared to those of matched healthy controls, VEGF levels are also much higher (Benoy, 2002). These results show that serum and plasma VEGF levels are affected by platelets, but more markedly so in serum.

2.1.5. Characterization of the Serum Proteome

The proteome describes the entire compliment of proteins expressed by a cell at a point in time. Alterations in protein abundance, function, and structure can serve to indicate pathological abnormalities even before clinical symptoms are observed. Therefore, if the early detection of diseases such as cancer is to become a reality, it is vital to identify useful diagnostic and prognostic biomarkers. The methods that have been evaluated for discovering proteins for diagnostic purposes are often based on separation (electrophoresis and chromatography) followed by MS for detection and identification. Since blood circulates throughout the body, early hypotheses suggested that the serum/plasma proteome contains a treasure trove of protein biomarkers. Without having any prior information, discovering these biomarkers requires analytical methods that can be used to examine as much of this biofluid proteome as possible. Therefore, much of the analytical development

in the past few years has focused on methods to identifying ever increasing numbers of proteins within serum and plasma.

2.1.6. The Dynamic Range Problem Related to Protein Concentration

At first glance, serum and plasma seem to be the ideal clinical samples for MS based proteomic analysis. They are relatively easily obtained from the patient and have a very high protein concentration (e.g., on the orders of tens of mg/ mL). The protein concentration, however, is deceiving. Twenty-two proteins make up approximately 99% of the protein content of serum and plasma (Figure 2.2) (Anderson and Anderson, 2002; Tirumalai, 2003). It is estimated that the protein concentrations in these samples span 10 orders of magnitude, and the prevailing thought is that specific disease biomarkers for diagnostic and prognostic purposes are most likely within the very low concentration range. It was recognized early on, particularly in the analysis of serum and plasma, that the high dynamic range of protein concentrations found in these two fluids was going to be problematic for downstream MS analysis (Anderson, 2005). Considering that the dynamic range of a mass spectrometer is on the order of 2 orders of magnitude, it is easy to figure out that a straightforward liquid chromatography (LC)-MS/MS analysis will result in the characterization of only the highest abundance, and probably least interesting, proteins. While strong cation exchange fractionation prior to reversed phase (RP) LC-MS/MS analysis has been shown to increase the ability to identify low abundant proteins in many proteomic studies (Fujii, 2004; Jin, 2005), this strategy alone is not sufficient to gain comprehensive coverage of the low abundance proteins within biofluids.

It was quickly recognized that to effectively characterize serum or plasma was going to require methods to remove the high abundance proteins prior to downstream analysis. One of the earliest approaches used to deplete high abundance proteins was to pass a serum/plasma sample over Cibacron Blue, a dye with high affinity for albumin (Zolotarjova, 2005). Albumin, as shown in Figure 2.2, comprises approximately 50% of the protein content of serum/plasma; therefore, removal of this single protein has an immediate impact on the dynamic range problem related to protein concentration. Recently, Agilent introduced the

multiple affinity removal system (MARS) for the immunodepletion of six high abundant proteins (i.e., albumin, IgG, IgA, transferrin, haptoglobin, and alpha-1-antitrypsin) in serum/plasma (Darde, 2007). The usefulness of this product in removing high abundant proteins is illustrated in Figure 2.3. Similar products have been developed, including a Top 20 depletion column from Sigma, and the Seppro MIXED12 IgY-based affinity LC column, for the depletion of the twelve highest abundance plasma proteins manufactured by GenWay Biotech Inc. (Gong, 2006). The reproducibility and effectiveness of these products to deplete major proteins in serum/plasma samples have always been a concern. In fact, a recent study published the results of the reproducibility of a MARS column across serum samples from patients with prostate cancer. They found that the depletion of high abundant proteins from all 250 serum samples was complete and reproducible, with a relative standard deviation below 7%, over a six week period (Darde, 2007). Another study comparing a series of sample preparation methods has also confirmed the effectiveness and robustness of immunoaffinity subtraction methods for simplifying the serum proteome prior to MS analysis (Whiteaker, 2007). Depletion of high abundant proteins is now considered an essential sample handling step in any serum/plasma study regardless of subsequent analytical strategies. There are always concerns, however, when using affinity-based depletion strategies that potentially important biomarkers will be lost either through the possible “sponge” effect of the high abundant proteins or by the nonspecific binding to the affinity column used. Indeed, studies have shown that proteins remain bound to the targeted high abundance proteins during their depletion (Gundry, 2007; Zhou, 2004). Moreover, major protein depletion alone certainly was not enough to deal with the dynamic range problem.

2.1.7. Major Protein Depletion Strategies

In a perfect world the best protein depletion option for human plasma would be to remove the top 50–100 most abundant proteins (the classic plasma proteins of little interest to the biomarker researcher) to greatly extend the dynamic range of proteome detection deep into the pg/mL range of plasma proteins for greater coverage and diversity of protein identifications.

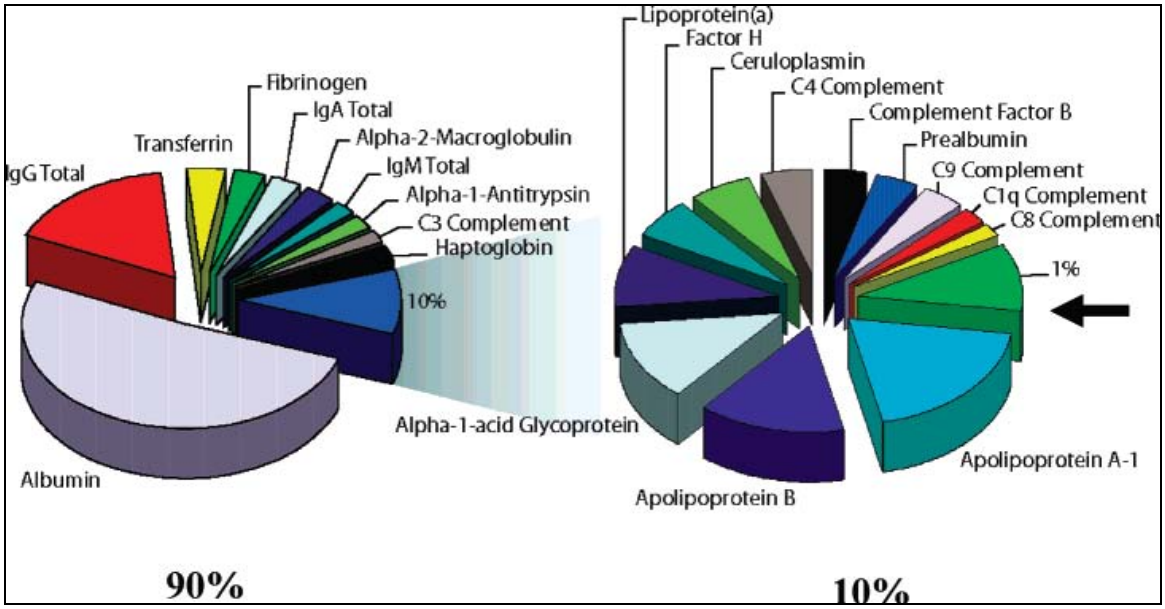

Figure 2.2. The dynamic range of protein concentrations in human serum. While the overall protein concentration of serum is high, 22 proteins make up 99% of the total protein amount.

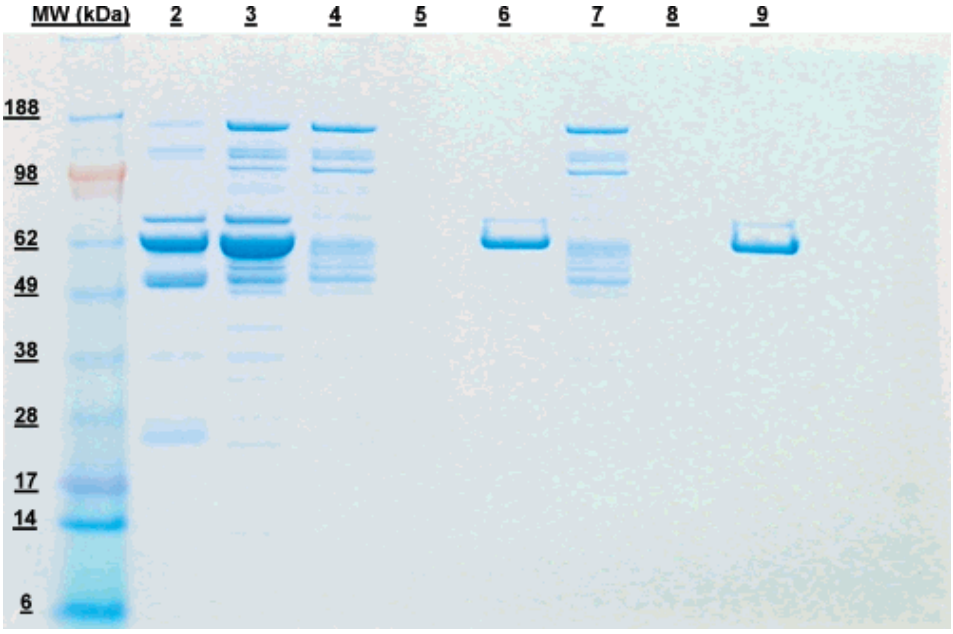

Figure 2.3. Depletion of serum using a multiple affinity removal system (MARS): lane 2, serum standard; lane 3, raw plasma; lane 4, plasma proteins that flow through a MARS immunodepletion column during the first washing step; lane 5, plasma proteins that flow through a MARS immunodepletion column during the second washing step; lane 6, elution of high abundant proteins that are retained by the MARS immunodepletion column. Lanes 7, 8, and 9 are replicates of lanes 4, 5, and 6, respectively, using a second MARS column.

This of course is not currently practical, but the intent has been well taken by others as there are a number of basic techniques that have been used to eliminate the high abundance proteins in plasma. The two largest contributors to the dynamic range challenge of plasma are human serum albumin (HSA) at ~50% of the total protein mass, and the immunoglobulin proteins which represent 20–25% of the total protein mass. Each has relatively high molecular weights, 64 kDa and ~150 kDa respectively, which have spawned methods to help selectively target them. Organic solvent precipitation (methanol, acetonitrile), affinity dye based depletion (Cibacron Blue), and simple ultra-filtration are commonly used general methods to either remove whole proteins entirely or remove the higher molecular weight component. Often, a series of increasingly concentrated acetonitrile fractions or “cuts” are taken to selectively precipitate out the higher molecular protein fraction. Such techniques are effective but act in a nonspecific manner and lack in reproducibility, especially concerning the quantitation of proteins remaining in solution. The introduction of affinity chromatography for depletion purposes now allows for the selective removal of virtually any protein of interest (although with imperfect efficiency) and when coupled to a high pressure liquid chromatography (HPLC) system, can provide a reasonably reproducible platform for repeated quantitative analysis (Jacobs, 2005).

One concern for depletion methodologies is that for every sample manipulation, there is a small but accumulative rate of error which is propagated into the analysis. This principle hold true for each step in the sample processing pipeline, especially for any depletion process. The hope is that any introduced error will be minimal in affecting experimental accuracy in comparison to the benefits gained from increasing the number of overall identifications. A second concern of the process is the loss of potential proteins of interest, whether due to selective or nonselective binding to the depleted protein or column surface, during the depletion method. For example, HSA is a known nonspecific binder as part of its biological role is to act as a molecular “sponge” of sorts to assist in the circulation and distribution of other proteins (Jacobs, 2005).

Depletion of the immunoglobulin class of proteins (IgG, IgA, IgM, IgE, etc.) is actually quite straightforward as researchers for some time have been extensively

targeting this group of proteins to develop multiple antibodies (i.e., Goat R-human IgG) and binding proteins (Concanavalin A, Protein G, Protein A, Protein L) for the selective binding, and eluting, of the various Ig classes. Though not as abundant as HSA, the removal of Ig proteins accomplishes not only a reduction of total protein content, but also greatly reduces the overall complexity and potential random background sequence generation that occurs once the CDR of the immunoglobulin has been reduced to peptide form (Jacobs, 2005).

Jacobs et al. have utilized both HSA depletion and IgG depletion methods in attempts to increase the potential dynamic range of detection for human plasma proteomics (Shen, 2005). Reducing both species effectively removes ~75% of the total protein content of the sample, but still leaves some higher abundant species in the 2–3 mg/mL range. In their studies, even after depletion, they were still able to detect a significant number of peptides from both HSA and Ig proteins from the “depleted” sample. The columns tested (Poros@ anti-HSA and protein G affinity depletion cartridges, Applied Biosystems) both claimed to have > 99% depletion of the specific component. This initially appears adequate for a depletion study, but when compared in depth, 99% depletion for HSA at ~45 mg/mL would correspond to on average 450 µg/mL of the protein remaining in the sample, still maintaining HSA near the top of the most abundant proteins present in plasma. This is not even taking under consideration likely fragmentation and partial protein components, which are proportionally present for every protein, but for albumin would constitute a significant percentage of the total protein content. Partial protein retention is also very likely for depletion of immunoglobulin proteins as well, especially when using Protein A/G depletion, which binds to a specific site on the Fc portion of the immunoglobulin, and would not recognize or bind to any separate light chain, fragment or portion that does not contain the binding site.

Also notably observed when analyzing the retentate from each depletion was a significant number of non HSA and non-Ig proteins retained on the column, a major concern of depletion protocols. Most of these extra identifications corresponded to higher abundance proteins, which suggests that the nonspecific interactions occurring during depletion (either with the column itself or with the retained HSA and IgG) are concentration dependent. However, this supposition is

difficult to prove because potentially retained lower abundant species would be difficult to detect in the enriched presence of HSA and immunoglobulins.

The obvious next step or progression is not only to remove the top two most abundant proteins but to attempt a simultaneous and reproducible removal of all of the highest abundant proteins. By combining various affinity materials into one depletion column, the depletion of multiple components can be accomplished in one step, simplifying the sample preparation and potentially decreasing errors in reproducibility. Such columns are now commercially available from multiple suppliers; MIXED12 column from GenWay and the MARS column from Agilent (Table 2.1). When using such columns, Jacobs et al. have been able to identify a number of new proteins not previously identified using only HSA or Ig depletion methods and have observed similar results of reproducibility and depletion levels as previously published results (Jacobs, 2005; Szafranski, 2004). Depletion results dealing with specific human plasma studies have revealed numerous secreted and known lower abundance proteins which have been very beneficial in ascertaining the approximate increase in dynamic range of our detections. Utilizing plasma samples has been very beneficial to use for such studies due to the large number of proteins with known plasma concentrations, making it very straightforward to infer, based upon the identification of these known proteins, the dynamic range of the detection methods.

Beyond what has already been discussed, there still remain some technical challenges associated with such multiple protein depletion strategies. First, most have very limited loading capacities, 15–25 µL volume of total plasma for the small columns and 30–40 µL for the larger columns, and since only 5-10% protein amount is expected to be recovered, multiple depletions steps for one sample are often required to generate enough sample for the following analysis. For a depletion of 1 mL of plasma, 20–40 separate HPLC runs need to be performed for each sample. Considering the recommended lifetime of each column is ~100–200 runs, this can be very limiting. Add into this the cost of each column, both small and large, can range between sixteen hundred to several thousand dollars each, this method, especially if you are conducting in-depth studies with several plasma samples, can greatly increase the overall baseline cost of analysis. Despite this, it

is becoming clear that such experiments are necessary in certain proteomic applications for the enhancement of detection of low abundance proteins.

Table 2.1. Major characteristics of some depletion columns

Column name (supplier)	Binding specificity						Loading capacity in µl serum	Method for depletion
	Albumin	IgG	α1-Anti-trypsin	IgA	Trans-ferrin	Hapto-globin		
Aurum Serum Protein minikit (Bio-Rad)	Dye-ligand, F3GA	Protein A	–	–	–	–	50	Spin-down columns
ProteoExtract™ Albumin/IgG Removal Kit (Merck Biosciences)	Novel affinity ligand	Protein A	–	–	–	–	35	Gravity flow columns
Multiple Affinity Removal System (Agilent Technologies)	pAb[a)]	pAb[a)]	pAb[a)]	pAb[a)]	pAb[a)]	pAb[a)]	30	LC-column
POROS® Affinity Depletion cartridges: Anti-HSA and Protein G (Applied Biosystems)	pAb[a)]	Protein G	–	–	–	–	5	LC-column
Albumin and IgG Removal Kit (Amersham Biosciences)	pAb[a)]	pAb[a)]	–	–	–	–	15	Spin-down columns

a) pAb, polyclonal antibodies

2.1.8. Current Issues in Clinical Proteomics

Although proteomics in general, and clinical proteomics in particular, offer much promise for biomarker discovery, issues of pre-analytical variables, analytical variability, and biological variation must be addressed if further progress is to be gained. A good understanding of how pre-analytical variables affect test results is important in any clinical laboratory and is equally important in biomarker research. Specimen manipulation, whether sample collection, pipetting, or diluting, contributes to preanalytical error. Whether looking for protein changes that act as potential biomarkers of disease, or using spectral patterns as protein fingerprints, Q understanding how the use of different blood collection tubes, coagulation times, storage conditions, or sample type, such as whole blood, plasma, or serum, affects MS protein spectra must be explored and considered. The Human Proteome Organization (HUPO) established a Specimen Committee in 2002 to study and address many of these issues (Colantonio and Chan, 2005).

A study by Marshall et al. highlights the importance of understanding the effects of pre-analytical variation in interpreting data produced through proteomic analysis

(Marshall, 2003). Using MALDI-TOF MS, the authors analyzed blood samples obtained from patients with myocardial infarction and observed changes in protein profiles that were generated not by pathophysiological processes but rather by the amount of time between sample draw and analysis (Marshall, 2003). They found that the pattern of protein fragments in both serum and plasma changed within as little as 2 h at room temperature (Marshall, 2003). Using different concentrations of protease inhibitors, they determined that proteases in serum and plasma remain active after blood collection and their activity has an impact on the spectra produced. This example highlights that failure to understand how pre-analytical variables affect proteomic results can lead to misinterpretation of data, but a better understanding of these variables should lead to improved experimental design and interpretation of data.

Another source of variation that must also be considered in biomarker research is biological variation (Fraser, 2001). In the context of proteomic research and biomarker discovery, biological variation, referred to as between-subject variation, is the sum of differences in protein expression between people, resulting, but not limited to, differences in age, gender, or race (Fraser, 2001). Another source of variance is within-subject variation. For any individual, many analytes fluctuate based on time of day, fasting state, or age. Although these fluctuations may not be clinically relevant, they do add an additional level of complexity in elucidating disease-induced protein changes from changes due to bio-rhythmic fluctuations. Comparison of complex protein samples, such as serum, between healthy and disease states adds yet an additional layer of complexity in elucidating disease-induced protein changes. Teasing out protein changes that are due to within subject variation, between-subject variation, and pathophysiological processes requires good experimental design, a solid understanding of the strengths and limitations of proteomic technologies used, and the proper utilization of statistical techniques.

2.2. Dye-Ligand Affinity Chromatography

In the last 20 years, protein-based drugs have become significant weapons in the war against disease. Approximately 1049 million grams of protein-based drugs

were produced worldwide in 1999, and their production is expected to rise to 1150 million grams by 2004. Within a decade, it is estimated that approximately 25% of all drugs in developed countries will fall in this category, especially as the number of candidate therapeutic targets is increased (Thomas, 2001).

Given the worldwide demand for pure therapeutic proteins, the biotechnology industry will soon suffer from a severe shortage of manufacturing capacity for such agents (Garber, 2001). To meet this demand, technical improvements will be needed in protein purification methods to give both good purification efficiency and high protein yields (Garber, 2001; Lowe, 2001). In addition, now that the human genome has been determined, scientists are faced with the challenge of studying large protein libraries as they examine the molecular workings of the cell (Geoffrey and McCarty, 2001). This will also require improved methods and materials for the purification of proteins (Wehr, 2001; Johnston, 2001; Kodadek, 2001).

One approach for dealing with these needs is to develop better affinity ligands for protein isolation. Synthetic compounds such as dyes and chlorotriazine-linked biomimetic agents are particularly appealing for use as ligands in large-scale affinity chromatography and high-throughput protein screening. Reasons for this include the low cost of these ligands, their resistance to chemical or biological degradation, and their ability to be sterilized and cleaned *in situ.* In addition, they can be readily immobilized to generate affinity adsorbents that have high binding capacities for proteins (Lowe, 2001; Labrou and Clonis, 1994; 2002; Clonis, 2004).

Dye-ligand affinity chromatography and *biomimetic affinity chromatography* are two chromatographic methods that are being explored for this purpose. These use either synthetic dyes or biomimetic molecules as immobilized ligands. The discovery of dye-ligands occurred accidentally in the late 1960s. At that time, scientists purifying the enzyme pyruvate kinase were puzzled when they found that a small dye (Blue Dextran) coeluted with this enzyme from a gel filtration column (Haeckel, 1968). It was later learned that this was caused by binding between the enzyme and dye, thus causing the dye to elute with the enzyme. This soon led to the first reported application of dyes in affinity chromatography when

Staal et al. used a Blue Dextran column in 1971 to purify pyruvate kinase from human erythrocytes (Staal, 1971).

The dyes originally employed as ligands in dye-affinity chromatography were obtained from the textile industry. In particular, chlorotriazine polysulfonated aromatic molecules, often referred to as triazine dyes, were used for this purpose. Over the past few decades, these dyes have found wide application as general ligands for the purification of albumin and other blood proteins, as well as for oxidoreductases, decarboxylases, glycolytic enzymes, nucleases, hydrolases, lyases, synthetases, and transferases (Labrou and Clonis, 1994; 2002).

Many dye-ligand adsorbents are now available from suppliers like Sigma-Aldrich and Amersham Pharmacia Biotech. Examples of these adsorbents include CB3GA-Agarose, Blue-Trisacryl, Reactive Brown 10-Sepharose, Reactive Gren 19-Sepharose, Reactive Red 120-Sepharose, and Reactive Yellow 3-Sepharose.

To increase the specificity of these supports, the concept of a biomimetic dye ligand was later introduced (Clonis, 2000; Lowe, 1992; 1986). In this approach, new dyes are designed that mimic the natural ligand of a targeted protein, such as by substituting the terminal 2-aminobenzene sulfonate moiety of the dye Cibacron Blue 3GA (CB-3GA). It has been found that these biomimetic dyes exhibit increased purification ability and specificity versus traditional dye-ligands, thus making them useful tools for simple and effective purification protocols.

Triazine dyes are the most common binding agents used in dye-ligand chromatography. The structures of these dyes consist of two distinct units joined through an amino-bridge, as illustrated in Figure 2.4. The first unit in this structure, the chromophore, contributes the color (usually based on an anthraquinone, azo, or phthalocyanine group). The other unit (usually 1,3,5-*sym*-trichlorotriazine) provides the site for covalent attachment to an insoluble support (Labrou, 2002; Denizli and Pişkin, 2001). Anthraquinone triazine dyes are the most widely used dyeligands in enzyme and protein purification. Of this group, the triazine dye CB3GA has received the most attention. Therefore, the following discussion on dye-ligand affinity chromatography focuses primarily on this dye and its analogs.

(a) Cibacron Blue F3GA

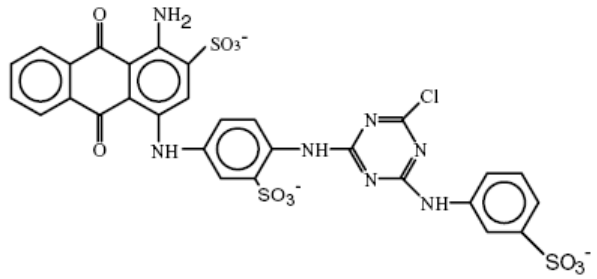

(b) Procion Red HE-3B

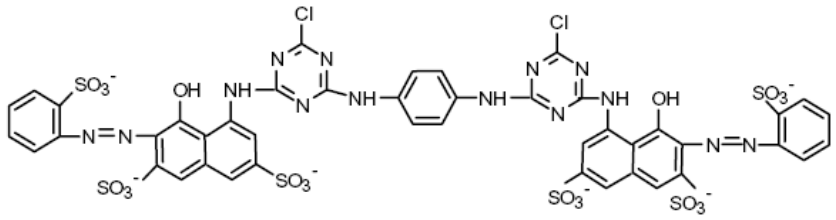

(c) Procion Rubine MX-B

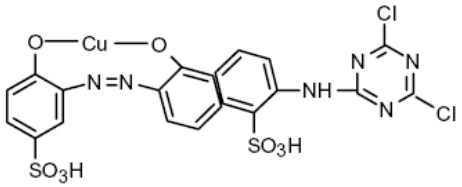

(d) Procion Yellow H-A

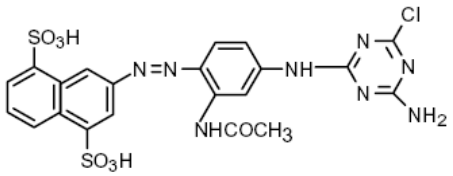

(e) Turquoise MX-G

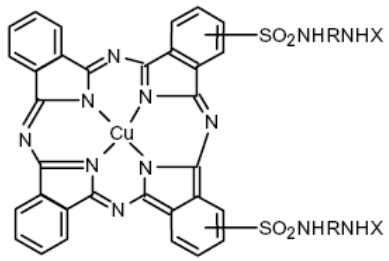

Figure 2.4. Structure of several representative triazine dyes: (a) Cibacron Blue 3GA, (b) Procion Red HE-3B, (c) Procion Rubine MX-B, (d) Procion Yellow H-A, and (e) Turquoise MX-G.

2.2.1 Immobilization of Dye-Ligands

Covalent attachment of a triazine dye like CB3GA onto an affinity support (e.g., carbohydrates such as agarose, dextran, and cellulose can be achieved under alkaline conditions by using nucleophilic displacement of the dye's chlorine atom by hydroxyl groups on the support's surface (Labrou and Clonis, 2002; Labrou, 2000; Labrou, 1995). A typical protocol for performing this with an agarose support is as follows. First, one gram of a washed agarose gel is combined with a solution of purified dye in water (5 to 20 mg dye in 1 ml), followed by the addition of a sodium chloride solution (22% w/v, 0.2 ml). This suspension is tumbled for 30 min at room temperature prior to adding solid sodium carbonate to give a final concentration for this salt of 1%. The reaction is then allowed to continue with shaking at 25 to 60°C for 1 to 8 h (Labrou, 1995). The actual time used in this last step depends on the reactivity of the dye molecule, with 4 to 8 h generally giving 2 to 4 μmol of immobilized dye per gram of moist gel. Next, the gel is washed extensively with distilled water, 1 *M* KCl, and 20% dimethyl sulfoxide (DMSO) until the washings are colorless. The gel is then stored until use as a suspension in 20% ethanol at 4°C (Labrou, 1995).

2.2.2 Selective Interactions of Dye-Ligands with Proteins

The first x-ray crystal structure that gave detailed information on dye-protein interactions was for the complex of CB-3GA with horse liver alcohol dehydrogenase (Biellmann, 1979). More recently, two other structures have been solved: one for the CB3GA-NAD(P)H:quinone reductase complex (Li, 1995) and the other for a CB3GA glutathione *S*-transferase complex (Oakley, 1999).

The results for the CB3GA NAD(P)H:quinone reductase complex indicate that the dye CB3GA and the AMP moiety of $NADP^+$ interact very similarly with the enzyme, with three of the ring systems of CB3GA mimicking AMP binding. In the case of the CB3GA glutathione *S*-transferase complex, the anthraquinone chromophore of the dye occupies the H-site of each enzyme subunit and makes van der Waals contacts with amino acids Phe-8, Val-10, Ile-104, Tyr-108, and Gly-205 (Figure 2.5). In addition, there is possible hydrogen bonding between the hydroxyl group

of Tyr-7 and the anthraquinone ring carbonyl group of CB3GA, as well as a salt bridge between the sulfonic acid group of CB3GA and the guanidyl group of Arg-13. Because there is no observed density for the rest of the dye-ligand in the glutathione *S*-transferase complex, it is believed that the remainder of the dye molecule exhibits a structural mobility that is too high to be characterized by crystallography (Oakley, 1999).

Recently, matrix-assisted laser desorption/ionization mass spectrometry (MALDI MS) was also applied to the study of dye-protein interactions (Fries and Zenobi, 2001, Salih and Zenobi, 1998). This approach has shown that the sulfonic acid groups of CB3GA bind only to arginine side chains, as opposed to binding to all basic sites (Arg, Lys, and His). This specific interaction is thought to represent the driving force in dye-protein binding. To explain this finding, the authors of this study noted that among all the amino acids, arginine has the highest gas-phase basicity and highest *pKa* value (*pKa* = 12.48 for the guanidino group). This could be the reason for the preferential selectivity of a sulfonate group (with a typical *pKa* much less than zero) for arginine over other basic amino acids. It was further suggested by these authors that the principal arginine-sulfonate interaction is a salt bridge, which is enhanced by ion-dipole interactions and hydrogen bonds that are especially favorable because of the near-perfect fit between these two bidentate binding groups (Fries and Zenobi, 2001).

2.2.3 Development of a Dye-Ligand Purification Method

The selection of a dye adsorbent for a particular macromolecule is currently an empirical process. The suitability of a range of dyes and adsorbents can be evaluated chromatographically by using small affinity columns (i.e., 0.5 to 1 ml in size). Detailed screening procedures that can be used for this purpose have been described elsewhere (Labrou, 2000).

During the development and optimization of a dye ligand purification, attention should be paid to variables such as the immobilized ligand concentration; the mobile phase pH, ionic strength, and composition; temperature; and sample size (Labrou and Clonis, 2002; Labrou, 2000). The pH, ionic strength, and temperature

of the initial equilibration buffer are all important factors that will influence the adsorption and elution of target proteins on a dye-ligand column. The influence of pH and ionic strength arises from the cation-exchange character of common dye ligands, which results from the presence of negatively charged sulfonic groups in these dyes (Labrou and Clonis, 2002).

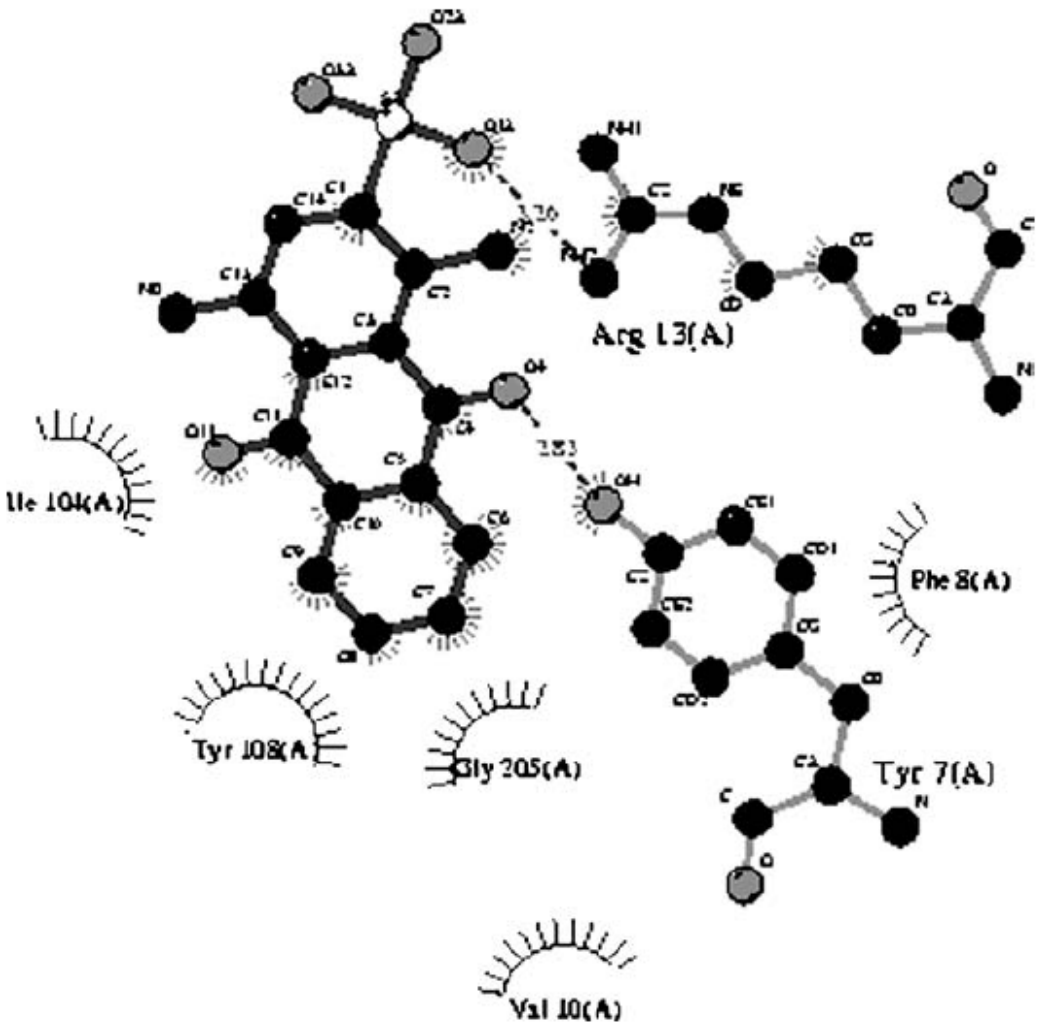

Figure 2.5. A LigPlot diagram of the Cibacron Blue 3GA/glutathione *S*-transferase complex (PDB code 20gs), illustrating some of the residues involved in van der Waals interactions.

The elution conditions used for a bound biomolecule should be compatible with the dye-ligand adsorbent, as well as effective in desorbing the retained molecule in a good yield and in its native state. The elution of bound proteins can be performed in either a nonspecificor biospecific manner (Labrou and Clonis, 2002; Frier,

2001). Nonspecific elution usually involves changing the pH or ionic strength of the mobile phase. An increase in pH generally weakens adsorption and promotes the elution of retained molecules. The ionic strength of the mobile phase is usually increased by adding a salt like KCl or NaCl. If the hydrophobic contribution to dye-protein binding is large, it is also possible to promote elution by altering the polarity of the mobile phase, such as by adding ethylene glycol or other organic solvents.

Nonspecific elution methods, although economical, generally give a lower degree of purification due to the coelution of nonspecifically bound proteins. Thus, biospecific elution is instead recommended for group-specific adsorbents like dye-ligand supports. Biospecific elution can be achieved in this case by including in the mobile phase an agent that competes with the immobilized ligand for its binding site on the target enzyme or protein. Examples of such competing agents can include substrates, products, cofactors, inhibitors, or compounds that produce allosteric changes in the binding of the immobilized dye to its target (Frier, 2001).

2.2.4 Recent Progress in Dye-Ligand Affinity Chromatography

New developments in dye-ligand techniques have recently appeared for both the traditional chromatographic mode and for alternative separation schemes like affinity partitioning, affinity precipitation, and expanded-bed chromatography (Zijlstra, 1998; Lali, 1999; Mattiasson, 1996; Garg, 1996). As one example, a PEG-CB3GA conjugate was used in an aqueous two-phase system for the isolation of IgG, where the partitioning of IgG into the top phase was obtained in the presence of a 10 m*M* potassium phosphate buffer (Zijlstra, 1998).

Affinity precipitation is a technique that integrates specific affinity interactions into a conventional precipitation method. This technique involves the use of a soluble ligand that binds the target molecule to form a complex that can be selectively precipitated, thus allowing the target molecule to be subsequently eluted in higher purity. This can be accomplished by using heterobifunctional ligands and reversibly soluble polymers (e.g., carboxymethyl cellulose) onto which the affinity ligand has been conjugated. Precipitation of a polymerligand- target protein complex in this method can be induced by a change in such conditions as

temperature, pH, or ionic strength (Lali, 1999). For instance, CB3GA conjugated to carboxymethyl cellulose was used for the affinity precipitation of lactate dehydrogenase. This gave a 23-fold purification from a crude porcine extract in a single precipitation step (Lali, 1999).

The efficiency of a chromatographic process can be significantly improved by pretreatment of an affinity matrix with certain water soluble polymers (Mattiasson, 1996; Garg, 1996). This technique is known as *polymer-shielded dye affinity chromatography*. In this method, the dye matrix complexes with a nonionic water-soluble polymer, such as poly(vinylpyrrolidone) or poly(vinyl alcohol), prior to the application of a sample. The purpose of these polymersis to shield the dye and prevent nonspecific interactions between the target protein and dye, as illustrated in Figure 2.6. This provides a faster purification than can be achieved on an unshielded column. Polymer-shielded dye-affinity chromatography has successfully been used in purifying a number of enzymes (Garg, 1996). For example, polymer-shielded dye affinity chromatography was used in an expanded-bed system with the support Streamline-CB3GA for the isolation of lactate dehydrogenase from a crude porcine muscle extract, resulting in 4.1-fold purification (Garg, 1996).

Dye-ligand affinity chromatography has also found wide use in the purification of pharmaceutical proteins (Koch, 1998; Swaminhatan and Khanna, 1999; Moore, 1997; Govoroum, 1997; Alderton, 1995; Allary, 1991). Examples include work with this method in purifying human component factor B, factor C2, factor II, factor IX, trypsin, chymotrypsin, and proteinase 3 (Garg, 1996). For instance, human recombinant alpha-interferon was purified in a single step on a mimetic dye-ligand matrix, yielding monomeric alpha-interferon with a specific activity of 2.8×10^{8} IU/mg (Swaminhatan and Khanna, 1999). Other examples have involved the purification of follicle-stimulating hormone (Moore, 1997), pituitary gonadotropins (Govoroum, 1997), ricin A chain (Alderton, 1995), and human serum albumin (Allary, 1991). In the case of the human serum albumin, a CB3GA-Sepharose adsorbent was used on a pilot scale to produce 250 g of albumin on a 50-l column, giving a product with a purity of 98 to 100% at a yield of 82%.

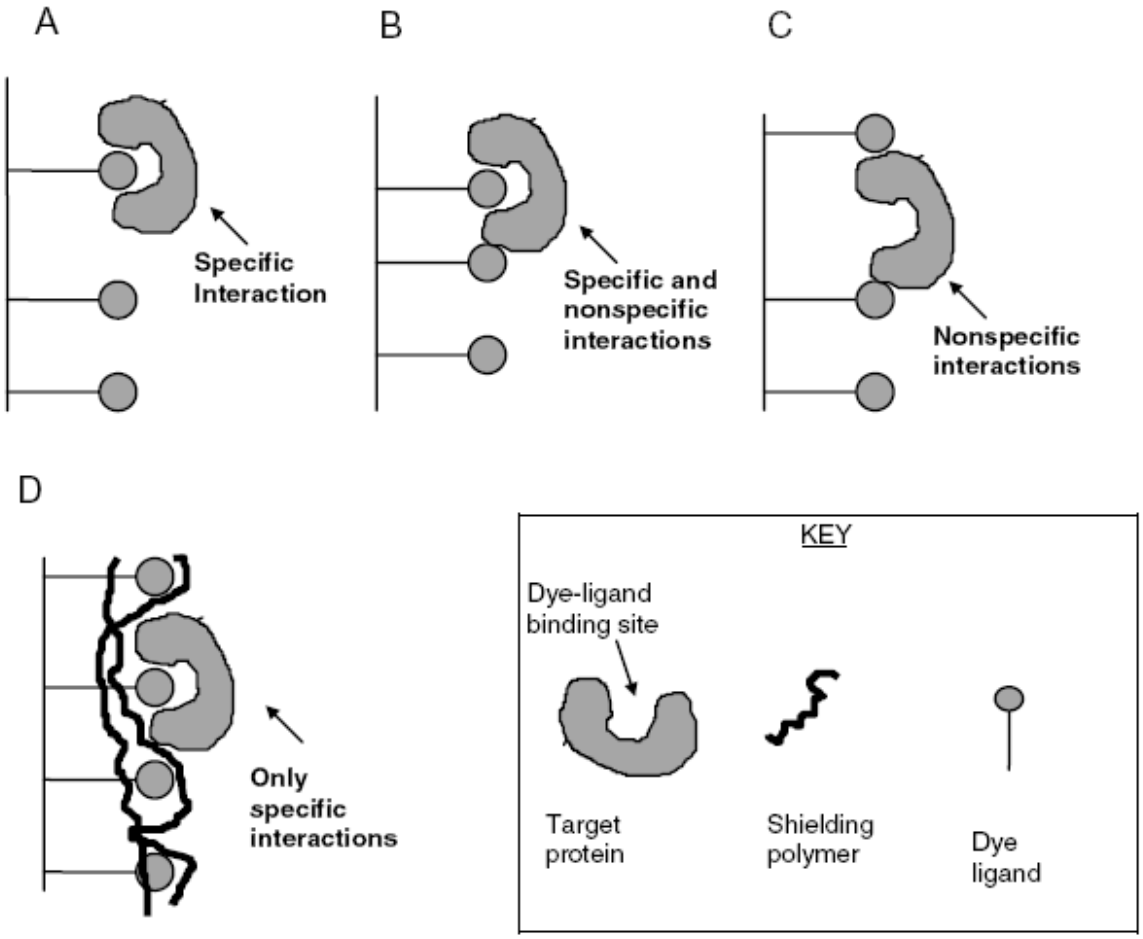

Figure 2.6. Polymer-shielded dye-affinity chromatography.

The long lifetime of dye-ligand adsorbents makes these attractive and economical for such purifications. Unfortunately, regulations dealing with the safety and toxicity issues that are associated with CB3GA have prevented albumin prepared by CB3GA adsorbents from being used in clinical applications. However, this type of albumin can be used as a component of cell culture media or as stabilizer for recombinant products (Bumouf and Radosevich, 2001).

Another application of dye-ligands has been in the removal of small hydrophobic molecules and ions from biological fluids using conventional affinity chromatography. For example, CB3GA coupled to poly(EGDMA-2-hydroxyethyl methacrylate) (pHEMA) microbeads was used to remove bilirubin from human plasma in a packed-bed system (Denizli, 1998). The same adsorbent was also used for the removal of Al^{3+} and Fe^{3+} from human plasma (Denizli, 1997; 1998;

Arıca, 1998). In addition, a dye-ligand column has been employed in the separation of G-DNA structures that are formed by guanosine-rich oligodeoxyribonucleotide. This particular separation was performed on a Reactive Green 19-agarose resin in the presence of Li^+ ions (Alberghina, 1999).

Recently, an affinity extraction with a reversed-micelle system was used in the extraction of lysozyme. The reversed micelle in this method was generated by using a CB3GA-lecithin conjugate in *n*-hexane and gave an overall recovery for lysozyme of 87% (Sun, 1998). This approach gave high selectivity, resulting from the presence of both biospecific and steric-hindrance effects, and it was found to be well suited for the purification of low molecular-weight proteins (Sun, 1998).

A future application for dye-ligands may be their use in the removal of toxic macromolecules from biological fluids, such as prion proteins, human immunodeficiency virus-1, or hepatitis B particles. Prion proteins have been shown to bind specifically to the azo dye Congo Red (Caspi, 1998). It is also known that immobilized CB3GA is able to adsorb envelope glycoproteins, such as the 140 kDa precursor and mature 120-kDa envelope glycoproteins from human immunodeficiency virus-1 (Hattori, 1997). In addition, it has been shown that this same dye can retain more than 99.5% of the hepatitis B particles from a human plasma sample (Brown and Combridge, 1986).

2.3. Molecular Imprinting

The structures, reactions and interactions of the molecular structures of living organisms are based on the ability of molecules to distinguish between the structures which they encounter. This ability is called the molecular recognition. Scientists have been trying to understand its underlying mechanism and thus to elucidate the interactions such as antibody-antigen, enzyme-substrate, hormone-receptor, DNA and RNA (Andersson, 1999). The ligand selectivity natures of protein and nucleic acid structures as well as their stability, pose a limit to their utility in abiotic environments. This has stimulated the development of synthetic recognition systems capable of displaying the same high selectivity and efficiency as their natural counterparts (Andersson, 1999). One synthetic approach to

molecular recognition that has been developed in the recent decades is the molecular imprinting whose concept is rather simple. Indeed, it relies upon the formation of complexes between a molecular template (the structure for which recognition is desired) and functionalized monomers, which are subsequently fixed throw a polymerisation reaction. Removal of the template species reveals “imprints” complementary in shape and functionality to the template (Figure 2.7) (Andersson, 1999).

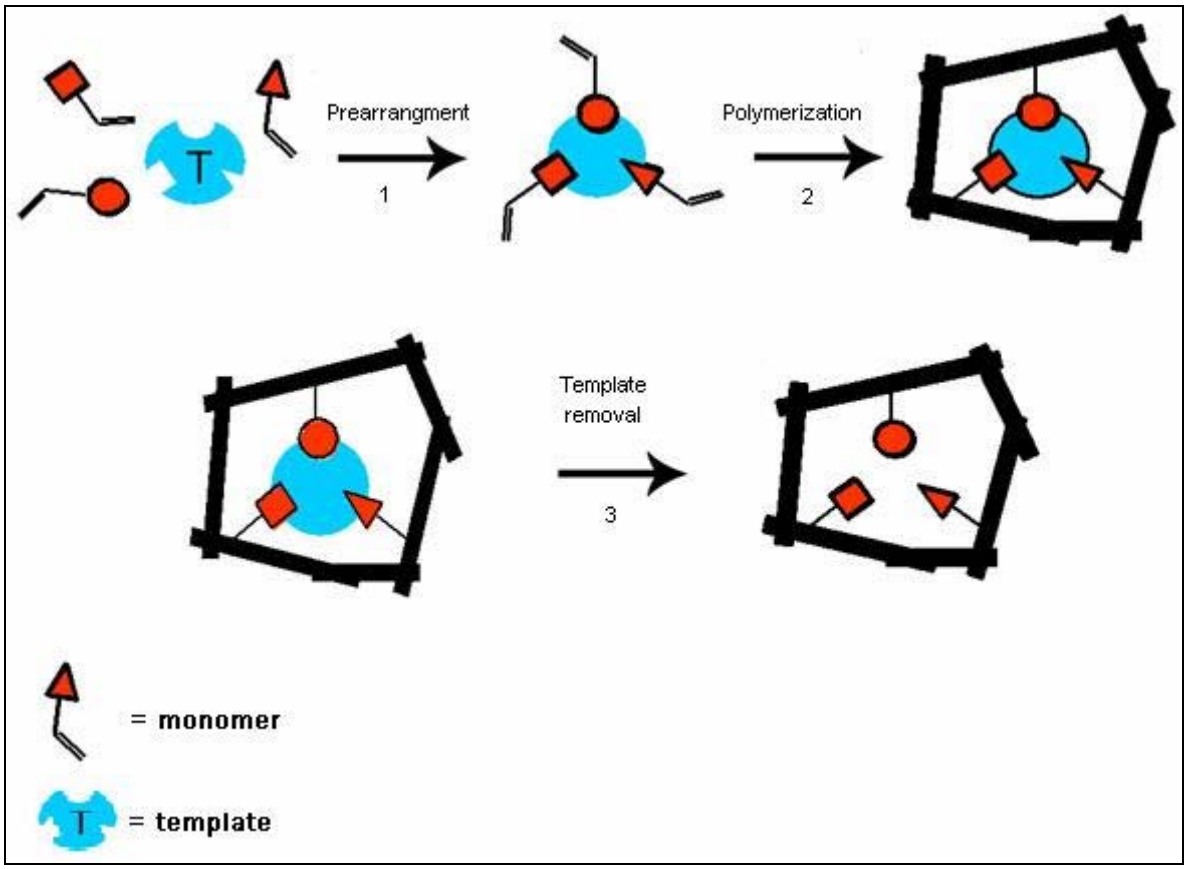

Figure 2.7. Schematic illustration of molecular imprinting principle: (1) preparation of covalent conjugate or noncovalent adduct between a functional monomer and a template molecule, (2) polymerisation of this monomertemplate conjugate and (3) removal of the template from the polymer.

In the first step, monomers, carrying suitable chemical functions, form a complex with the template through covalent or non-covalent interaction (Belmont, 2006). During the second step the polymer chains start to form, they are still flexible in the beginning, but as the polymerisation proceeds, they become cross-linked and the functional groups of the interacting monomers are held in place and topographically complementary to the template. In the third step, the templates are

removed from the polymer; binding sites complementary to the target molecule in size, shapes, and position of functional groups are left as cavities (Komiyama, 2003). Their evidence is preserved by the cross linked structure as a memory imprinted on the polymer which is now capable of selectively rebinding the target (or its analogue) (Komiyama, 2003). Thus, molecular imprinted polymers (MIP) possess two of the most important features of biological receptors: the ability to recognize and bind specific target molecules (Belmont, 2006). Their obtainment is easy and inexpensive and they can be easily adapted to different chemistry fields (i.e. chromatographic stationary phases, sensors, catalysis, immunoassays and adsorption). Accordingly, the use of MIP as selective sorbents seems extremely promising (Martin-Esteban, 2001).

2.3.1. Historical Perspective

The focus on molecular imprinting technique and its applications is relatively recent but the concept itself has a long history. The first recognized examples of molecular imprinting were achieved by the Soviet chemist Polyakov. He prepared rigid matrices made of silica by acidification of sodium silicate solutions followed by drying; the effects on the pore structure of the rigid matrix were studied by adding compounds such as benzene and toluene during the drying and then washing them off. In a published paper in 1931 it was demonstrated that under certain conditions the silica matrix was readsorbing slightly more of the different additive in whose presence it was prepared (Polyakov, 1931). Later, in 1942, Linus Pauling tried to prepare antibodies in vitro by non-covalent modification of serum globulins using different compounds as antigen templates: methylene blue, an arsenic acid derivative and a polysaccharide (Pauling, 1942). The results indicated that the renatured antibody could precipitate the template more efficiently than structurally related compounds; this apparent success led Pauling to apply the imprinting in an abiotic system, silica. These experiments used a similar method as that of Polyakov with the difference that the template was introduced prior to the polymerisation, whereas Polyakov introduced during the drying process. The results were clear: the silica prepared in the presence of any of these “pattern molecules”, bound the pattern molecule in preference to the others. Shortly after these results several research groups started to use this method. In 1955, Dickey,

Haldeman and Emmett, presented concurring and more detailed hypotheses to explain the observed template dependent selectivity of the silica (Dickey, 1955). This “footprint” theory was later supported by Beckett and Youssef with the most important findings being the recognition properties of the imprinted silica adversely dependent on the amount of remaining template (Beckett and Youssef, 1963). Moreover, Bartels used UV spectroscopy to demonstrate a specific pre-organization of silica acids around the template (1,10-phenantroline) in the polymerisation structure (Bartels, 1967). During all this period the main applications for the silica imprinting were as chromatographic stationary phases in column or thin layer format. Several other examples of practical uses with molecularly imprinted silica have been addressed, however the interest in silica experienced a decline by the end of 1960’s mostly due to limitations in stability and reproducibility of imprinted silica materials. The year of 1972 marked the start of molecular imprinting as we know it today, when the laboratories of Wulff (Wulff and Sarhan, 1972) and Klotz (Takagishi and Klotz, 1972) independently reported the preparation of organic polymers with predetermined ligand selectivities. Template molecules, or derivatives, which were present during polymerisation, were recognized by the resultant molecularly imprinted polymers (MIP). The groups of Wulff, Mosbach and Shea were the pioneers for the current molecular imprinting techniques. Klotz et al. reported that poly(ethyleneimine), cross-linked by disulfide bridges in the presence of methyl orange, exhibited enhanced adsorption capacity for this template in aqueous media as related to polymers cross-linked in the absence of template, whereas Wulff et al. reported chiral recognition of D-glyceric acid in a divinylbenzene polymer prepared in the presence of D-glyceric-p(vinylanilide)- 2,3-O-p(vinylphenylboronate), which was covalently incorporated in the polymer and subsequently hydrolyzed (Wulff, 1995). This was the first example of reversible covalent interactions as the basis for recognition; later on, many other MIP protocols on covalent imprinting were developed during the 1970’s and early 1980’s. The first steps on the non-covalent approach were taken by Arshady & Mosbach who prepared N-methyl-N,N-diallylamine (MDAA) MIP based on electrostatic prearrangement in water/DMF between two template dyes (rhodanile blue and safranine O) and the functional monomers N,N’-phenylenediacrylamide and 3,5 bis(acryloylamido) benzoic acid. Selectivity was demonstrated by batchwise ligand binding studies and chromatographic evaluations (Arshady and

Mosbach, 1981; Norrlow, 1984). This non-covalent approach was then refined by the use of acetonitrile as a polymerisation solvent and ethylene glycol dimethacrylate (EGDMA) as the cross-linker. These were important leading steps to the more versatile methodology employed in recent years. Extensive chromatographic investigations and direct physical studies of the pre-polymerisation mixture established the non-covalent approach as a general method for achieving pre determined recognition; it is still by far the most widely used approach. In parallel, the metal coordination approach was further developed by the groups of Fujii (Fujii, 1985), and Arnold (Dhal, 1991; 1992). During the past few years an exponential interest on the molecular imprinting was generated by the increase of studies based on systems similar to the one developed by the group of Mosbach, the general demonstrations of the versatility of the non-covalent approach, as well as the use of molecular imprinting in various applications. For example, the work published by Vlatakis et al., which involved the use of theophylline and diazepam MIP in an assay format, was the first demonstrating that MIP system may rival the selectivity of polyclonal antibodies (Vlatakis, 1993). This work received much attention and represents one of the most cited works in the area.

2.3.2. Approaches to Molecular Imprinting

Although the non-covalent imprinting is the most commonly used, there are many other approaches that can be differentiated by the polymer framework constituents (i.e. organic matrix/inorganic matrix) or by the interactions involved in the prearrangement and in the rebinding process (i.e. reversible covalent, metal ion coordination or non-covalent). Despite these distinctions many parallels may be drawn on aspects of molecular recognition and in the applications and methods for evaluation of the MIP (Andersson, 1999). Depending on the nature of the interactions between the monomers and the templates, they can be placed via a covalent linkage (in covalent imprinting), placed nearby through non-covalent interactions (in non-covalent imprinting) or by metal ion coordination. In either case, these bonds should be reversible in order to enable template extraction after polymerisation and rebinding of the target molecule (Komiyama, 2003).

2.3.2.1. Covalent Imprinting

In covalent imprinting, the monomers and the template are covalently linked during the polymerisation process. After the polymerisation, the template is removed from the polymeric matrix by chemical cleavage and during the rebinding process the same covalent bonds will be formed. These covalent linkages lead to a very stable and stoichiometric template-monomer or guestmonomer complex. The main disadvantages include a troublesome and less economical synthesis of the monomer-template complex, a possible diminution of the imprinting effect since the template removal step requires severe conditions, and a slow binding kinetics. This last disadvantage would be a serious problem if the polymer is to be used in rapid chromatography, columns for adsorption or in a biosensor (Table 2.2). Binding kinetics is thus an important factor to take into account when choosing the functional monomers which, with the limited choice of solvents and applications, are the main reasons why the covalent approach has played a small role in the molecular imprinting research (Belmont, 2006).

2.3.2.2. Non-covalent Imprinting

In non-covalent imprinting the functional monomers connect with the template by non-covalent interactions (ionic interactions, hydrogen bonds and hydrophobic interactions), for that reason the connection strength is weak (Komiyama, 2003). After polymerisation the template is removed from the polymer by a simple solvent extraction with an appropriate solvent. The rebinding to the polymer cavities by a guest molecule occurs based on the same non-covalent interactions. In general the non-covalent approach is less clear-cut (the monomer-template is labile and not strictly stoichiometric) (Komiyama, 2003). The interactions are weaker and habitually forbid the use of polar protic solvents, in particular water, which would interfere in complex formation (Belmont, 2006). The monomers are added in considerable excess in order to ensure an effective imprinting by a completely degree of complexation with the functional groups of the template. As a result, the functional groups in the polymer are not exclusively situated in the recognition sites, which inevitably lead to non specific binding (Komiyama, 2003). Despite these drawbacks, the non-covalent method has key advantages that led to an

advance in the field of molecular imprinting (Table 2.2) it is easier to attain and applicable to a wider spectrum of templates, which are simply removed from the polymer under very mild conditions as well as the target binding/release, avoiding the problem of slow binding kinetics (Komiyama, 2003). In biology, molecular recognition is mostly based on noncovalent interactions. Also the polymerisation method selected for this project is based on these connections. Mosbach and his co-workers were the first showing that non-covalent linkages between functional monomer and template work sufficiently for molecular imprinting (Arshady and Mosbach, 1981). For instance in the imprinting of methacrylic acid with theophylline (drug), a non-covalent monomer-template adduct was formed through hydrogen bonding and electrostatic interaction (Arshady and Mosbach, 1981). Indeed, imprints against molecules such as drugs, hormones, pesticides, amino acids, peptides, proteins, co-enzymes and nucleotide bases have been generated in this way, making this approach the most common applied on molecular imprinting in the later years.

Table 2.2. Advantages and disadvantages of the covalent and the non-covalent imprinting.

	Covalent	Non-covalent
Monomer- template stability	+	-
Monomer-template stoichiometry	+	-
Polymerisation conditions	-	+
Removal of the template	-	+
Guest-binding and guest-release kinetics	-	+
Economical	-	+

2.3.2.3. Other Approaches

As an alternative to use covalent imprinting to solve the above-mentioned problems is the use of metal containing monomers. The complex used for imprinting generally consists of polymerizable ligand(s) to complex the metal ion (generally a transition metal ion) which in turn coordinates to the template. These coordination bonds are often stable in polar solvents including water, which is a

substantial advantage when using biomacromolecules as templates (Belmont, 2006). Another advantage is the possibility of using stoichiometric template monomer ratios and increasing the binding site homogeneity and selectivity of the polymer (Belmont, 2006). This approach was first reported by Fujii et al., in the imprinting of amino acids (Fujii, 1985). The group of Arnold investigated different metals and polymerizable ligands for the imprinting of templates including bis-imidazoles in organic matrixes and on solid supports (Mallik, 1994). Recently it was shown that imprinted polymers prepared for cholesterol using Cu^{2+} acrylate, in place of acrylic acid, resulted in MIP with higher capacities (Sreenivasan, 2001) and a ferric acrylate-containing MIP for cholesterol has also been reported (Sreenivasan and Sivakumar, 2003). Another approach is the semi-covalent imprinting introduced by Whitcombe and co-workers in 1995 (Whitcombe, 1995), where the advantage of covalent imprinting (clear-cut nature) and that of non-covalent imprinting (fast guest binding) were combined to address the problem of slow binding kinetics. In this hybrid method the polymers were prepared as in covalent imprinting whereas the guest binding employed non covalent interactions. This was achieved by using carbonate esters which after hydrolysis leave a phenol residue in the matrix capable of rebinding the template. Molecular imprinting by the use of inorganic materials, such as sol-gel made of silica or TiO_2 were also applied. Some bulk materials have been effectively imprinted this way using the noncovalent (Glad, 1985; Dai, 1997) or covalent (Katz, 2000) approaches or films (Makote, 1998). The resultant imprint left in the gel by the template has been used with a wide range of compounds such as ion (Dai, 1997), organic molecules (Makote, 1998) and enzyme recognition (Glad, 1985), or even as shape-selective catalysts (Katz, 2000). TiO_2 gel works as an organic receptor since a liberated hydroxyl group (Ti-OH) in the gel can be a binding site for t he target molecule (Ichinose, 2002; Lee, 1998).

2.3.3. Reagents and Experimental Procedures

In general, the chemicals required for a standard imprinting process are (1) functional monomers, (2) templates, (3) crosslinking agents, (4) solvents for the polymerisation and (5) solvents (or bond-cleaving agents) to remove the templates from the polymers. They are the key elements and their proper selection will

ensure that polymers with appropriate properties are obtained to a particular application (Martin-Esteban, 2001). All kinds of polymerisation (radial, anion, cation and condensation) can be employed for molecular imprinting (Komiyama, 2003).

2.3.3.1. Template and Monomers

For a good specificity and selectivity of the polymer, the cavities formed during the polymerisation should retain their conformation even after the template removal and should possess a good accessibility for later rebinding of the target molecule (Belmont, 2006). The first step in the preparation of imprinted polymers consists of an arrangement with the template and the monomer(s) in a solvent. The selection of the monomer is dependent upon the template characteristics. The template has to contain in its structure functional chemical groups capable of interacting with the monomer(s) with sufficient strength to form a stable complex. Until now, the most frequently employed monomers have been acrylic or vinylic. There is a wide range of monomers available for non-covalent imprinting that can be basic (vinylpyridines) or acid (Methacrylic acid (MAA)), hydrogen bonding (acrylamides), hydrophobic (styrene) and others. With MAA the used templates have been mainly restricted to those able to interact by hydrogen bonding (Esteban, 2001). In fact, steroids such as Progesterone, Testosterone, β-Estradiol and Estrone were used as templates for MAA-containing imprinted polymers (Rachkov, 1998). This study showed that molecules with a relatively rigid structure and the OH group at the C-17 position (e.g. Testosterone, 17-β-estradiol) are better succeed as templates for MAA. Also 4-vinylpyridine was successfully used for 17β-estadiol as template (Le Noir, 2006; 2007a; 2007b). During the recent years, other polymers like polyphenols and polyurethanes (Belmont, 2006), and commercially available polymers such as polyvinyl chloride (PVC), polysulfone, polystyrene and polyacrylonitrile (Kobayashi, 2002) have been studied into specific applications or for being easier to synthesize the imprinted polymers in a desired shape. Resembling this previous study (Kobayashi, 2002) a commercial polymer was used in this work. Concerning the relative amounts of the template-monomers, it is important to point out that since the template–monomer interactions are governed by an equilibrium process, a high amount of monomer is used in order to assure

the equilibrium to form the template–monomer complex. The main disadvantage is that the excess of free monomers leads to the formation of non-specific binding sites. The solvent used during the pre-polymerisation step is also of prime importance since it also has a direct influence on the strength of the template–monomer interaction. Finally, the template size and shape has a strong influence on the selectivity of the obtained polymers. In general, even small structural differences near the functional group responsible for the interaction with the monomer can lead to the formation of highly selective polymers preventing the binding of structurally related compounds. In some cases, however, the absence or presence of groups far from the functional groups has allowed formation of highly selective imprinted polymers (Martin-Esteban, 2001).

2.3.3.2. Solvents

Apart from its influence on the template–monomer strength interactions mentioned previously, the solvent used in the pre-polymerisation structure plays an important role in the morphology of the obtained polymer in terms of specific surface area and pore diameter (Martin-Esteban, 2001). Generally, a low surface area and low porosity leads to low template recognition in the subsequent rebinding experiments owing to slow diffusion of the target molecule through the porous structure. It is quite difficult to predict in advance the right solvent for the successful production of polymer because even when using a solvent capable of stabilizing the template–monomer complex during the prepolymerisation step it is possible to obtain a polymer with an inadequate morphology, which decreases the template recognition (Martin-Esteban, 2001). Solvents with a low dielectric constant (poor solvents), such as chloroform and toluene, are thus preferred to good ones since they offer an adequate medium to stabilize hydrogen bonding and/or electrostatic interactions between monomer(s) and templates leading to precipitation of growing chains during the polymerisation process (Martin-Esteban, 2001). When solvents with higher dielectric constants (ex. acetonitrile) were used, the obtained polymers usually showed a lower affinity to rebind the template. Protic solvents, such as water and methanol, are not recommended since they not only hinder polymerisation but also disrupt the template–monomer hydrogen bonding interactions (Martin- Esteban, 2001). The solvent used in this work for the

pre-polymerisation mixture was dimethyl acetamide (DMAc) since it has been reported as a good solvent for the polymer chosen (Zhao, 2004). When the molecular imprinted polymer is prepared it is necessary to remove the template in order to obtain free binding sites. This step is usually carried out by washing the polymer repeatedly with a solvent capable of disrupting the template–monomer interactions or by Soxhlet Extraction.

2.3.3.3. Crosslinking Agents

In order to guarantee the stability of the template–monomer complex during polymerisation and to increase polymer porosity, a high degree of cross-linking is necessary. The cross-linkers make the imprinted polymers insoluble in solvents and facilitate their practical applications (Komiyama, 2003). The mole ratio of cross linking agent to functional monomer is also important. The presence of a cross-linker not only preserves the binding sites but also has a direct influence on the physical and chemical properties of the polymeric matrix. If the ratios are too small, the guest-binding sites are located so closely to each other that they cannot work independently (Komiyama, 2003). Ethylene glycol dimethacrylate (EGDMA) is the cross-linker often used in methacrylate-based systems, since it provides mechanical and thermal stability, good wettability and rapid mass transfer. For instance, it has been reported that at least 50% of the total monomer in a MAA-ethylene glycol dimethacrylate (EGDMA) system has to be EGDMA, otherwise no recognition can take place (Sellergren, 1989).

2.3.4. Characterization of Molecularly Imprinted Polymers

The imprinting concept may suggest a homogeneous binding site distribution, however experimental work has demonstrated that a heterogeneous distribution is the most common situation (Garcia-Calzon and Diaz-Garcia, 2007). Several reasons have been suggested for the heterogeneous binding sites in MIPs: amorphous nature of the polymer and the low number of templated sites; dissociation of the template-functional monomer aggregate in solution; clusters formation by interaction of the templates during the recognition process and collapse the binding sites by template solvent extraction (Garcia-Calzon and Diaz

Garcia, 2007). Therefore it is of great importance to characterize the binding sites of the MIPs. For instance, to characterize the shape by means of the specific surface area, specific pore volume and pore size distribution, a BET method combined with nitrogen adsorption can be used (Le Noir, 2007a;b). To characterize the rebinding properties and selectivity of MIPs, experimental methods such as batch rebinding approaches and frontal chromatography can be applied (Garcia-Calzon and Diaz-Garcia, 2007). Another option is to use radiometric assays (Le Noir, 2006, 2007a;b). A more quantitative approach to characterize the imprinted polymer heterogeneity includes analytical and numerical methods used for calculating the adsorption isotherms and the adsorption energy distribution. During the last 5 years, several models have been proposed to describe the heterogeneity of binding sites in MIPs making use of this methods (Garcia-Calzon and Diaz-Garcia, 2007).

2.3.5. Applications of Molecular Imprinted Polymers

2.3.5.1. Solid Phase Extraction

Solid phase extraction (SPE) consists of the selective pre-concentration (enrichment) of a compound to be analysed on a stationary phase, followed by elution and collection of the fractions containing the analyte. These fractions are then analyzed by chromatography in order to quantify their content. This pre concentration step allows analysis of samples with very low concentrations. The first indication of the MIP potential technique in SPE was given by Sellergren with pentamidine MIP (Sellergren, 1994). The fact that not all the template can be extracted after MIP preparation is a potential problem for application of MIP as solid-phase extraction materials. Several reports indicate that residues of template molecules interfere with the analyte response (Andersson, 1999). To solve this problem, the use of a “dummy” template can be an alternative (Matsui, 2000). Another limiting aspect relates to the extraction step, where the proper choice of extraction solvent is essential for the degree of preconcentration. For instance, Mullett and Lai, (1998) demonstrated that a small pulse (20 µl) of the appropriate solvent may be used to disrupt the electrostatic interactions between the MIP and the template. Despite of these drawbacks, the use of MIP in SPE matrices

appears as one of the most promising application areas for molecular imprinting. For example, a non-covalent molecularly imprinted polymer (MIP) of cholesterol, prepared by UV initiated polymerisation, was used as SPE sorbent for direct extraction of cholesterol from different biological samples (Shi, 2006). Under the optimal conditions, high recoveries of spiked human serum (91.1%), yolk (80.4%), cow milk (86.6%), shrimp (78.2%), pork (81.4%) and beef (80.1%) were obtained (Shi, 2006). Another example is the MIP prepared with caffeine as template, by thermal polymerisation (60°C) (Theodoridis, 2002). This MIP was used as a SPE sorbent for selective trapping and pre-concentration of caffeine. Recoveries of 81.0, 83.4 and 82.6% were obtained from two beverages extracts and spiked human plasma, respectively (Theodoridis, 2002). Even more recently, MIP solid phases for extraction of cocaine metabolites directly from water were designed by Zurutuza and co-workers by using a synthetic analogue of benzoylecgonine as the template. Successfully detection of clinically relevant concentrations (in the µg/ml range) were reported (Zurutuza, 2005). Presently, most of the methods developed are based on polymers prepared by bulk polymerisation. In the traditional bulk polymerisation the polymer is ground and sieved until the desired particle size (Theodoridis, 2002; Zurutuza, 2005; Shi, 2006). This leads to heterogeneous particles which limits scale-up and commercialization of SPE methods. New polymerisation strategies are now being developed for the obtainment of homogenous imprinted particles of the desired size and shape. In addition, the preparation of polymers with capacity to recognize analytes in aqueous samples has to be improved for different types of molecules with environmental impact.

2.3.5.2. Liquid Chromatography and Chromatography Based Methods

MIP have been employed as stationary phases for column chromatography ever since the development of the first truly functional silica-derived imprinted polymer systems. This method is very common to analyze the selectivity of MIP systems. Nevertheless these MIP - stationary phases have not yet been developed with the aim of future commercial applications. Some examples of MIP-based stationary phases for HPLC and related chromatographic techniques are presented here. For example, Kempe's group described that S-naproxen MIP utilized as HPLC stationary phase were giving excellent results comparable with direct resolution of

naxopren on conventional chiral stationary phases (Kempe and Mosbach, 1994). These authors verified that this new type of stationary phase was able to distinguish between naxopren and related compounds such as ibuprofen and ketoprofen. This consisted in a significant improvement in comparison with conventional stationary phases since none of these two molecules could be resolved. The interest in developing imprinted polymer matrices selective for biologically active substances has also induced the production of a significant number of chromatographic stationary phases. Many of these studies were carried out to produce analytical procedures for substances of clinical or environmental concern. Synthetic and endogenous substances have been used as templates: a number of antibiotics such as vancomycin, cefazolin and phenethicillin were imprinted on cyclodextrin molecules (Asanuma, 2001); the anticancer drugs such as piritrexim (Lai, 2003), trimethoprim (Lai, 2002a), harmine and harmaline (Xie, 2002) and also β-blockers (Haginaka and Sanbe, 2003a), chloramphenicol (Suarez-Rodriguez and Diaz-Garcia, 2001), and nicotinamide (Fu, 2001). For example, cortisol (Baggiani, 2000), estradiol (Haginaka, 2001), and cholesterol (Hwang and Lee, 2002) are also interesting templates for molecular imprinting in chromatography approaches, both from a fundamental perspective and on account of their biological activities, because of the rigidity of their steroid ring system and their inherently well-defined placement of functionality. Estrogenic substance imprinted polymers have also been used for simulated drug screening (Ye, 2001). Finally, both the D1 protein binding herbicide atrazine (Matsui, 1995) and bisphenol A (Haginaka and Sanbe, 2003b) have been used to develop chromatographic stationary phases selective for these substances, on account of interest in their hazardous influence on the environment. MIP-based chromatographic stationary phases have and might continue to play a pivotal role in the development of our understanding of the molecular level events underlying ligand—molecularly imprinted polymer recognition. Furthermore, MIP still offers potential for the development of tailormade HPLC stationary phases for specific separation problems.

2.3.5.3. Equlibrium Ligand-Binding Assays – Antibody and Receptor Mimics

MIP can also serve as artificial antibodies and be used as recognition elements in immunoassays (Belmont, 2006). It was the published work by Mosbach et al. on radioimmunoassays for theophylline and diapezam (Vlatakis, 1993) that opened a new application field and an exponential rise in the number of publications on MIP per year. More recently, such assays have been done in competitive mode using radioligands, enzymes or fluorophores as labels for detection. An example using fluorophores is the work developed by Surugiu, (2001) who developed competitive enzyme immunoassays based on chemiluminescence imaging and polymer microspheres imprinted against the herbicide 2,4-Dichlorophenoxyacetic acid (2,4-D) as recognition element. With the 2,4-D imprinted polymer microspheres detection limits of 34 nM were obtained in buffer with a useful concentration range from 68 nM to 680 µM. These range was only slightly narrower than comparable antibody-based assays, which had, however lower detection limits. Cross-reactivities of related compounds were also studied and results were similar to those reported for monoclonal antibodies raised against 2,4-D, and sometimes even better (Surugiu, 2001). From this example we can conclude that the use of antibody and receptor binding mimics is of particular interest, especially for small, non-immunogenic molecules where it is impossible to raise antibodies without conjugating the antigen to a carrier protein, or for immunosuppressive drugs. Further advantages of such systems are their low cost and the elimination of the need for laboratory animals in antibody production.

2.3.5.4. Sensor and Membrane Systems

The development of sensor systems is a demanding task. Ideally, the sensing tools should be selective, provide a rapid response, have a detection limit as low as possible and be stable for a long time and under different conditions. The first steps in the investigation of several ways to develop MIP sensors were done by the group of Mosbach however the sensor response times were generally too long (Hedborg, 1993). In recent years much effort has been dedicated to find general signalling mechanisms for MIP sensors (Andersson, 1999). The incorporation of signalling elements directly into the polymer structure is an attractive approach

which has a lot of attention in recent times. The most successful example are the luminescent sensor systems developed for detection of the chemical warfare nerve gases Sarin and Soman via imprinting of the Soman hydrolysis product pinaconyl methyl phosphonate (PMP) (Jenkins, 1997). A portable model of the sensor had been developed and characteristics of this system were excellent as compared to previous works (Jenkins, 1997). MIP membranes can also be used as selective adsorbents for solid-phase extra tion and thin films of imprinted material deposited on solid surfaces are intended to act as sensing elements (Andersson, 1999). For instance, a recent study for MIP membranes were SPE is applied was made by Ulbricht and Malaisamy; it consisted in the preparation of porous membranes by immersion precipitation phase inversion of cellulose acetate-sulfonated polysulfone (CA-SPS) blends with different compositions with the fluorescent dye Rhodamine B (RhB) as template (Ulbricht and Malaisamy, 2005). The MIP were analysed by scanning force microscopy (SFM), scanning electron microscopy (SEM) and gas adsorption isotherm method (BET) and binding tests obtained by SPE gave very positive results for the CA-SPS in a 95:5 blend.

2.3.5.5. Synthesis and Catalysis

The exact location and orientation of functional groups in the binding sites of imprinted polymers has also allowed for their application as microreactors for synthesis or catalysis (Belmont, 2006). In the case of synthesis the geometry of the binding sites is used to influence the stereochemical course of a reaction by maintaining the reactants in a certain position. This principle was demonstrated when producing specific enantiomeric cyclopropane derivatives (Shea, 1980): the hydroxyl groups in the binding sites of a MIP imprinted with cyclobutane dicarboxylic ester were esterified with fumaryl chloride. Then, after alkylation, they generated the desired cyclopropane derivative. Binding sites can be also used for catalysis in the way that the template can be a transition state or coenzyme analogues. After the template removal one or more guest molecules are introduced in the sites. The interaction between these molecules and the functional groups located in the three dimensional scaffold permits the precise arrangement of chemical functionality between the guest molecule and the

functional groups and to obtain defined reaction mechanisms. Examples for catalysis are carbon-carbon bond formation (Matsui, 1996), elimination (Beach and Shea, 1994) or metal mediated reactions using MIP as enzyme mimics or coenzymes (Gamez, 1995). The use of MIP as enzyme mimics is commonly regarded as the most challenging with respect to applications in chemical synthesis, but also other applications for MIP in synthetic chemistry, like equilibrium shifting (Ye, 1999) or protecting groups (Alexander, 1999), have been focus of interest.

2.4. Cryogels

At present, polymeric gels have applications in many different areas of biotechnology including use as chromatographic materials, carriers for the immobilization of molecules and cells, matrices for electrophoresis and immunodiffusion, and as a gel basis for solid cultural media. A variety of problems associated with using polymer gels, as well as the broad range of biological objects encountered, lead to new, often contradictory, requirements for the gels. These requirements stimulate the development and commercialization of new gel materials for biological applications. One of the new types of polymer gels with considerable potential in biotechnology is ‘cryogels’ (from the Greek krios (kryos) meaning frost or ice) (Lozinsky, 2002). Cryogels are formed as a result of cryogenic treatment (freezing, storage in the frozen state for a definite time and defrosting) of low- or highmolecular- weight precursors, as well as colloid systems – all capable of gelling. Cryogels were first reported ~40 years ago and their properties, which are rather unusual for polymer gels, soon attracted attention. The biomedical and biotechnological potential of these materials has now been recognized (Lozinsky, 1998; 2001; 2002; Nambu, 1990; Kaetsu, 1993; Suzuki and Hirasa, 1993, Lozinsky and Plieva, 1998; Hassan and Peppas, 2000).

2.4.1. Gels and Cryogels – What is the difference?

Polymeric materials combined under the name ‘gels’ are the systems ‘polymer – immobilized (solvate) solvent’, in which macromolecules connected via non-fluctuating bonds form a 3D-network (i.e. via the bonds that, to a large extent,

remain unchanged with time). The gel morphology (homo- or heterophase) is determined by the method of gel preparation, and the nature of the bonds is determined by the chemical structure of the polymers. The role of the solvent immobilized within a 3D-polymer network in gels is crucial because the solvent does not allow the formation of a compact polymer mass, preventing the collapse of the system. Gels are physical objects that can withstand considerable reversible deformation without flowing or destruction. According to the nature of intermolecular bonds in the junctions of polymer network, gels can be divided into two groups: chemical and physical gels. A more detailed classification of gels, which reflects the particular process resulting in gel-formation, is presented in Table 2.3. Given that the biotechnological applications of cryogels are discussed, they deserve a more detailed consideration, especially regarding the properties that distinguish them from other gel types.

The formation of cryogels is schematically presented in Figure 2.8, in which the features of cryotropic gelation processes are also listed. Cryotropic gelation produces polymeric materials with essentially different morphology compared with gels obtained in non-frozen systems. Cryogels could be of any chemical type – covalent, ionic or non-covalent. Obviously, only the precursors of heat induced (thermotropic) gels cannot be used for the preparation of cryogels.

With some exceptions, freeze-dried polymeric materials soaked in solvent (in which the polymer swells without dissolution) can be considered as materials with macro and microstructure similar to that of cryogels. The solvent freezing followed by the sublimation of solvent crystals (ice in case of aqueous systems) forms a system of interconnected pores in the polymeric material. However, no gel formation takes place per se in unfrozen liquid microphase (Figure 2.8, unfrozen liquid microphase, UFLMP). Freeze-dried materials can be produced only as relatively thin objects, for example, films, plates or small beads. The production of freeze-dried cylinders or thick blocks is impractical from a technical point of view. On the contrary, cryogels can be formed in any desirable shape, for example, blocks, cylinders, tubes, granules and disks. Moreover, the production of cryogels is simpler than production of freezedried materials because solvent removal under reduced pressure is not necessary.

Table 2.3. Classification of polymeric gels and gel formation processes.

Type	Physicochemical causes of gel-formation	Examples	Comments
		Polymeric gels	
Chemotropic gels	Intermolecular chemical bonds resulting in 3D covalent network	– Polyacrylamide gels; – Ion-exchange resins based on polystyrene or polyacrylate matrices; – Cross-linked dextran gels known as Sephadexes, etc.	This is a large group of gels; the gel-formation occurs during branched polymerization of monomeric precursors, or during covalent cross-linking of polymeric precursors. The gels are widely used in biotechnology.
Ionotropic gels	Ion-exchange reactions giving rise to stable intermolecular ionic (salt) bonds	– Gels based on polyelectrolyte complexes like alginate-polylysine or chitosan-polyphosphate mixed matrices, etc.	These gels are stable in media of definite composition but could easily be dissolved by changing, for example, the pH or ionic composition in outer liquid medium. The gels are used as carriers of immobilized (encapsulated) microbial, plant and animal cells.
Chelatotropic gels	Chelating reactions giving rise to stable intermolecular coordination bonds	Gels formed on addition of multivalent strongly coordinating metal ions (e.g., Cu(II) or Co(II)) to chitosan solutions or Cr(III) ions to carboxymethyl cellulose solution or alginate gels cross-linked by, for example, calcium ions.	Ca-alginategels are used for cell immobilization, other chelatropic gels have not yet found biotechnological applications.
Solvotropic (or solvatotropic) gels	Gelation due to the changes of solvent composition	The gels formed as a result of so-called coacervation phenomenon; such type of gelation is an intermediate stage in the processes of wet-formation of films and fibers, for example, from cellulose nitrates or cellulose acetates.	Gels are formed, when a non-solvent is added to the polymer solution thus reducing the polymer affinity to the medium and promoting non-covalent polymer–polymer interactions. No documented biotechnological application.
Thermotropic gels	Gelation caused by heating of an initial polymer system	– Gels of hydrophobically modified hydroxyethyl cellulose; – Ovalbumin and egg white gels.	Intermolecular hydrophobic interactions have a significant role in the gel-formation.
Psychrotropic (from ψυχρα – psychria – chill) gels	Gelation caused by chilling (no freezing) of initial polymer system	– Gelatine gels; – Starch gels; – Agarose and agar–agar gels; – Carrageenan gels.	Psychrotropic gels are well known; they are related to the physical ones. The gels are widely used in biotechnology as solid media for cell cultivation, as chromatographic materials or as electrophoresis matrices.
Cryotropic (from κρυοσ – kryos – frost, ice) gels (**cryogels**)	Gelation induced by freezing of an initial system.		

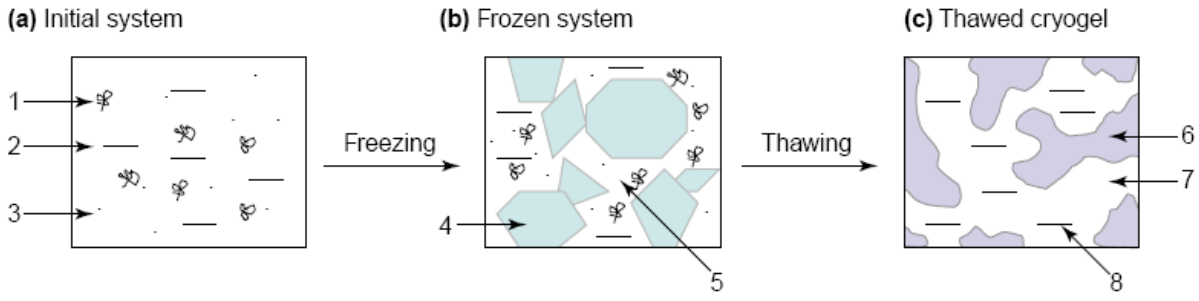

Figure 2.8. Scheme of formation of macroporous gels. (1) macromolecules in a solution; (2) solvent; (3) low-molecular solutes; (4) polycrystals of frozen solvent; (5) unfrozen liquid microphase; (6) polymeric framework of a cryogel; (7) macropores; (8) solvent.

A system of large interconnected pores is a main characteristic feature of cryogels; some cryogels possess spongy morphology. The pore system in such sponge-like gels ensures unhindered convectional transport of solutes within the cryogels, contrary to diffusion of solutes in traditional homophase gels.

The size of macropores within cryogels varies from tens or even hundreds to only a few micrometers. The interconnected system of large pores makes various cryogels promising materials for the production of new chromatographic matrices tailormade for the separation of biological nano- and microparticles (plasmids, viruses, cell organelles and even intact cells), and also for the implementation as carriers for immobilization of molecules and cells.

2.4.2. Cryogels in Bioseparation

A crucial element of modern process biotechnology is the separation and purification of the target product from a fermentation broth or cell rupture supernatant. Chromatography, both analytical and large-scale, is the predominant technology in downstream separations. Traditional packed-bed chromatography with immobile stationary phase, despite its elegance and high resolving power, has a major limitation: incapability of processing particulate-containing fluids, for example, cell suspensions or non-clarified crude cell homogenates. Particulate material is trapped between the beads of the chromatographic carrier resulting in increased flow resistance of the column and complete blockage of the flow. To address this drawback, expanded-bed chromatography has been proposed (Bioseparation, 1999). However, despite all its advantages, expanded bed chromatography requires a special type of columns and equipment and cannot be fitted in traditional packed-bed chromatographic systems. It is attractive to have a packed-bed chromatographic carrier with pores large enough to accommodate cell debris and even the whole cells without being blocked. The porosity of cryogels makes them appropriate candidates as the basis for such supermacroporous chromatographic materials.

Owing to supermacroporosity and interconnected pore-structure, such a chromatographic matrix has a very low flow resistance. Water passes freely

through the column at linear flow rate (volumetric flow rate divided by cross-section area of the column) of ~750–2000 cm/h at a pressure of ~0.01 MPa. For comparison, HPLC operates at flow rates of 300–1700 cm/h at excessive pressures of 2–10 Mpa (Arvidsson, 2003) and expanded bed chromatography at flow rates of 200–400 cm/h at excessive pressure ~0.01 MPa (Bioseparation 1999). Thus, it is reasonable to assume that continuous supermacroporous beds produced by the cryotropic gelation would allow chromatographic process at flow rates comparable with those in HPLC and exceeding those used in expanded bed chromatography, while using only minimal pressures typical for low-pressure protein chromatography. Owing to the large pore size in such cryogels, crude homogenate can be processed directly with no need for the clarification.

Owing to the low diffusivity of nanoparticles, and even more so for cells, an efficient convectional transport within the pores of the matrix is needed for chromatographic separation of these objects within a reasonable time. Pore size in traditional chromatographic adsorbents is usually so that 95% of convective flow takes place in the liquid in between the beads of the chromatographic matrix. Even in the ideal case of most densely packed spheres, the interparticle volume is ~27% of the total column volume – in practice it is higher owing to the irregularities of size and shape of the beads. To improve the convectional transport, the columns with large pore size, as well as minimal dead volume, are required. The enforced convectional transport is realized in monolithic columns (Josic, 2001; Tennikova and Freitag, 2000; Rodriguez, 1997).

Extensive experience of working with individual biomolecules has been based on the existence of highly efficient techniques for isolation and purification of molecular entities with molecular weights $<10^6$ Da. However, the purification of objects, often combined under the name of biological ‘nanoparticles’ (such as plasmids, cell organelles, viruses, protein inclusion bodies and macromolecular assemblies) still remain a challenge. Large particle sizes (20–300 nm), low diffusion rates and complex molecular surfaces distinguish such objects from soluble macromolecules (commonly <10 nm).

Macroporous inorganic chromatographic matrices, similar to porous glasses, seem to meet these requirements. They are available with a variety of pore sizes in the micrometer range, mechanically stable and sustain thermal sterilization. Although the use of these matrices for virus-specific immunosorbents has been reported (Nijayou and Quash, 1991), the brittleness, pronounced non-specific sorption and chemical instability in alkaline media limit their application. The larger the virus particles, the more pronounced the differences in capacities between Sepharose 4B and cryogel-based immunosorbent Thus, cryogels present a very interesting chromatographic material allowing the direct separation of proteins from unprocessed crude extracts or even from fermentation broth in the case of extracellulary expressed proteins. Cryogel based chromatographic materials open a whole new area of bioseparation, in which bioparticles, similar to viruses, microbial cells and even mammalian cells, are isolated and separated in chromatographic mode.

2.4.3. Cryogel Matrices for Immobilization of Biopolymers

It is evident that the use of cryogels as matrices of immobilized biopolymers (enzymes, polysaccharides, nucleic acids) is reasonable in cases where unique properties of cryogels give better results than traditional gel carriers. For instance, the biocatalyst produced by the immobilization of enzymes in the macropores of cryogels allows processing of macromolecular substrates because they diffuse undisturbed in the macropores (Kokufuta and Jinbo, 1992; Hayashi, 1993; Lozinsky, 1995; Kumakura, 1997). Supermacroporous continuous beds, such as cryogel columns developed for the separation of bioparticles, are perfectly suited for the plug-flow bioreactors. The ability of macroporous PVA cryogels to retain water strongly turned out to be useful for the immobilized biocatalysts functioning in non-aqueous media. The cryogel matrix provides the water needed for enzyme to catalyze the reaction in organic media (Belokon, 2000; Plieva, 2000; Bacheva, 2001; Filippova, 2001).

An interesting, although as yet practically unexplored, area is the use of cryogels produced from stimulus responsive polymers. These gels change drastically the swelling degree in response to external stimuli such as temperature, pH, ionic

strength and the presence of certain chemicals (Galaev and Mattiasson, 1999). The activity of enzymes immobilized in stimulus responsive gels depends on the swelling state of the matrix and hence responds to the stimuli changing the swelling degree of the gel (Chen 2002). The rate of the response decreases with increase in gel size owing to the increased distance for water transport into or out of the gel, thus limiting the application of such systems. Thin walls represent the gel phase in cryogels, whereas most of the total volume is occupied by the interconnected system of large pores. Therefore, the transport of water in stimulus-responsive cryogel will proceed within thin walls of the gel phase, whereas in the pores water transport proceeds unhindered. Hence, stimulus-responsive cryogels respond much faster to the stimuli than ordinary gels (Lozinsky, 1997). Therefore, the use of enzymes immobilized in stimuli-responsive cryogels is promising in cases where a fast response of the system is crucial.

Given that the walls of macropores in cryogels consist of highly concentrated microporous gel (Lozinsky, 2002), the diffusion of macromolecules in the pore walls is limited, if at all possible. The biopolymers could be immobilized in cryogels either via entrapment within the walls or via the attachment to the inner surface of the macropores. The former example is the immobilisation in spongy cryogels produced by the radiation cryopolymerisation of certain acrylate monomers in the presence of biopolymers to be entrapped (Kaetsu, 1993; Kumakura, 1997; 2001; Sutani, 2001). The enzymes immobilized in this way are separated from the outer medium by a dense polymer network and hence are accessible only for low molecular weight substrates. However, the diffusion time of the substrates in pore walls is short owing to the small width of the walls.

2.4.4. Cryogels as Carriers for Cell Immobilization

Suitable physicochemical properties and specific porosity of various cryogels are attractive for their implementation as carriers for cell immobilization. Cell immobilization using cryogel-type carriers, analogous to the immobilization of biopolymers, could be accomplished either via attachment (covalent or adsorption) or entrapment techniques. In the former case, supermacroporous matrices are used, for instance, for chemical coupling of E. coli cells with aldehyde derivative of

cryoPAAG (Lusta, 1988). When immobilizing cells via the entrapment approach, there are two opportunities depending on the type of carrier: entrapment of cells within thin pore walls of supermacroporous cryogel and cell entrapment inside the macropores in cryogels such as cryoPVAG.

For cell entrapment in pore walls of spongy cryogels, a biomass (microbes, spores, organelles) is suspended in a solution of gel precursors (monomers for polymerisation gelation (Kaetsu, 1993; Kumakura, 2001; Lusta, 2000) or reactive polymer and cross-linking agent (Cocquemcot, 1979; Scardi, 1987) and the mixture is cryogenically treated. This gives rise to the supermacroporous matrix containing immobilized cells entrapped in the cross linked gel phase of pore walls. It is noteworthy that such biomass-containing material could be fabricated not only from organic but also from inorganic polymer, for example, cryo-silica gel (silica gel formed under freeze-thaw conditions) (Slabova, 1988).

Cell entrapment in macroporous PVA cryogels results in very efficient immobilized systems (Lozinsky and Plieva, 1998), in which the cells are caged in gel pores, of which the size is only somewhat less then the cell size. The cells are situated in favorable microenvironment because virtually no barriers arise for diffusion of substrates and metabolites (Lozinsky, 1995; Ariga, 1994; Gordon, 1999). CryoPVAG as a carrier of immobilized cells has other useful properties: high thermostability and gel strength, and the non-brittle viscoelastic matrix is not prone to abrasive erosion even at intense stirring. Also, the matrix is resistant to biological degradation and is practically insensitive to culture media compositions. PVA is a biologically compatible, non-toxic and low-cost polymer. The immobilization procedure is not complicated: a biomass is mixed with the solution of PVA and cryoprotectant (if required for cryosensitive strains), then frozen, kept frozen for a definite time and finally thawed. Cell bearing composites prepared this way can be of any desirable shape: beads, films, blocks, tubes, and so on. However, the better form for the majority of bioreactors is beaded biocatalysts, and therefore several constructions of cryogranulating devices have been elaborated (Lozinsky, 2001; Hayashi, 1993; Prusse, 1998). All the above-described features make such carriers promising for industrial application, and the data on scaled-up

implementation of cryoPVAG-immobilized cells have already been published (Okazaki, 1995).

2.5. Particle Embedded Cryogels

The advantage of the particle loaded cryogel adsorbents over packed bed systems and chemically functionalized cryogel adsorbents for protein applications is the combination of both high flow rate and a high capacity. This originates from the fact that macroporous cryogels, when compared to chromatographic beads, have a very low flow resistance. The big pores in the membrane structure ensure convective transport of the target molecules to the active binding sites located on the surface of the embedded particles. Meanwhile, the use of small particles creates a high adsorption/affinity area per unit of column volume. The embedding of particles in a macroporous matrix makes the column insensitive for possible particle deformation.

Recently Savina et al. (Savina, 2005) developed cryogel monoliths with high amount of functional groups for protein adsorption by graft polymerization of *N*,*N*-dimethylaminoethyl methacrylate (DMAEMA) onto the polyacrylamide-based cryogel pore surface initiated using potassium diperiodatocuprate and the BSA binding capacity of the obtained cryogel was increased. Yao et al. developed a novel polyacrylamide-based cryogel monolith by embedding nanosize Fe_3O_4 adsorbent particles in cryogel matrix with their partial surfaces exposed to the liquid in cryogel pores (Yao, 2006). These nanoparticles have large specific area and high protein loadings (Peng, 2004) and served as effective binding sites for protein adsorption. It was found that BSA adsorption capacity of this cryogel was also improved due to these nano-size adsorbent particles (Yao, 2006). Baydemir et al. prepared bilirubin imprinted particles embedded supermacroporous poly(hydroxyethyl methacrylate) based cryogels and obtained high surface area adsorbents and high bilirubin removal efficiency (Baydemir, 2009).

3. MATERIALS AND METHODS

3.1. General Procedures

2-Hydroxyethyl methacrylate (HEMA) and poly ethylene glycol diacrylate (PEGDA) was purchased from Sigma (St. Louis, MO, USA), N,N,N,N-tetra-methyl-ethylenediamine (TEMED) and ammonium persulfate (APS) were from BioRad (Hercules, CA, USA), methylene-bis-acrylamide (MBAAm) was from Acros (Geel, Belgium). Cibacron Blue F3GA (CB) was obtained from Polyscience (Warrington, USA) and used without further purification. L-phenyl alanine and methacryloyl chloride were also obtained from Sigma. For the synthesis of PGMA beads; glycidyl methacrylate (GMA, Fluka A.G., Buchs, Switzerland) was purified by vacuum distillation and stored in a refrigerator until use. Poly (vinyl alcohol) (PVAL, M_W: 30.000-70.000, Sigma, St. Louis, MO, USA) was selected as the steric stabilizer. Human Serum Albumin (HSA), human transferrin (HTR) and myoglobin (MYB) from equine skeletal muscle were purchased from Sigma with purity of 98-100%. All other chemicals were of reagent grade and were purchased from Merck AG (Darmstadt, Germany). All reagents were used as purchased without any purification. All water used in the experiments was purified using a Barnstead (Dubuque, IA) ROpure LP® reverse osmosis unit. Buffer and sample solutions were prefiltered through a 0.2-µm membrane (Sartorius, Gottingen, Germany). All glassware was extensively washed with dilute nitric acid before use.

3.2. Preparation of PHEMA Cryogel Column

Production is carried out in partially frozen reaction system where ice crystals perform as pore-forming material (porogen) and the gelation proceeds in non-frozen microphase of the apparently frozen reaction system. When gelation in microphase is completed, melting of the reaction system results in a system of large pores (the space previously occupied by ice crystals) surrounded by walls of dense hydrogel formed in the unfrozen microphase (Figure 3.1). The PHEMA cryogel was prepared by dissolving at 5 different monomer/crosslinker (HEMA/MBAAm) ratios (5, 6, 8, 10 and 20 mmol of HEMA, 1 mmol of MBAAm) in deionized water with a final monomer concentration of 10%. After free radical

polymerization was initiated by TEMED (1%, w/w) and APS (1% w/w), the monomer mixtures were immediately poured into glass columns (4 mL, ID 10 mm) and frozen at –12°C for 16 h. The PHEMA cryogel was allowed to thaw at room temperature in order to form supermacropores. The defrosted PHEMA cryogel was washed with deionized water to remove unreacted monomers and stored at 4°C in the swollen state.

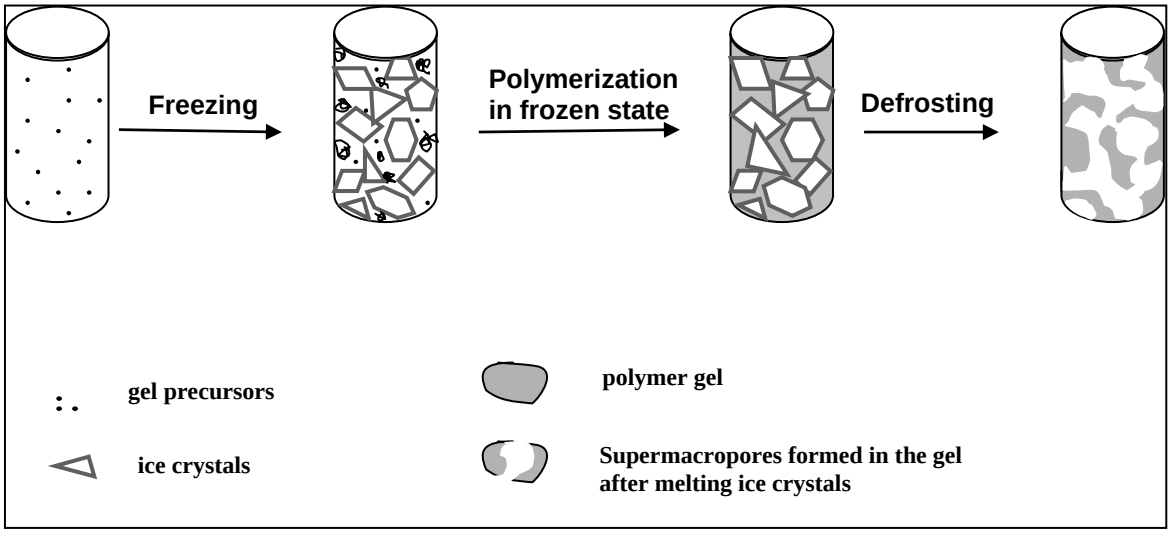

Figure 3.1. Production Scheme of Cryogels.

3.3. CB Attached PHEMA (PHEMA-CB) Cryogel

CB immobilization studies were carried out in a recirculating system equipped with a water jacket for temperature control as in (Figure 3.2). The cryogel was washed with 250 mL of water. Then, 30 mL of CB solution (5 mg/mL) for 5 mL cryogel was pumped through the glass column under recirculation at 60°C for 30 min. During recirculation 0.75 g NaCl was added and incubated for 1 hour at the same temperature. Then temperature was increased gradually up to 80°C in 2 hour by adding 0.075 g Na_2CO_3. Under these experimental conditions, a chemical reaction took place between the group of the CB containing chloride and the hydroxyl group of the PHEMA cryogel. After incubation, the PHEMA-CB cryogel was washed with 2 L of 1.0 M NaCl solution and distilled water until all the physically adsorbed CB was removed. The modified cryogel was then stored at 4°C with 0.02% sodium azide to prevent microbial contamination.

Figure 3.2. Dye attachment procedure of PHEMA cryogel.

3.4. Preparation of MAPA Incorporated PHEMA (PHEMAPA) Cryogel

3.4.1. Synthesis of N-methacryloyl-L-phenylalanine (MAPA)

The following experimental procedure was applied for the synthesis of N-methacryloyl-L-phenylalanine (MAPA): Phenylalanine (5.0 g) and $NaNO_2$ (0.2 g) were dissolved in 30 mL of K_2CO_3 aqueous solution (5%, w/v). This solution was cooled down to 0°C. Methacryloyl chloride (4.0 mL) was slowly poured into this solution under nitrogen atmosphere and this solution was then stirred magnetically at room temperature for 2 h. At the end of this chemical reaction period, the pH of the solution was adjusted to 7.0 and subsequently the solution was extracted with ethyl acetate. The aqueous phase was evaporated in a rotary evaporator. The residue (i.e., MAPA) was crystallized from ether and cyclohexane. The structure analysis of the synthesized MAPA was completed using ^1H NMR (Bruker, UltraShield 400 MHz) spectroscopy in $CDCl_3$. The residual non-deuterated solvent ($CHCl_3$) served as an internal reference. Chemical shifts are reported in ppm (δ) downfield relative to $CHCl_3$.

3.4.2. Preparation of HSA-Imprinted PHEMAPA (PHEMAPA-HSA) Cryogel

HSA-MAPA complex was prepared by adding 1 mM of MAPA solution to 1 mM HSA solution. This mixture was incubated for 3 h for the formation of a complex between HSA and MAPA monomer before the polymerization process. The

monomer mixture was prepared by dissolving 6 mmol of HEMA and 1 mmol of MBAAm in 14 mL of deionized water with a monomer concentration of 10%. After 1 mL of HSA-MAPA complex was added to the monomer mixture, the final monomer solution was degassed under vacuum for about 5 min to eliminate soluble oxygen. The free radical polymerization was initiated by adding APS and TEMED (1% (w/v) of the total monomers) in an ice bath at 0°C. Immediately, the reaction mixture was poured into 4 plastic syringes (4 mL, id. 10 mm) with closed outlets at the bottom and was frozen at -12°C for 24 h. The PHEMAPA-HSA cryogel was thawed at room temperature. The non-imprinted (PHEMAPA) cryogel was prepared in the same manner without using HSA as template.

After washing with 200 ml of water, the removal of template (HSA) was performed using 0.1 M acetate buffer (pH 4.0) containing 10% ethylene glycol which was pumped through the PHEMAPA-HSA cryogel for at least 2 h at room temperature. This procedure was repeated until no HSA leakage was observed. Then, the cryogel was washed with 50 mM NaOH for sterilization. The amount of HSA extracted from the cryogel structure was determined at 595 nm by Bradford method using spectrophotometer (UV–1601, Shimadzu, Japan). A calibration curve was prepared using HSA solution as a standard. The experiments were performed in replicates of three, and the samples were analyzed in replicates of three as well. After cleaning procedure, the cryogel was stored in a buffer containing 0.02% sodium azide at 4°C until use.

3.5. Preparation of PGMA Beads Embedded PHEMA (PGMA/PHEMA) Composite Cryogel

3.5.1. Preparation of the HSA-Surface Imprinted PGMA (PGMA-HSA) Beads

The minidispersion polymerization was used for the surface imprinting process. For this purpose, two aqueous phases were prepared. To form the first aqueous phase, 0.375 g of PVAL was dissolved in 20 mL of deionized (DI) water. A second aqueous phase of 0.2 g of PVAL was dissolved in 400 mL of DI water. A 0.8 mL of GMA and 4.2 mL of EGDMA were then mixed to form the oil phase. The monomer mixture oil phase was slowly added into the first aqueous phase, followed by

homogenization at 24 000 rpm with a homogenizer (T10 basic, Ika-Ultra Turrax, Germany) to form a minisuspension. Subsequently, 12.4 µmol of the template protein (HSA) was added to the minisuspension and mixed with a magnetic stirrer for 30 min to allow effective monomer-template interaction. The minisuspension with the HSA was then added into the second aqueous phase under stirring and transferred into a 1 L three-neck round-bottomed flask. The flask was mechanically stirred at 300 rpm and slowly heated. After the prepolymerization mixture had reached 40 °C, the reaction vessel was prepurged with nitrogen gas for 15 min to displace the oxygen, and finally, sodium bisulfite (0.230 g), followed by APS (1% w/v), was added into the mixture as initiators for polymerization for 24 h. The polymer product was then washed five times each with DI water and four times with excess ethanol to remove the surfactant or any unreacted monomer and initiator, and six times with DI water. For each washing step, the solution was centrifuged (Universal 320R, Hettich Zentrifugen, Germany) at 9000 rpm for 1 h to isolate the polymeric product from the washing medium. Non-imprinted PGMA beads (PGMA) were prepared in a similar manner as above, except without the addition of the template protein. Upon completion of the polymerization reaction, the PGMA was washed in a similar way as that for the imprinted particles.

3.5.2. Preparation of HSA-Surface Imprinted PGMA Beads Embedded PHEMA (HSA-PGMA/PHEMA) Composite Cryogel

The monomer mixture was prepared by dissolving 6 mmol of HEMA and 1 mmol of PEGDA in 15 mL of deionized water with a monomer concentration of 10%. After the PGMA-HSA beads were loaded in the monomer mixture (150 mg bead per mL of monomer), the final monomer solution was degassed under vacuum for about 5 min to eliminate soluble oxygen. The free radical polymerization was initiated by adding APS and TEMED (1% (w/v) of the total monomers) in an ice bath at 0°C. Immediately, the reaction mixture was poured into 4 plastic syringes (4 mL, id. 10 mm) with closed outlets at the bottom and was frozen at -16°C for 24 h. The HSA surface-imprinted (PGMA-HSA/PHEMA) composite cryogel was thawed at room temperature. The non-imprinted (PGMA/PHEMA) cryogel was prepared in the same manner by loading non-imprinted PGMA beads.

After washing with 200 mL of water, the removal of template (HSA) was performed using a solution of SDS and acetic acid (10% w/v: 10% v/v) which was pumped through the PGMA-HSA/PHEMA cryogel for at least 2 h at room temperature. This procedure was repeated until no HSA leakage was observed. Then, the cryogel was washed with 50 mM NaOH for sterilization. The amount of HSA extracted from the cryogel structure was determined at 595 nm by Bradford method using spectrophotometer (UV–1601, Shimadzu, Japan). A calibration curve was prepared using HSA solutions as a standard. The experiments were performed in replicates of three, and the samples were analyzed in replicates of three as well. After cleaning procedure, the cryogel was kept in a buffer. The washed imprinted polymer was diluted with DI water to 200 mL and kept as a suspension containing 0.02% sodium azide at 4°C until use.

3.6. Characterization Studies

3.6.1. Swelling Properties of Cryogel

The gelation yield was determined as follows: the swollen cryogel sample (1 ml) was put in an oven at 60 °C for drying. After drying till constant weight, the mass of the dried sample was determined (m_{dried}). The gel fraction yield was defined as (m_{dried}/m_t) x100%, where m_t is the total mass of the monomers in the feed mixture.

The swelling degrees of PHEMA based cryogels were determined as follows: samples of swollen gels (1mL by each) on porous filter were sucked dry and then weighed ($m_{wet\ gel}$). After drying to constant weight in the oven at 60°C, the weight of dried samples was determined ($m_{dry\ gel}$). The degree of swelling was calculated as: $S_w/_w = (m_{wet\ gel} - m_{dry\ gel})/m_{dry\ gel}$. The standard deviation of 3 measured samples is shown.

The total volume of supermacropores in the swollen cryogel was roughly estimated as follows: the weight of the sample ($m_{squeezed\ gel}$) was determined after squeezing the free water from the swollen gel matrix, the porosity was calculated as follows: $(m_{swollen\ gel} - m_{squeezed\ gel})/m_{swollen\ gel} \times 100\%$. The percent of swollen gel

weight is also calculated as $(m_{swollen\ gel} - m_{dried})/m_{swollen\ gel} \times 100\%$. All measurements were done in triplicate and the average values are presented.

The flow-rate of water passing through the cryogel was measured at the constant hydrostatic pressure equal to 100 cm of water-column corresponding to a pressure of ca. 0.01 MPa. At least three measurements were done for each sample.

3.6.2. ^{1}H-NMR and FTIR Studies

The proton NMR spectrum of MAPA monomer was taken in $CDCl_3$ on a JEOL GX-400-300 MHz instrument. The residual non-deuterated solvent (TMS) served as an internal reference. Chemical shifts were reported in ppm (δ) downfield relative to TMS.

FTIR spectra of MAPA monomer, HSA-MAPA complex and other cryogels were obtained by using a FTIR spectrophotometer (FTIR 8000 Series, Shimadzu, Japan). The dry particles (about 0.1 g) was thoroughly mixed with KBr (0.1 g, IR Grade, Merck, Germany), and pressed into a pellet and the FTIR spectrum was then recorded.

3.6.3. Surface Morphology

The surface morphology of the cryogel was examined using scanning electron microscopy (SEM). The sample was fixed in 2.5% glutaraldehyde for overnight. Then the sample was dehydrated at -50 °C in lyophilizate. (Lyophilizer, Christ Alpha 1-2 LD plus, Germany). Finally, it was coated with gold-palladium (40:60) and examined using a JEOL JSM 5600 scanning electron microscope (Tokyo, Japan).

3.6.4. Surface Area Measurements

The specific surface area of all cryogels was measured according to the Brunauer-Emmett-Teller (BET) model using multi point analysis and a Flowsorb II 2300 from Micromeritics Instrument Corporation, Norcross, GA.

3.6.5. Elemental Analysis

The degree of CB immobilization for PHEMA-CB cryogel was evaluated by elemental analysis from sulfur stoichiometry using a Leco Elemental Analyzer (Model CHNS-932).

3.7. Adsorption Studies

3.7.1. Adsorption of HSA from Aqueous Solutions

All HSA adsorption study on cryogel was carried out in a recirculation system equipped with a water jacket for temperature control. The PHEMA-CB cryogel was washed with 30 mL of water and then equilibrated with 50 mM acetate buffer (pH 5.0) for 30 min. Then, the HSA solution was pumped through the column under recirculation for 2 hour. Effects of HSA concentration, flow rate, pH of the medium, temperature and ionic strength on the adsorption capacity were studied. The effect of the initial concentration of HSA on adsorption capacity was studied by changing the concentration of HSA between 0.5-80 mg/mL. The effect of flow rate on adsorption capacity was investigated at different flow rates changing between 0.5-4.0 mL/min pumped through the column under recirculation for 60 min with 2 mg/mL of HSA solution in 50 mM acetate buffer (pH 5.0, 10 mL). The effect of pH on the adsorption capacity was determined by changing pH of the solution between 4.0 and 8.0. The effect of temperature on the adsorption capacity was determined by changing temperature of the solution between 4.0 °C and 50 °C. The observation of the effect of ionic strength was carried out in solutions containing different amounts of NaCl.

The PHEMAPA-HSA cryogel was washed with 30 mL of water and then equilibrated with 50 mM phosphate buffer (pH 6.0) for 30 min. Then, the HSA solution was pumped through the column under recirculation for 2 hour. Effects of HSA concentration, flow rate, pH of the medium, temperature and ionic strength on the adsorption capacity were studied. The effect of the initial concentration of HSA on adsorption capacity was studied by changing the concentration of HSA between 0.5-5.0 mg/mL. The effect of flow rate on adsorption capacity was

investigated at different flow rates changing between 0.5-4.0 mL/min pumped through the column under recirculation for 60 min with 2 mg/mL of HSA solution in 50 mM phosphate buffer (pH 6.0, 10 mL). The effect of pH on the adsorption capacity was determined by changing pH of the solution between 4.0 and 8.0. The effect of temperature on the adsorption capacity was determined by changing temperature of the solution between 4.0 °C and 50 °C. The observation of the effect of ionic strength was carried out in solutions containing different amounts of NaCl.

The PGMA-HSA/PHEMA composite cryogel was washed with 30 mL of water and then equilibrated with 50 mM acetate buffer (pH 5.0) for 30 min. Then, the HSA solution was pumped through the column under recirculation for 2 hour. Effects of HSA concentration, flow rate and pH of the medium, on the adsorption capacity were studied. The effect of the initial concentration of HSA on adsorption capacity was studied by changing the concentration of HSA between 0.5-80 mg/mL. The effect of flow rate on adsorption capacity was investigated at different flow rates changing between 0.5-3.0 mL/min pumped through the column under recirculation for 60 min with 2 mg/mL of HSA solution in 50 mM acetate buffer (pH 5.0, 10 mL). The effect of pH on the adsorption capacity was determined by changing pH of the solution between 4.0 and 7.0.

The adsorption amount for all cryogel system was followed by monitoring the decrease in visible absorbance at 595 nm by Bradford method. The amount of adsorbed HSA was calculated as;

$$q=[(C_o-C)V]/m \qquad (3.1)$$

Here, q is the amount of HSA adsorbed onto unit mass of cryogel (mg/g); C_o and C are the concentrations of HSA in the initial solution and in the aqueous phase after treatment for certain period of time, respectively (mg/mL); V is the volume of the aqueous phase (mL); and m is the mass of the cryogel used (g). Each experiment was performed three for quality control and statistical calculations.

3.8. Selectivity Studies for HSA-Imprinted Cryogel

The HSA selectivity of HSA-imprinted cryogel (for PHEMAPA and PGMA/PHEMA) was investigated by competitive adsorptions of HTR and MYB as model proteins in 50 mM of pH 5.0 acetate buffer solution. The selectivity of the HSA-imprinted cryogel for HSA (Mw: 67.0 kDa, pI: 4.9) with the competitive proteins HTR (Mw: 80.0 kDa, pI: 5.2) and MYB (Mw: 17.0 kDa, pI: 6.8-7.2) was evaluated in a circulating system with 0.4 g of the MIP cryogel, using a peristaltic pump for 2 h. After competitive adsorption equilibrium was reached, the remaining samples were detected separately for each protein by Analytical LC system (Ultimate-3000, Dionex, USA) equipped with Ultimate-3000 pump, Ultimate-3000 Autosampler, Ultimate-3000 Column Department, Ultimate-3000 Variable Wavelength Detector. Separation was carried out by PepSwift Monolithic PS-DVB column (Length/I.D; 5 cm/500 μm). Mobile phases A and B were prepared using water with 0.05% TFA and water/acetonitrile (50:50, v/v) with 0.04% TFA, respectively. The chromatographic separation was performed using a linear gradient at 20 µL/min flow rate. After a 1 min starting period with 90% mobile phase A, a linear gradient started from 10% B in 2 min, continued with increasing B from 10% to 90% in 10 min and finished with increasing B from 90% to 10% in 20 min. 1 µL of protein solution was injected to the column. Absorbance was monitored at 280 nm. The separation was performed at 60 °C temperature.

The distribution coefficients (K_d) for HTR and MYB with respect to HSA were calculated by the following equation;

$$K_d = [(C_i - C_f)/C_f] \times V/m \quad (3.2)$$

in which K_d represents the distribution coefficient for the metal ion (mL/g); C_i and C_f are initial and final concentrations of proteins (mg/mL), respectively. V is the volume of the solution (mL) and m is the weight of the cryogel used in the column (g). The selectivity coefficient (k) for the binding of HSA with competing species (i.e, HTR and MYB) was determined by the following equation;

$$k = K_{d\ (template)} / K_{d\ (competing\ protein)} \quad (3.3)$$

in which, $K_{d\ (template)}$ is the distribution coefficient of the template protein (HSA) and $K_{d(competing\ protein)}$ is the distribution coefficient of the competing proteins (HTR and MYB). The relative selectivity coefficient, which was used to estimate the effect of imprinting on protein selectivity, can be defined from the following equation;

$$k=k_{MIP}/\ k_{NIP} \qquad (3.4)$$

in which k_{MIP} is for MIP cryogel, k_{NIP} is for NIP cryogel.

3.9. Depletion of HSA from Human Serum

3.9.1. Depletion Procedures

The blood is collected from thoroughly healthy voluntary blood donors. Each unit separately controlled and found negative for HSA antigen and HIV I, II and hepatitis C antibodies. No preservatives are added to the samples. The blood samples were centrifuged at 3000 rpm for 10 min at room temperature to separate the serum. The serum samples were filtered using 0.45 µm cellulose acetate microspin filters (Alltech, Deerfield IL, USA) and frozen at -20ºC. Equilibration of the cryogel column was performed by passing four column volumes of phosphate buffer saline (PBS pH: 7.4, NaCl: 0.9%) before injection of the serum. Then, 10 ml of the freshly separated human serum flow through the cryogel column pre-equilibrated with 50 mM of PBS for 1 h. The amount of HSA adsorbed by cryogels was determined by measuring the initial and final concentration of HSA in serum (Mesa Hospital, Ankara). 50 mM of PBS was used for dilution of human serum by 1/2, 1/5, 1/10 ratios.

3.9.2. Fast Protein Liquid Chromatography (FPLC) and SDS-PAGE Imaging

Fast protein liquid chromatography, usually referred to as FPLC, is a form of column chromatography, used to separate or purify proteins from complex mixtures by using ion chromatography. Columns used with an FPLC can separate

macromolecules based on size, charge distribution, hydrophobicity or biorecognition.

FPLC separation was performed using an AKTA-FPLC (Amersham Bioscience, Uppsala, Sweden) system equipped monitor, INV-907 injection valve and Frac920 fraction collector. Separation for all cryogel column was carried out at GE Healthcare column (10/10, 19-5001-01) (Figure 3.3).

2 mL of injection volume of human serum, diluted (1:10) with PBS (50 mM, pH 7.4), was applied. FPLC mobile phases A and B were prepared using 50 mM phosphate buffer (pH 7.0) and phosphate buffer (7.0) containing 1.0 M NaCl, respectively. The chromatographic separation was performed using a linear gradient at 3.0 mL/min flow rate. After a 9.0 min starting period with 100% mobile phase A, a linear gradient started from 0% B to 100% B in 3.0 min, continued with 4.0 min 100% eluent B and finished last 4 min 100% buffer A. All buffers and protein solutions were filtered before use. Absorbance was monitored at 280 nm.

Figure 3.3. Photograph of FPLC system and applied column.

Electrophoresis is the process of moving charged molecules in solution by applying an electric field across the mixture. Because molecules in an electric field move with a speed dependent on their charge, shape, and size, electrophoresis has been extensively developed for molecular separations. As an analytical tool, electrophoresis is simple and relatively rapid. It is used chiefly for analysis and purification of very large molecules such as proteins and nucleic acids, but can also be applied to simpler charged molecules, including charged sugars, amino acids, peptides, nucleotides and simple ions. Highly sensitive detection methods have been developed to monitor and analyze electrophoretic separations. Sodium dodecyl sulphate (SDS) was used for making all proteins negative (Laemmli, 1970).

SDS-polyacrylamide gel electrophoresis (SDS-PAGE) was carried out 12% acrylamide separating gel (in 1.5 M Tris-HCI pH 8.8) and a 5% acrylamide stacking gel (in 1.0 M Tris-HCI pH 6.8) containing 12% SDS. 20.0 µg/µL total protein solution was loaded. Initial, and desorbed samples (15 µL,) were taken and mixed with 15 µL bromophenol (0.002% bromophenol blue in 50% aqueous glycerol containing 1% mercaptoethanol). This sample was runned through Tris-glycine buffer at pH 8.3 containing 0.1% SDS. Electrophoresis was run at a current of 15 mA for 1.0 hour and 50 mA for 5 hour. These currents were used for 5% stacking and 12% separating gel respectively (Westermeier, 1997). Colloidal Coomassie Blue G-250 staining protocol was used and destained in water. ImageQuant 300 (Amersham, USA) was used for monitoring the image.

3.9. Desorption and Repeated Use

Desorption of the adsorbed HSA from cryogel was studied in continuous experimental setup. HSA adsorbed PHEMA-CB cryogel was desorbed with 50 mM pH 7.0 phosphate buffer containing 1M NaCl solution. HSA adsorbed PHEMAPA cryogel was desorbed with 0.1 M acetate buffer containing %10 ethylene glycol (pH 4.0) solution. HSA adsorbed PGMA/PHEMA composite cryogel was desorbed with a solution of SDS and acetic acid (10% w/v: 10% v/v). All desorption media was maintained for 2.0 hour at room temperature. The final HSA concentration in

the desorption medium was determined at 595 nm by Bradford method. Desorption ratio for HSA was calculated with the following expression:

$$\text{Desorption ratio (\%)} = \frac{\text{Amount of HSA released}}{\text{Amount of HSA adsorbed}} \text{ X } 100 \qquad (3.5)$$

In order to show the reusability of cryogel, adsorption-desorption cycle was repeated ten times by using the same cryogel.

4. RESULTS AND DISCUSSION

4.1. Structure and Swelling Characterization of Cryogels

When cryogels are produced, polymerization takes place in the non-frozen fluids containing concentrated dissolved monomers and initiator. The ice crystals formed during freezing perform as porogen. Thus, the shape and size of the crystals formed determine the shape and size of the pores formed after defrosting the sample. In general, the size of ice crystals depends on how fast the system is frozen, provided other parameters (e.g. concentration of the dissolved substances, volume and geometrical shape of the sample) remain the same (Plieva, 2000). The freezing rate is determined by the starting temperature, which was maintained in our case close to 0°C as all the solutions before mixing were kept in an ice bath, and the freezing temperature. In order to obtain a reproducible freezing pattern, several precautions were taken: the samples of small size and uniform shape (4 mL syringes filled with 4 mL solution) were used and the time was accurately controlled from the moment when the monomer and initiator solutions were mixed (the start of polymerization reaction) to the moment when the plastic syringes filled with polymerization solution were submerged into the cooling liquid of the cryostat.

The different pore morphology resulted in different flow resistance of the columns filled with PHEMA-6 to PHEMA-20 cryogels produced, respectively (estimated as water flow rate through the monolithic cryogel at hydrostatic pressure equal to 1 m of water column). The flow rate of water through the PHEMA-20 cryogel column was 334 cm/h, whereas different pore morphology in PHEMA-6 cryogel resulted in a drastic decrease of the flow rate to 76 cm/h (Table 4.1).

PHEMA cryogels can be dried at 60 °C and stored nearly indefinitely in the dry state. A dry cryogel sample slowly adsorbs water vapors about 100% of its weight. When submerged into liquid, dry cryogels rehydrated within less than a minute without deterioration of their supermacroporous structure. This property of cryogels makes them very attractive as potential chromatographic carriers. An important feature of the chromatographic material is the pore volume. On average,

dry polymer constitutes only 3–4% of the total weight of completely swollen cryogel. About 4–5% of the weight is composed of water tightly bound by the polymer (adsorbed from water vapor). Together, polymer with tightly bound water forms the pore walls. Thus, the remaining nearly 90% of the cryogel weight is represented by the water inside the pores. Due to the elasticity of cryogels, a large amount of water in large pores could be squeezed mechanically from the swollen monolithic samples. It indicates that the main part of the cryogel volume is composed of the interconnected supermacropores.

Table 4.1. Preparation conditions and swelling ratios of PHEMA cryogels.

HEMA/mBAAm	Notation for prepared PHEMA cryogels	Yield (%)	Linear flow resistance (cm/h)	Porosity (%)	Swelling degree
5/1	PHEMA–5	89.8	55	57.9	8.8
6/1	PHEMA–6	99.4	76	62.0	9,6
8/1	**PHEMA–8**	**95.3**	**84**	**65.2**	**10.1**
10/1	PHEMA–10	91.7	126	68.3	10.0
20/1	PHEMA–20	91.1	334	76.6	10.1

The equilibrium swelling degree of the PHEMA cryogel was changed between 8.8-10.1 g H_2O/g cryogel by changing the crosslinker ratio. PHEMA monolithic cryogel is opaque, sponge like and elastic. This cryogel can be easily compressed by hand to remove water accumulated inside the pores. When the compressed piece of cryogel was submerged in water, it soaked in water and within 1-2 s restored its original size and shape. Macroporosity increases by the increasing HEMA/crosslinker ratio. Table 4.1 shows the effect of crosslinker amount on swelling properties of cryogels. The amount of the crosslinker (i.e. mBAAm) in the reaction feed was changed in order to obtain different swelling properties of PHEMA cryogels. The prepared PHEMA-6 cryogel has the highest crosslinker concentration resulted in the highest gel fraction yield of 99.4%, however it has a rather low water uptake and swelling ratio (62%). As the mol ratio of

HEMA/mBAAm increases, the mBAAm concentration decreases in the reaction feed. The PHEMA-20 cryogels have lowest amount of crosslinker content.

Different morphology of cryogels formed with different amount of crosslinker, is clearly reflected in the different morphology of pores in the resulting cryogel samples (Figure 4.1). The PHEMA-6 cryogel has different pore structure with an apparent bimodal pore size distribution. There are supermacropores with hundred-micrometer size and small pores about 0.1–3 μm in size (Figure 4.1A). The PHEMA-20 cryogel has large (5–100 μm) interconnected pores (supermacropores) separated with smooth, nonporous dense gel walls (Figure 4.1B).

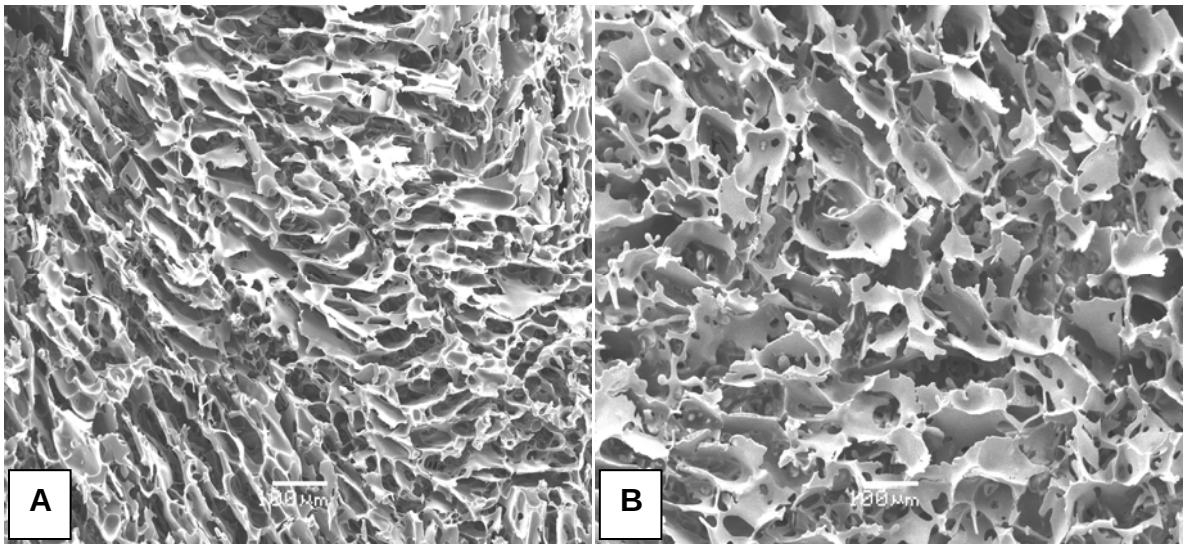

Figure 4.1. SEM Micrographs of PHEMA Cryogels. A) PHEMA-6 cryogel B) PHEMA-20 cryogel.

Specific surface area, total pore volume and average pore diameter of PHEMA cryogels are presented in Table 4.2. The specific surface areas of PHEMA cryogel were determined by a multipoint BET apparatus to be 25.0 m^2/g cryogel in average. It should be noted that there is no detectable difference in the specific surface area of PHEMA cryogel with different cross-linker ratios due to the low specific surface area that multipoint BET apparatus can detect. The sizes of the pores on PHEMA cryogel were determined via a BJH instrument to average out to 78.2 Å in diameter, in which the pore diameters range from 20 Å to 245 Å,

suggesting the presence of macropores on the surface of PHEMA cryogel. This pore diameter is convenient for convection of high viscosity fluids such as blood.

Table 4.2. Physical properties of PHEMA cryogels with different cross-linker ratio.

Notation for Cryogels	Surface Area[a] (m^2/g)	Total Pore Volume[b] (ml/g)	Average Pore Diameter[c] (Å)
PHEMA–5	25.2	0.038	74.0
PHEMA–6	25.8	0.041	77.1
PHEMA–8	**25.0**	**0.045**	**78.2**
PHEMA–10	n.a	n.a	n.a
PHEMA–20	n.a	n.a	n.a

a. Determined using multipoint BET method.

b. BJH cumulative desorption pore volume of pores between 20 and 245 Å.

c. BJH desorption average pore diameter of pores between 20 and 245 Å.

n.a. Not avaible.

In this thesis, HEMA/crosslinker ratio (i.e. MBAAm, PEGDA) was selected as 8/1 due to the low flow resistance with the large interconnected pores and the highest gel fraction yield.

4.2. Cibacron Blue F3GA Immobilized PHEMA Cryogel (PHEMA-CB)

CB was covalently attached to the PHEMA cryogel via the nucleophilic substitution reaction between the chloride of their triazine ring and the hydroxyl groups of the PHEMA under alkaline conditions (Figure 4.2). The highest dye surface density was 33.9 µmol/g. It should be noted that *no* dye leakage was observed in any medium used throughout this study, even over long periods of time (more than 32 weeks).

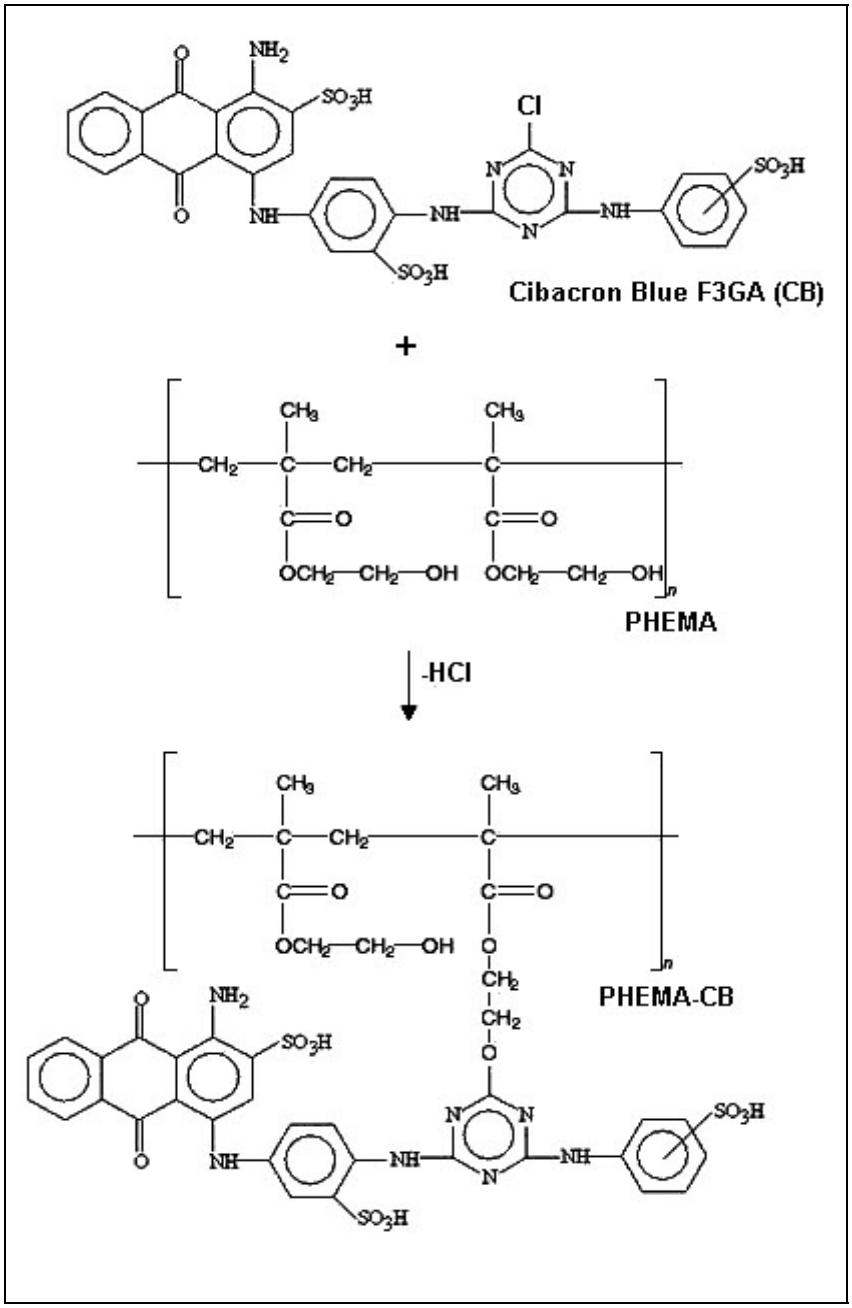

Figure 4.2. A schematic structure of CB immobilized cryogel (PHEMA-CB).

The SEM of the internal structure of the monolithic cryogel is shown in Figure 4.3. It can be seen that the surface morphology was not changed after CB immobilization procedure.

PHEMA-CB cryogel has nonporous and thin polymer walls, large continuous interconnected pores (10–100 μm in diameter) that provide channels for the mobile phase to flow through.

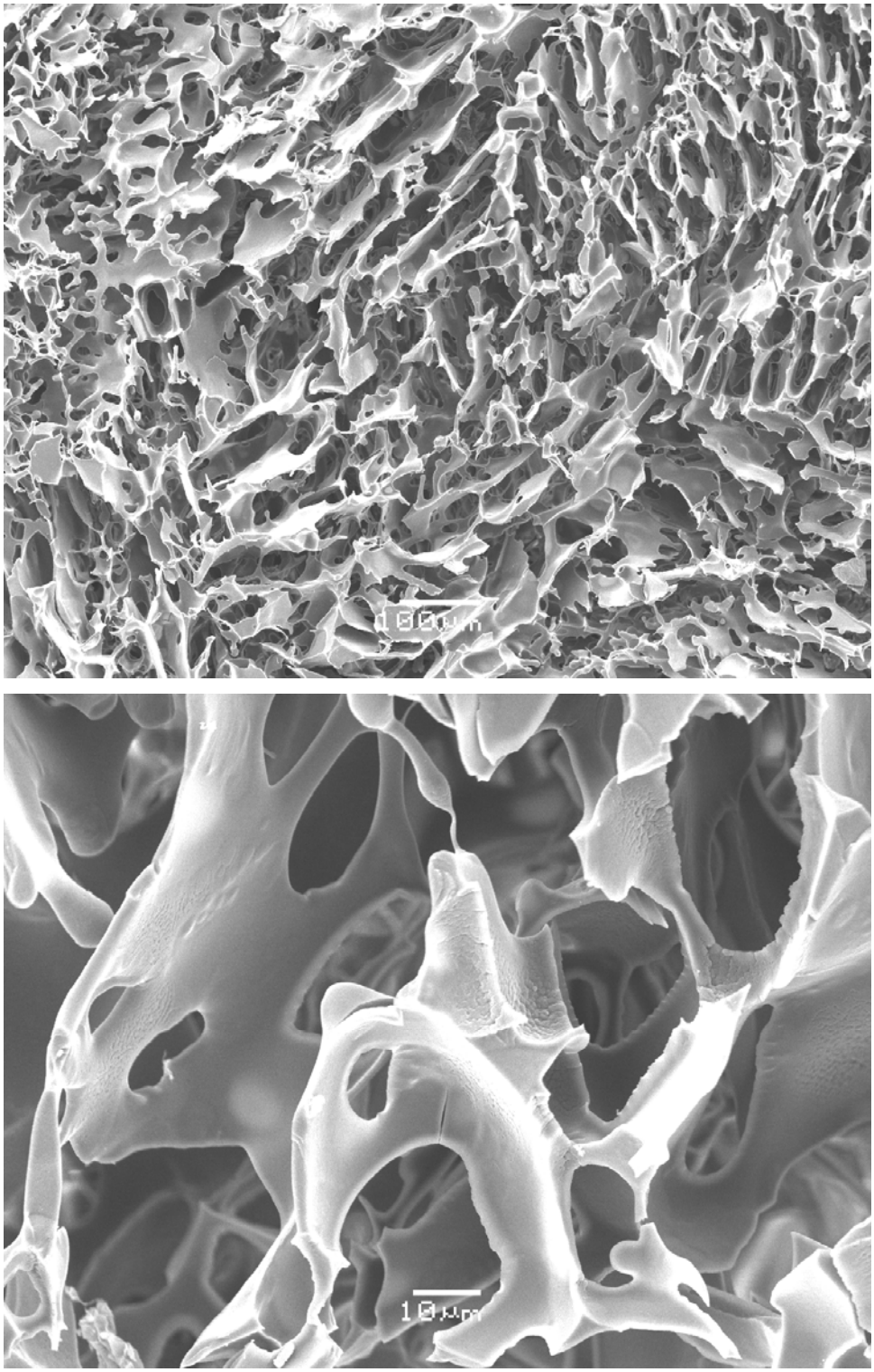

Figure 4.3. SEM photographs of PHEMA-CB cryogel.

Pore size of the matrix is much larger than the size of the protein molecules such as HSA (Hydrodynamic radius of HSA: 3.9 nm), allowing them to pass easily. The transport of solutes inside the cryogel column proceeded mainly due to the

convection rather than due to the diffusion. As a result of the convective flow of the solution through the pores, the mass transfer resistance is practically negligible.

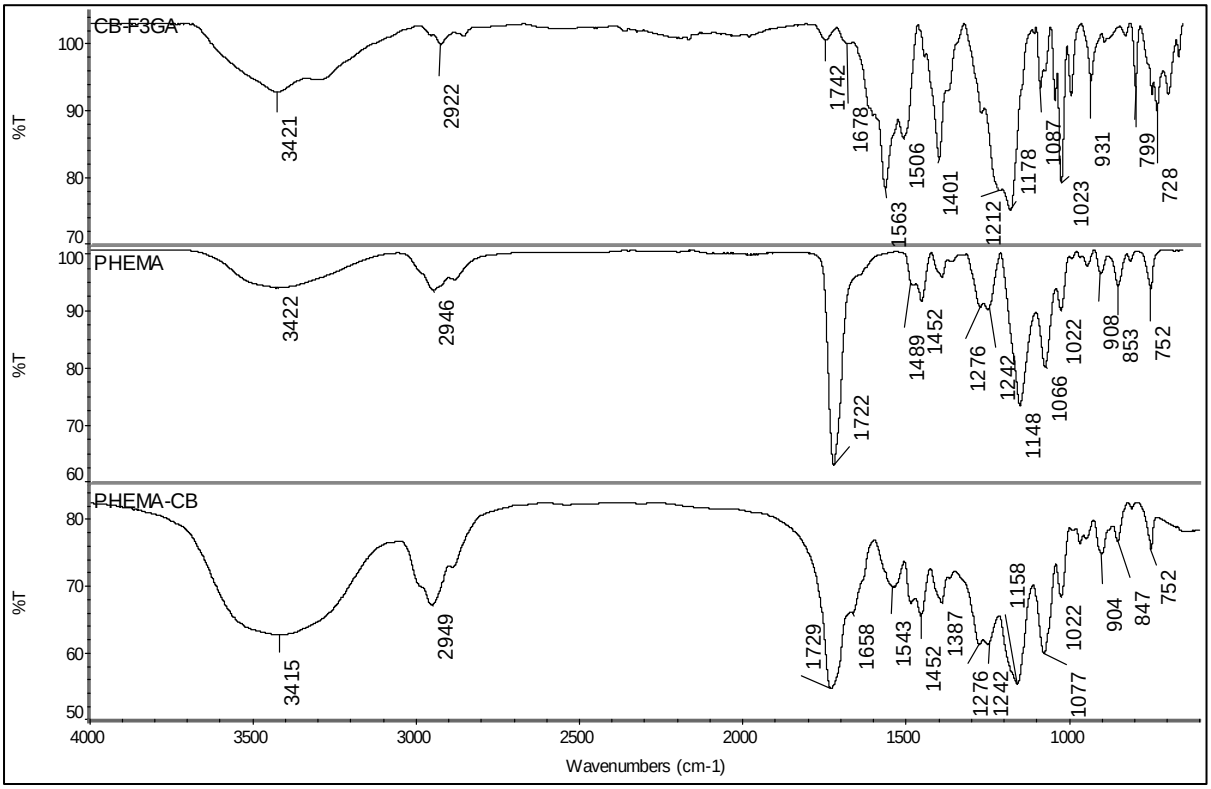

Figure 4.4. The FTIR spectra of CB, PHEMA and PHEMA-CB in the range of 4000-600 cm^{-1}.

The FTIR spectra in Figure 4.4 show the structural evaluation of functional groups for the incorporation of CB molecules into PHEMA. A broad peak of O-H stretching vibration around 3426 cm^{-1} has appeared for all CB, PHEMA and PHEMA-CB. The N-H stretching vibration bands of CB (upper side of Figure 4.4.) appear around 3400 cm^{-1} frequency range as multiple bands. The different amine groups of the dye could have a tendency to be free and H-bonded. That is why this spectral situation is regular. The band having moderate intensity at 1742 cm^{-1}, a shoulder at 1678 cm^{-1} and then sharp bands at 1563 cm^{-1} and 1506 cm^{-1} are the spectral evidences that characterize the C=O, C-N and C-C stretching vibrations of the structure. The band at 1212 cm^{-1} and the broad band at nearly 25 cm^{-1} below and above this frequency characterize the S=O stretching vibrations. The band that can be seen obviously at 1087 cm^{-1} belongs to the C-Cl stretching. At the lower wave number such as 1023 cm^{-1} S-O stretching vibration band is also seen

in the spectrum. In addition, it is possible to see the C-Cl stretching vibrations of the dye at different wave numbers in the range of 600–900 cm^{-1}. The characteristic C=O stretching vibrations for PHEMA and PHEMA-CB can be seen sharply at 1722 cm^{-1} and 1726 cm^{-1}, respectively. The amide I and amide II vibration bands at 1650 cm^{-1} and 1543 cm^{-1} in PHEMA-CB (lower side of Figure 4.4.) confirms the covalent attachment of CB to PHEMA while no amine groups observed in PHEMA. The peaks at 1276 cm^{-1} and 1158 cm^{-1} characterize the C-O stretching vibrations in PHEMA-CB. The conversion of the C-Cl stretching vibration of the CB at 1087 cm^{-1} to a weak shoulder at 1077 cm^{-1} proves the covalent attachment of CB to PHEMA. In addition, the decrease in the intensity of the same stretching vibrations of CB at 600–900 cm^{-1} frequency intervals also confirms the presence of CB in PHEMA.

4.2.1. Adsorption Studies of PHEMA-CB Cryogel

4.2.1.1. Adsorption of HSA from Aqueous Solutions

4.2.1.1.1. Effect of pH

Figure 4.5 shows the effect of pH on the adsorption of HSA onto PHEMA-CB cryogel. The maximum adsorption of HSA was observed at pH 5.0, which is the isoelectric point of HSA. The HSA adsorption capacity decreased above and below pH 5.0. The decrease in the HSA adsorption capacity can be attributed to electrostatic repulsion effects between the identically charged groups. At the isoelectric point, proteins have no net charge and therefore, the maximum protein adsorption from aqueous solution is usually observed at this point. In addition, the interactions between CB and HSA may result both from the ionization states of several groups on both the HSA and amino acid side chains in HSA structure, and from the conformational state of HSA at this pH. It should be also noted that nonspecific adsorption (i.e. adsorption on PHEMA cryogel) was independent of pH and it was observed same at all the pH values.

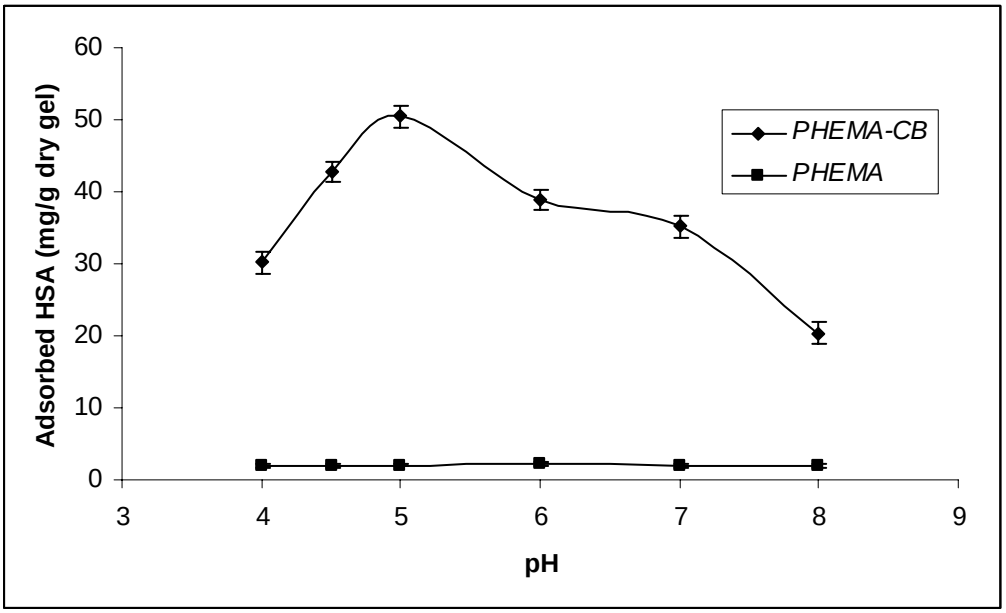

Figure 4.5. Effect of pH on HSA adsorption onto PHEMA-CB cryogel. Experimental conditions: T: 20ºC, flow-rate: 0.5 mL/min, HSA concentration: 2 mg/mL, $V_{solution}$: 10 mL, $m_{dry\ cryogel}$: 0.4 g.

4.2.1.1.2. Effect of Flow Rate

The HSA adsorption of the PHEMA-CB decreased drastically from 50.4 mg/g to 7.5 mg/g as the flow rate was increased from 0.5 mL/min to 4.0 mL/min, respectively (and, as a consequence, with the increase of the Reynolds number) (Figure 4.6). At a higher Reynolds number, the retention time of HSA in the PHEMA-CB cryogel column was not sufficiently long for the adsorption equilibrium to be reached; the solution left the PHEMA-CB cryogel column before the equilibrium was achieved, resulting in an earlier breakthrough time. At a lower Reynolds number, the retention time in the PHEMA-CB cryogel column was longer. Thus, HSA molecules would have more time to diffuse properly into the pores of cryogel and bind to binding sites at lower flow rates, and hence a better adsorption amount is achieved at a flow rate of 0.5 mL/min.

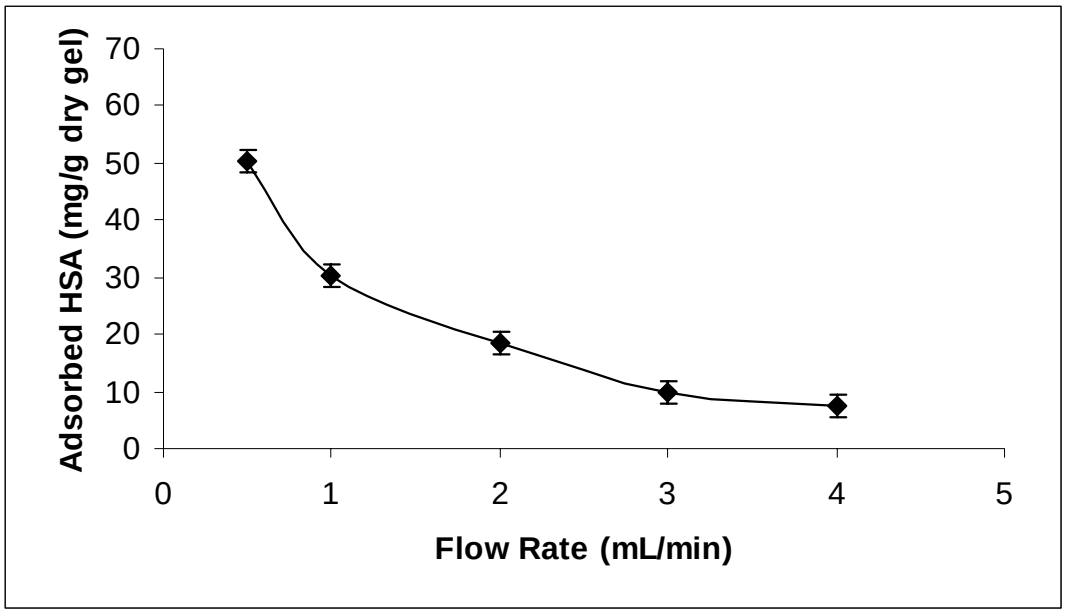

Figure 4.6. Effect of flow-rate on HSA adsorption onto PHEMA-CB cryogel. Experimental conditions: running buffer: 50 mM acetate buffer, pH 5.0, T: 20ºC, HSA concentration: 2 mg/mL, $V_{solution}$: 10 mL, $m_{dry\ cryogel}$: 0.4 g.

4.2.1.1.3. Effect of Initial Concentration

One of the main requirements in dye-affinity chromatography is the specificity of the affinity adsorbent for the target molecule. The nonspecific interaction between the PHEMA and HSA should be lower to consider the interaction as specific. Figure 4.7 shows the HSA adsorption capacity of the PHEMA-CB cryogel. The amount of HSA adsorbed per unit mass of the PHEMA-CB cryogel increased first with the initial concentration of HSA then reached a plateau value at 40 mg/mL which represents saturation of the active adsorption sites (which are available and accessible for HSA) on the cryogel.

The maximum HSA adsorption capacity by the PHEMA-CB cryogel was found to be 343.4 mg/g dry gel on the average. It should be noted that the HSA adsorption onto PHEMA cryogel was 170-fold lower (about 2.02 mg/g) at the same conditions. The increase in the HSA binding capacity may have resulted from cooperative effect of different interaction mechanisms such as hydrophobic, electrostatic, and hydrogen bonding caused by the acidic groups and aromatic structures on the CB and by groups on the side chains of amino acids on the HSA.

It should be mentioned that CB is not very hydrophobic overall, but it has planar aromatic surfaces that prefer to interact with hydrophobic groups in HSA structure.

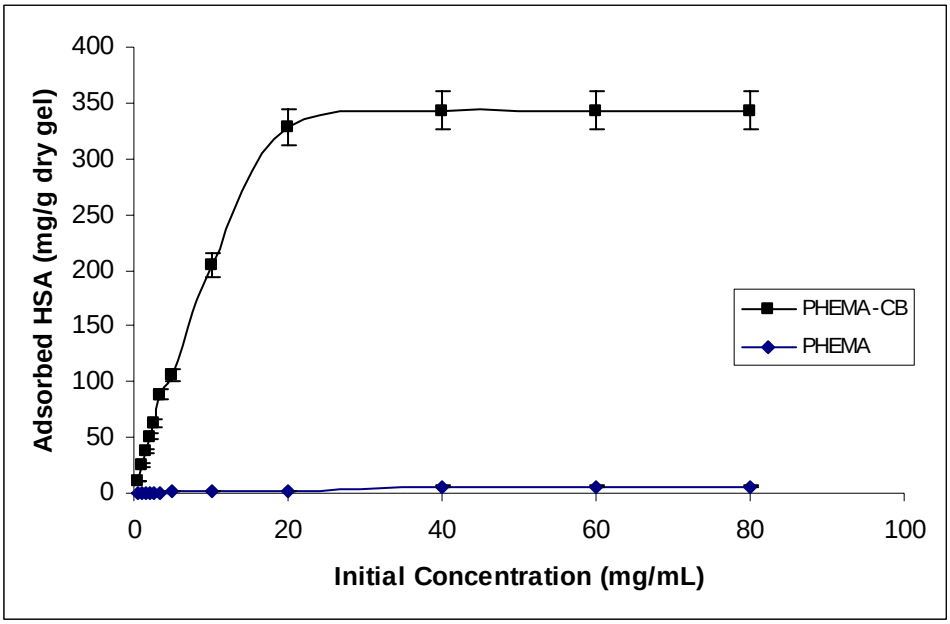

Figure 4.7. Effect of initial concentration on HSA adsorption onto PHEMA-CB cryogel. Experimental conditions: running buffer: 50 mM acetate buffer, pH 5.0, T: 20ºC, flow rate: 0.5 mL/min, $V_{solution:}$ 10 mL, $m_{dry\ cryogel}$: 0.4 g.

Modeling of the equilibrium data has been done using the Langmuir and Freundlich isotherms (Finette, 1997). A good fit to the Langmuir isotherm;

$$C_e/Q_e = (1/Q_{max} .b) + C_e. (1/Q_{max}) \qquad (4.1)$$

where, Q_e is the theoretical maximum adsorption capacity for Langmuir adsorption isotherm (mg/g), C_e is the equilibrium HSA concentration (mg/mL), b is the Langmuir adsorption equilibrium constant (mg/mL) which indicates the monolayer adsorption. A linearized plot of C_e/Q_e versus C_e (Figure 4.8) gives Q_{max} and b.

It has been reported that the effect of isotherm shape with a view to predicting if an adsorption system is ‘‘favorable’’ or ‘‘unfavorable’’ (Wan Ngah, 2002). The essential features of a Langmuir isotherm can be expressed in terms of a dimensionless constant separation factor or equilibrium parameter, R_L; which is defined by:

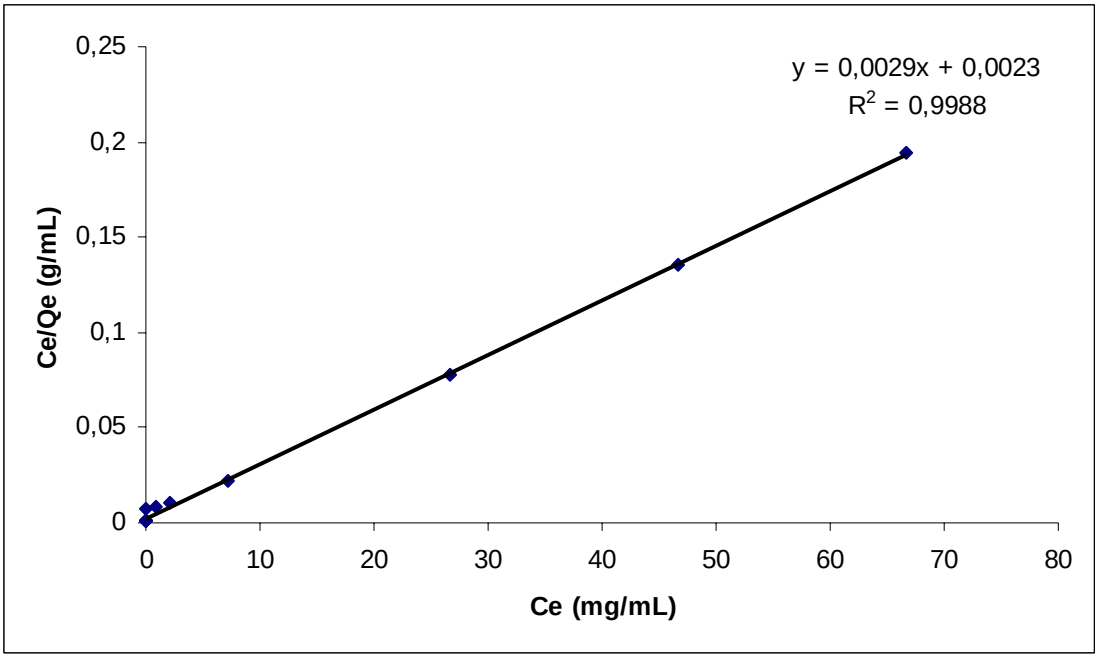

Figure 4.8. Linear plot of Langmuir adsorption isotherm for PHEMA-CB cryogel.

$$R_L = 1 / (1 + b.C_o) \quad (4.2)$$

where C_o is the initial HSA concentration (mg/mL), and b is the Langmuir adsorption equilibrium constant (mL/mg). The parameter $R_L > 1$; $R_L = 1$; $0 < R_L < 1$; $R_L = 0$ indicates the isotherm shape according to unfavorable, linear, favorable and irreversible, respectively. The values of R_L calculated for different initial HSA concentration for PHEMA-CB cryogel are given in Table 4.3. The R_L values show that favorable adsorption of HSA on PHEMA-CB cryogel takes place; therefore the PHEMA-CB cryogel is a favorable adsorbent.

Table 4.3. The R_L values based on the Langmuir equation.

Initial concentration (mg/mL)	R_L
0.5	0.613
1.0	0.442
2.0	0.284
5.0	0.137
10	0.074
20	0.038
40	0.019
80	0.010

The other well known isotherm, which is frequently used to describe adsorption behavior, is the Freundlich isotherm. The Freundlich isotherm used for isothermal adsorption is a special case for heterogeneous surface energy in which the energy term in the Langmuir equation varies as a function of surface coverage strictly due to variation of the sorption. The Freundlich equation is:

$$Q_e = Q_F . C_e^{1/n} \qquad (4.3)$$

where Q_F is roughly an indicator of the adsorption capacity and *1/n* is the Freundlich exponent which represents the heterogeneity of the system. Q_F and *1/n* can be determined from the linear plot of *ln* Q_e versus *ln* C_e (Figure 4.9). The Freundlich isotherm describes reversible adsorption and is not restricted to the formation of the monolayer. A more homogeneous system will have *n* value approaching unity while a more heterogeneous system will have an *n* value approaching zero (Umpleby, 2001).

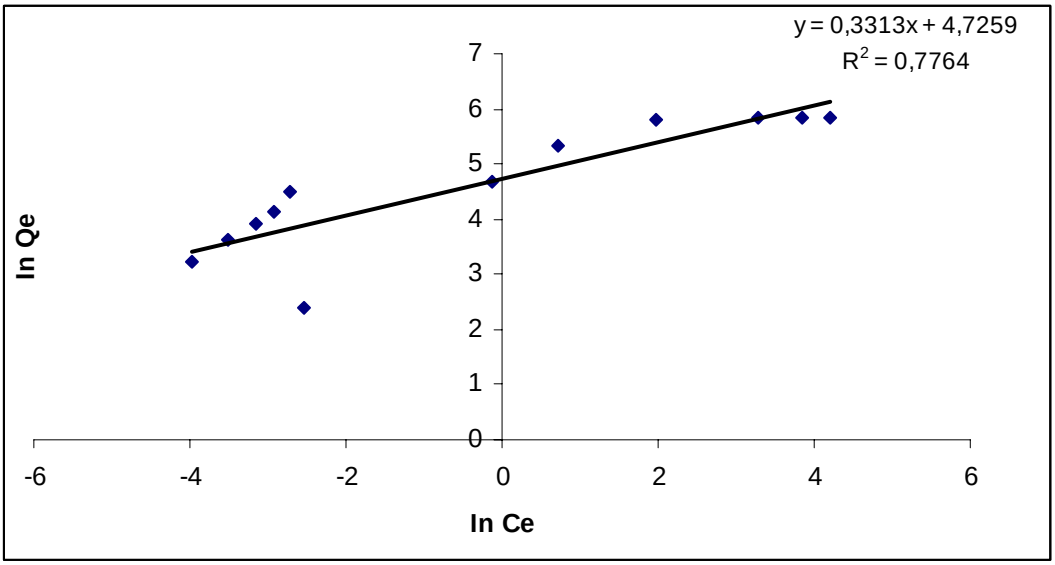

Figure 4.9. Linear plot of Freundlich adsorption isotherm for PHEMA-CB cryogel.

Table 4.4. Langmuir and Freundlich isotherm constants for PHEMA-CB cryogel.

Notation for cryogel	Experimental	Langmuir constants				Freundlich constants		
	Q_e (mg/g)	Q_{max} (mg/g)	b (mg/mL)	R_L	R^2	Q_F (mg/g)	n	R^2
PHEMA-CB	343.4	344.8	1.26	0.019	0.9988	112.8	3.02	0.7764

The experimental data tend to be better fitted with Langmuir rather than Freundlich isotherm, since the correlation coefficient (R^2) was high (0.99) (Table 4.4). The maximum amount of adsorption (343.4 mg/g) obtained from experimental results is also very close to the calculated Langmuir adsorption capacity (344.8 mg/g). The Langmuir and Freundlich constants with the correlation coefficients are given in Table 4.4. In Figure 4.10, the experimental adsorption behavior was compared with Langmuir and Freundlich adsorption isotherms. It can be concluded that the adsorption of HSA onto PHEMA-CB cryogel is a monolayer adsorption.

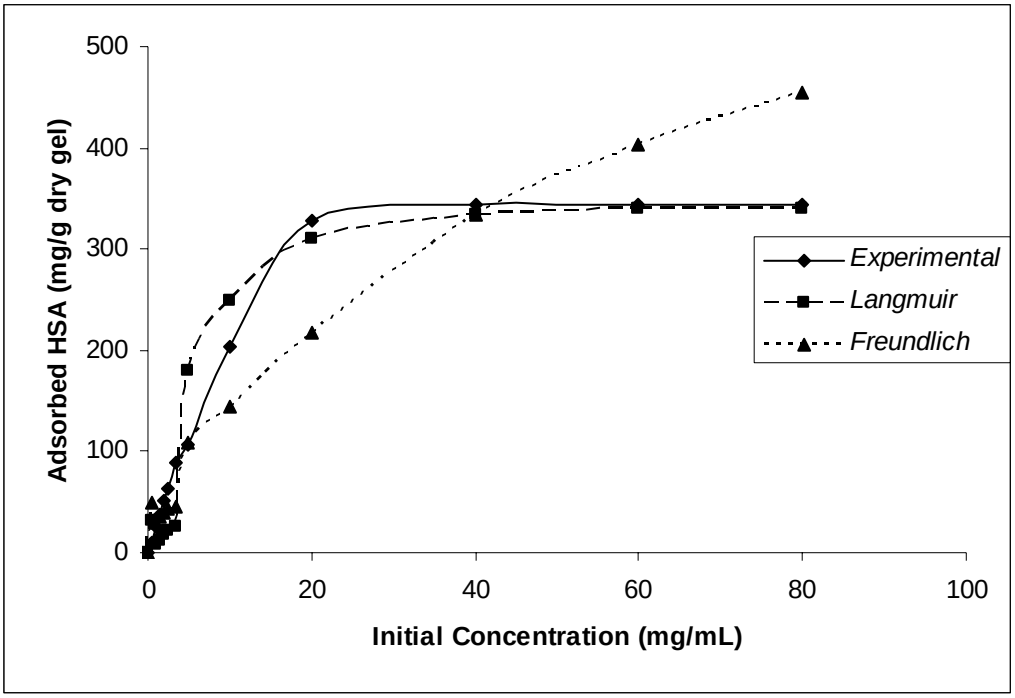

Figure 4.10. Experimental data for HSA adsorption on PHEMA-CB cryogel fitted to Langmuir and Freundlich isotherms, respectively. Experimental conditions: running buffer: 50 mM acetate buffer, pH 5.0, T: 20ºC, flow rate: 0.5 mL/min, $m_{dry\ cryogel}$: 0.4 g.

In order to examine the controlling mechanism of adsorption process such as mass transfer and chemical reaction, kinetic models were used to test experimental data. The kinetic models (Pseudo-first and second-order equations) can be used in this case assuming that the measured concentrations are equal to adsorbent surface concentrations. The first-order rate equation of Lagergren is one of the most widely used for the adsorption of solute from a liquid solution (Cheung, 2001). It can be represented as follows:

$$\Delta q_t/d_t=k_1(Q_e-q_t) \quad (4.4)$$

where k_1 is the rate constant of pseudo-first order adsorption (1/min) and Q_e and q_t denote the amounts of adsorbed protein at equilibrium and at time t (mg/g), respectively. After integration by applying boundary conditions, $q_t=0$ at t=0 and $q_t=q_t$ at t=t, gives

$$\log[Q_e/(Q_e-q_t)]= (k_1t)/2.303 \quad (4.5)$$

Equation 4.6 can be rearranged to obtain a linear form

$$\log(Q_e-q_t)= \log(Q_e) - (k_1t)/2.303 \quad (4.6)$$

a plot of $\log(Q_e)$ versus t should give a straight line to confirm the applicability of the kinetic model. In a true first-order process $\log(Q_e)$ should be equal to the interception point of a plot of $\log(Q_e-q_t)$ via t.

In addition, a pseudo-second order equation based on adsorption equilibrium capacity may be expressed in the form,

$$\Delta q_t/dt = k_2 (Q_e-q_t)^2 \quad (4.7)$$

where k_2 (g/mg.min) is the rate constant of pseudo-first order adsorption process. Integrating equation 4.7, q and applying the boundary conditions, $q_t=0$ at t=0 and $q_t=q_t$ at t=t, leads to

$$1/(Q_e-q_t) = (1/Q_e) + k_2t \quad (4.8)$$

or equivalently for linear form

$$(t/q_t)= (1/k_2Q_e^2) + (1/Q_e)\, t \quad (4.9)$$

a plot of t/q_t versus t should give a linear relationship for the applicability of the second-order kinetics. The rate constant (k_2) and adsorption at equilibrium (Q_e) can be obtained from the intercept and slope, respectively.

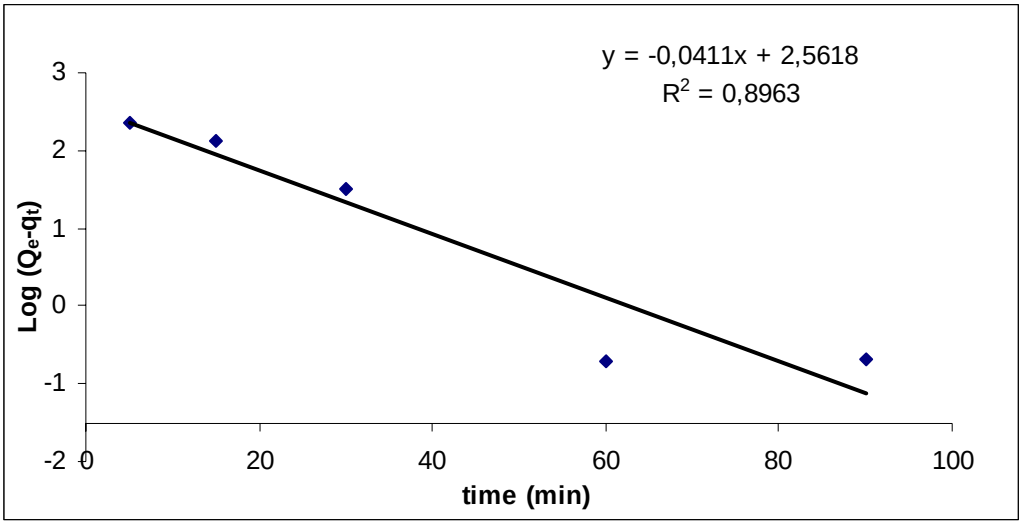

Figure 4.11. Pseudo-first-order kinetic of the experimental data for the adsorbent.

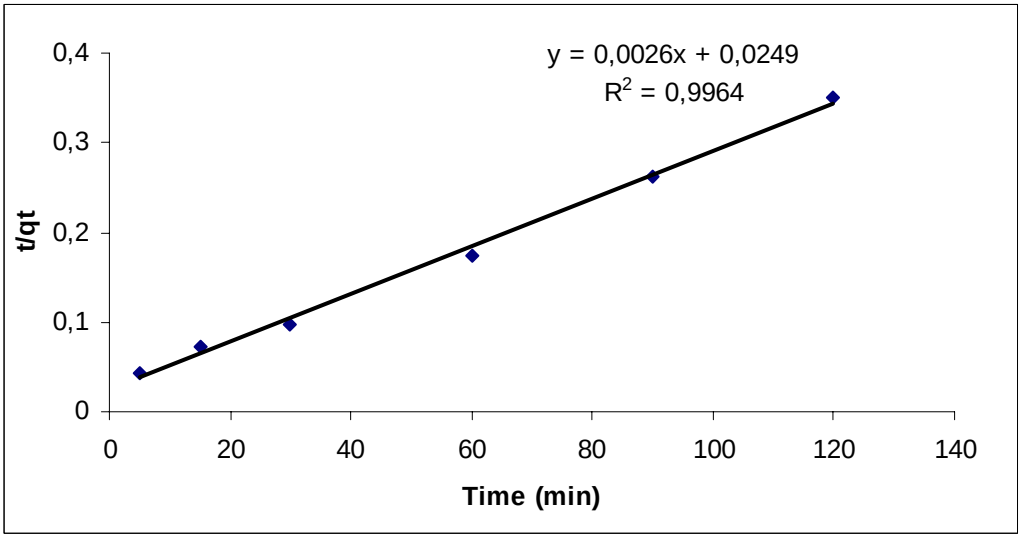

Figure 4.12. Pseudo-second-order kinetic of the experimental data for the adsorbent.

Table 4.5. The first and second order kinetic constants for PHEMA-CB cryogel.

Equilibrium	**Experimental**	**First-order kinetic**			**Second-order kinetic**		
Conc. (mg/mL)	**Q_e** (mg/g)	**k_1** (1/min)	**Q_e** (mg/g)	**R^2**	**k_2** (g/mg.min)	**Q_e** (mg/g)	**R^2**
40.0	343.4	0.095	12.96	0.8963	2.71×10^{-4}	384.61	0.9964

A comparison of the experimental adsorption capacity and the theoretical values which obtained from Figure 4.11 and 4.12 are presented in Table 4.5. The correlation coefficient for the linear plot of log (Q_e-q_t) vs. t for the pseudo-first order equation is lower than the correlation coefficient for the pseudo-second order equation. These values show that this adsorbent system is not so well described by pseudo-first-order kinetic model. Moreover, the rate constant for second-order kinetic (k_2) is lower than first-order rate constant (k_1), which denotes the adsorption rate was controlled by second-order kinetic. By these results, it is suggested that the pseudo-second order adsorption mechanism is predominant and that the overall rate of the HSA adsorption process appeared to be controlled by chemical process.

4.2.1.1.4. Effect of Ionic Strength

The ionic interactions give an essential contribution to the recognition and binding process. The effect of NaCl concentration on HSA adsorption is presented in Figure 4.13, which shows that the adsorption capacity decreases with increasing ionic strength of the binding acetate buffer. HSA adsorption amount decreased from 50.4 to 11.5 mg/g with the increasing NaCl concentration. Increasing the NaCl concentration could promote the adsorption of the dye molecules to the polymer surface by hydrophobic interaction. Moreover, the hydrophobic interactions between the immobilized dye molecules themselves would also become strong, because it has been observed that the salt addition to a dye solution caused the stacking of the free dye molecules. Thus, the numbers of the immobilized dye molecules accessible to HSA would decrease as the ionic strength increased, and the adsorption of the HSA to immobilized dye became difficult. It is also suggested that an increase in NaCl concentration result in the reduction of electrostatic interactions through masking of sulfonic acid groups of CB by sodium ions (Denizli, 2001). It should be also noted that a significant decrease of HSA adsorption onto PHEMA cryogel was not observed. It has been reported that the situation is particularly anxious when electrostatic and hydrophobic interactions occur at the same time, since an increase in the ionic strength of the solution decreases the former type of interaction.

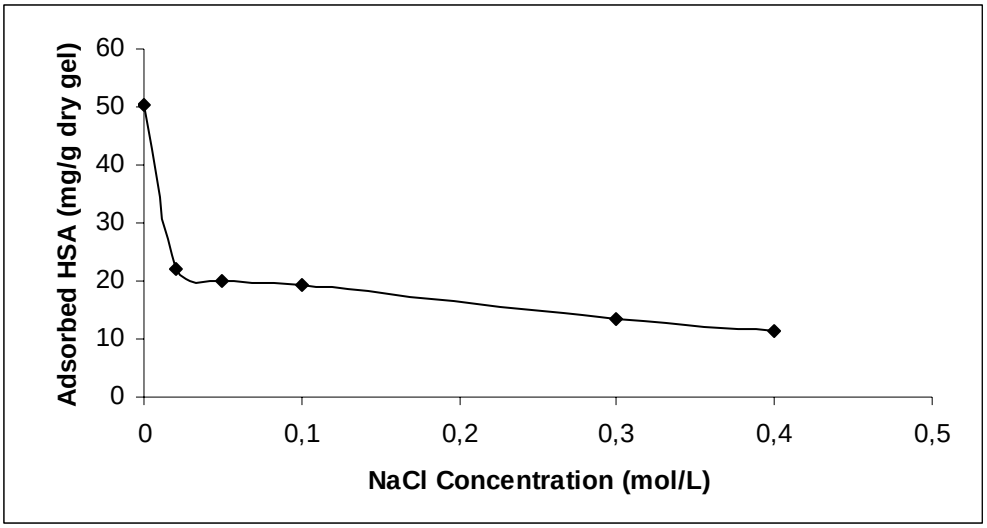

Figure 4.13. Effect of ionic strength on HSA adsorption onto the PHEMA-CB cryogel. Experimental conditions; running buffer: 50 mM acetate buffer (pH 5.0), T: 20ºC, flow rate: 0.5 mL/min, HSA concentration: 2 mg/mL, $V_{solution:}$ 10 mL, $m_{dry\ cryogel}$: 0.4 g.

4.2.1.1.5. Effect of Temperature

The increased temperature enhances protein retention and the lowered temperature generally promotes the protein elution. Effect of temperature on the adsorption of HSA on PHEMA-CB cryogel was presented in Figure 4.14. As shown in the Figure 4.14, adsorption of HSA on the PHEMA-CB cryogel slightly increased with increasing temperature. The aromatic groups of CB interact with protein molecules via hydrophobic interactions. As the temperature increases, the hydrophobic groups of HSA come out to interact with antraquinone moiety of CB. In fact, a hydrophobic interaction is an entropy-driven process. Since ΔH may be a small positive or negative value, ΔG is controlled by a positive entropy change and thus increases with temperature. In addition to, Van der Waals attraction forces, which operate in hydrophobic interactions increase with increasing temperature.

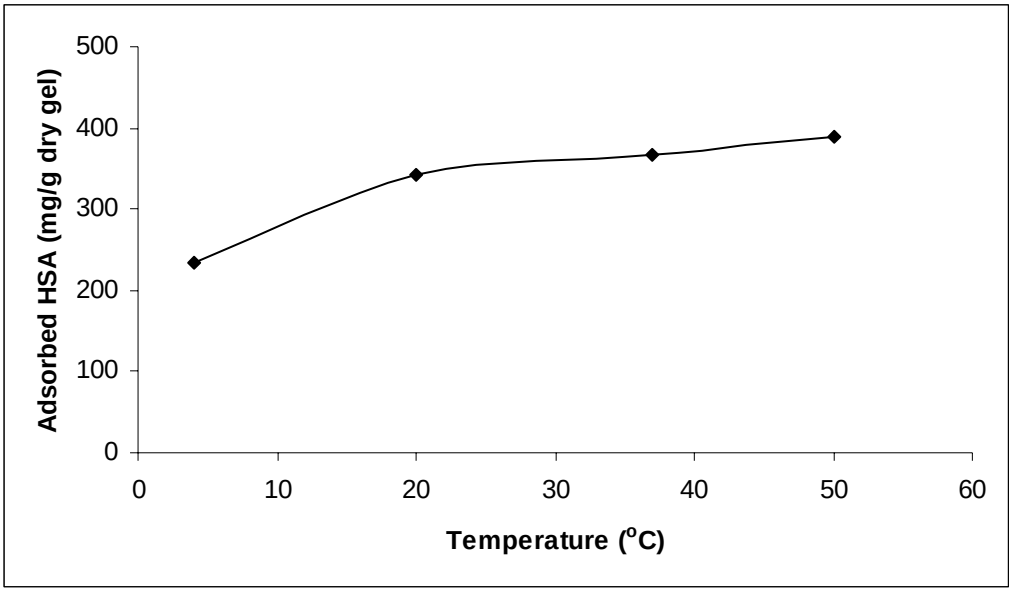

Figure 4.14. Effect of temperature on HSA adsorption onto the PHEMA-CB cryogel. Experimental conditions; running buffer: 50 mM acetate buffer (pH 5.0), flow rate: 0.5 mL/min, HSA concentration: 2 mg/mL, $V_{solution}$: 10 mL, $m_{dry\ cryogel}$: 0.4 g.

4.2.1.2. Adsorption of HSA from Human Serum

Adsorption efficiency of PHEMA-CB cryogel was investigated by circulating the whole serum in one-step affinity column system. The main advantage of cryogels was flow the whole serum through to column without any blockage due to the interconnected supermacroporous structure (Noppe, 2007; Garipcan, 2002; Ozcan, 2006; Arvidson, 2003). Figure 4.15 shows the depletion efficiency of HSA from human serum with different serum dilution ratios. PBS was used for dilution of human serum by 1/2, 1/5, 1/10 ratios. The maximum adsorption capacity for PHEMA-CB cryogel column was obtained as 948.7 mg/g cryogel for non-diluted serum. The adsorption capacity decreased with increasing dilution ratios while the depletion ratio of HSA remained as 77 % in serum sample. The elution of bound HSA to PHEMA-CB column was obtained by 50 mM pH 7.0 phosphate buffer containing 1M NaCl solution. Desorption ratio was achieved as 92 % in elution buffer. No reduction in column capacity has been observed with re-use of the PHEMA-CB cryogel up to ten times (data not shown).

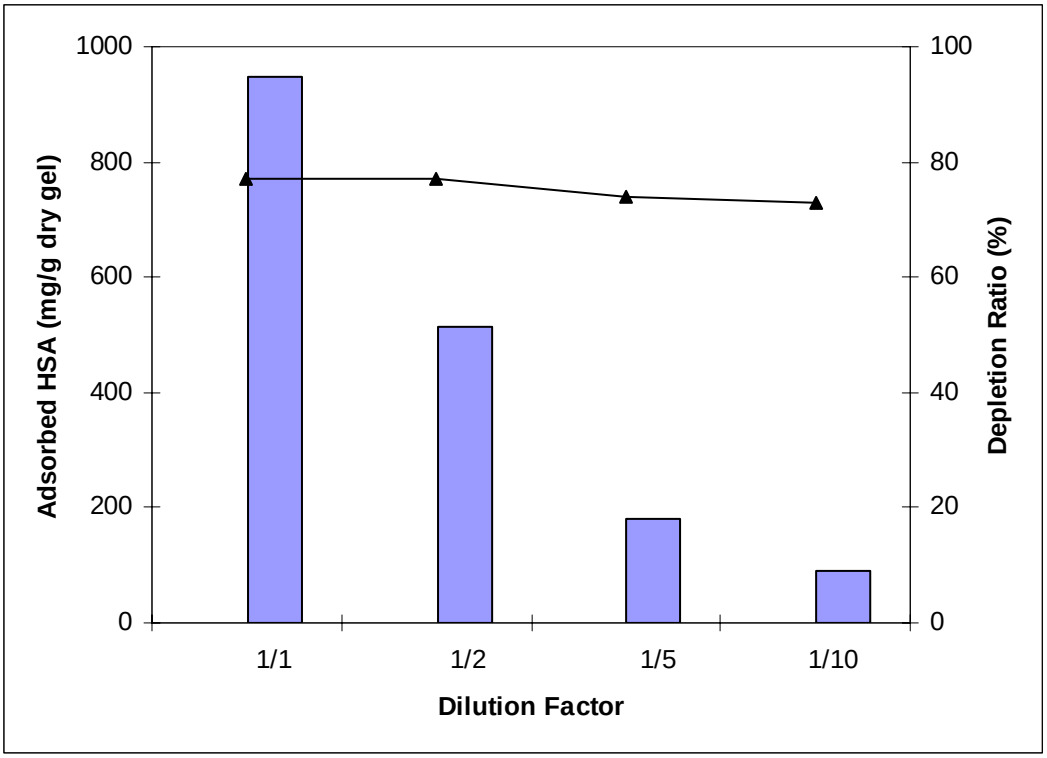

Figure 4.15. Depletion efficiency of HSA with different dilution ratios of human serum in PHEMA-CB column. ∏ Adsorbed HSA (mg/g dry cryogel). ▲Depletion ratio (%) of HSA in human serum. Experimental conditions; dilution buffer: 50 mM of PBS (pH 7.4), flow rate: 0.5 mL/min, HSA initial concentration: 48 mg/mL, $V_{solution}$: 10 mL, $m_{dry\ cryogel}$: 0.4 g.

The FPLC step focused on the rapid removal of the high abundant proteins from the human serum. PHEMA-CB cryogel column with a high binding capacity, well suited for depletion, was optimized for FPLC application. As shown in Figure 4.16, optimization of the depletion step allowed the use of a step elution at high flow rate (3 mL/min) with low back pressure (0.25 mPa) to speed up the purification. This was particularly advantageous when working with this potentially unstable sample.

In Figure 4.16, high abundant proteins such as HSA were eluted from human serum by linear gradient of two mobile phases A and B. After a 9.0 min starting period with 100% mobile phase A, a linear gradient started from 0% B to 100% B in 3.0 min, continued with 4.0 min 100% eluent B and finished last 4 min 100% buffer A.

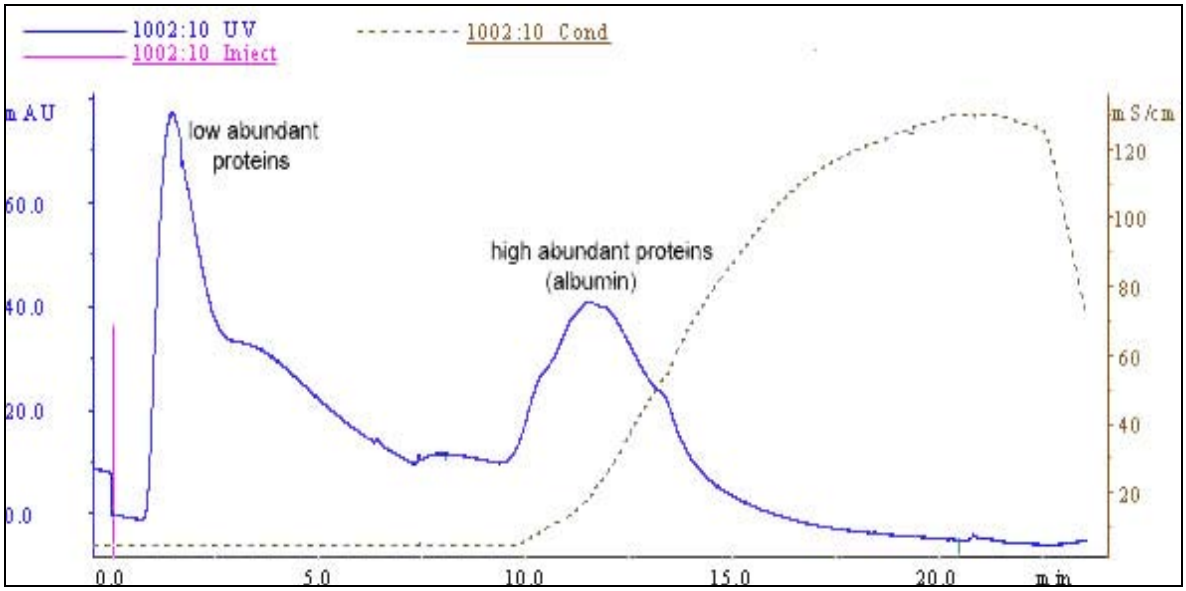

Figure 4.16. Separation of serum proteins via PHEMA-CB column with FPLC. Experimental conditions; sample volume: 2 mL, mobile phase A: 50 mM phosphate buffer (pH 7.0), mobile phase B: 50 mM phosphate buffer (pH 7.0) + 1.0 M NaCl, flow rate: 3 mL/min, column volume: 8 mL, back pressure: 0.25 mPa, λ: 280 nm.

Figure 4.17 shows the SDS-PAGE analysis of human serum before and after treatment with PHEMA-CB cryogel column. Lane 1 and Lane 2 correspond to Standard HSA and IgG samples (1 mg/mL), respectively, in order to control the molecular weight marker. As seen in Lane 3, the high abundant protein albumin masked the low abundant proteins in human serum. After three repeated treatment with PHEMA-CB cryogel column, the decrease in HSA concentration clearly seen in Lane 4. Furthermore, the number of bands increased as observed on the right side of Figure 4.17. It was monitored 20 serum proteins in Lane 4. The elution of HSA was placed in Lane 6. PHEMA-CB cryogel column was prepared for depletion of high abundant proteins such as HSA in human serum. CB based ligands may also bind many other abundant serum proteins (Gianazza and Arnaud, 1982). Therefore, the presence of additional bands was as a consequence of low capacity adsorption of IgG (12% of removal efficiency) in human serum.

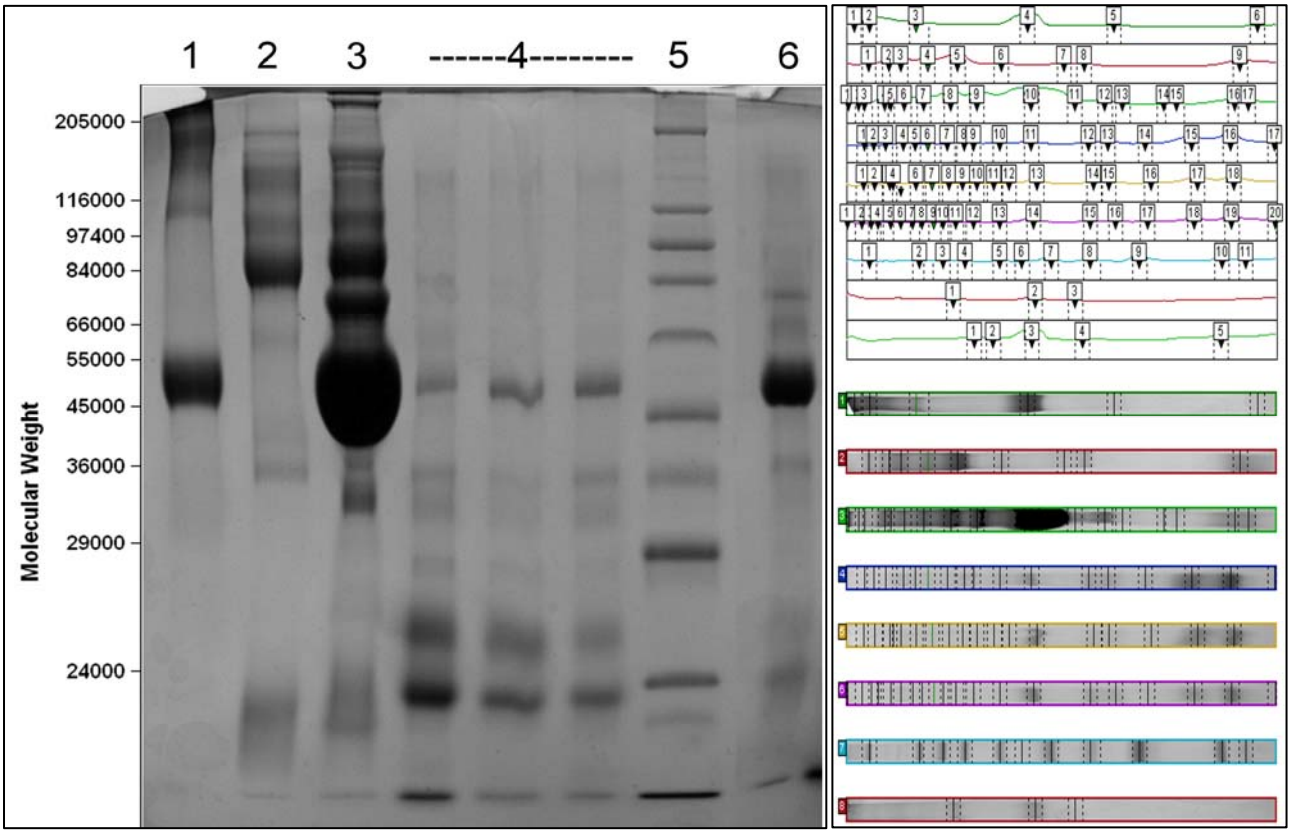

Figure 4.17. SDS-PAGE analysis of human serum before and after treatment with PHEMA-CB cryogel column. 5–12% SDS-PAGE, Lane 1: Standard HSA (1 mg/mL), Lane 2: Standard IgG (1mg/mL), Lane 3: untreated human serum, Lane 4: human serum after three repeated treatment with cryogel column, Lane 5: Wide range Sigma Marker (Molecular Weight, Da), Lane 6: the elution from the cryogel column.

4.2.2. Desorption and Reusability

In general, the regeneration of adsorption columns is a crucial step to render these columns more affordable for laboratory and commercial applications. Desorption ratios as high as 95% have been achieved and after 10 adsorption-desorption cycles, the PHEMA-CB cryogel column maintained of about 90% of initial binding capacity (Figure 4.18).

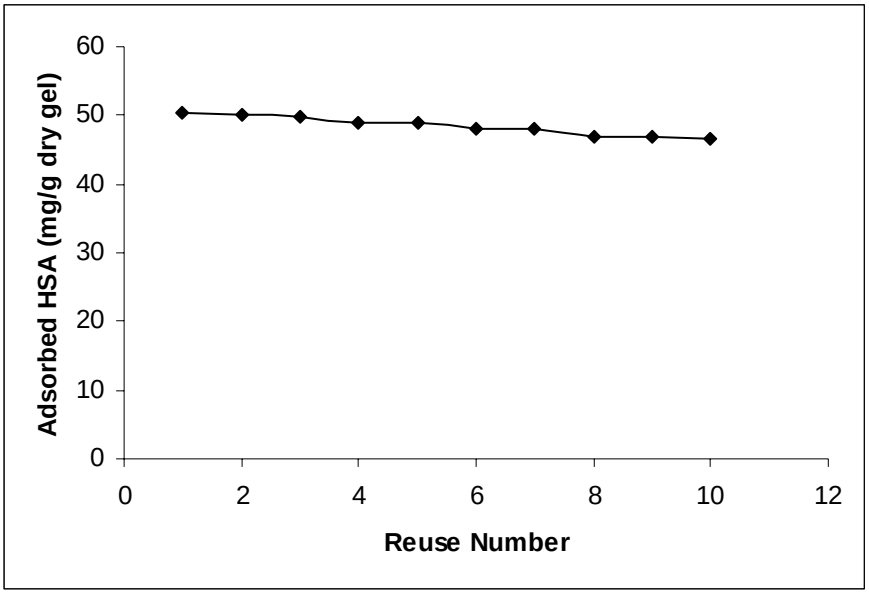

Figure 4.18. Adsorption-desorption cycle showing the reusability potential of PHEMA-CB cryogel column. Desorption buffer: 50 mM phosphate buffer (pH 7.0) + 1M NaCl; HSA concentration: 2 mg/mL, flow rate: 0.5 mL/min, T: 20ºC, $m_{dry\ cryogel}$: 0.4 g.

4.2.3. Binding Properties of CB Bound to HSA

CB is a derivative of monochlorotriazine dye (Figure 2.4a), containing three titratable acidic sulfonate groups and four basic primary and secondary aromatic amine groups, which binds with considerable specificity and affinity to nucleotide dependent enzymes and to a series of other proteins including serum albumin (Kopperschlager, 1982). For instance, Odabaşı and Denizli observed an increase in the level of HSA adsorption onto a CB-immobilized PHEMA adsorbent (Odabaşı, 2004). However, the exact binding mechanism of immobilized CB and the origin of its selectivity towards HSA currently remain mysterious. Thus, seeking ways to address a binding mechanism for HSA + CB mutual relationship has been of primary importance in the development of more efficient affinity separation systems.

CB was favorably docked by DOCKv6.2 (UCSF) into binding site II (ibuprofen/indomethacine binding site) of HSA using the X-ray coordinates of HSA (PDB ID: 2BXQ, Ghuman, 2005), shown in Figure 4.19, while it was determined

that CB does not bind binding site I (phenylbutazone/diazepam binding site) of HSA. Out of 4 different docked conformers of CB, energetically the most favorable CB conformer was selected.

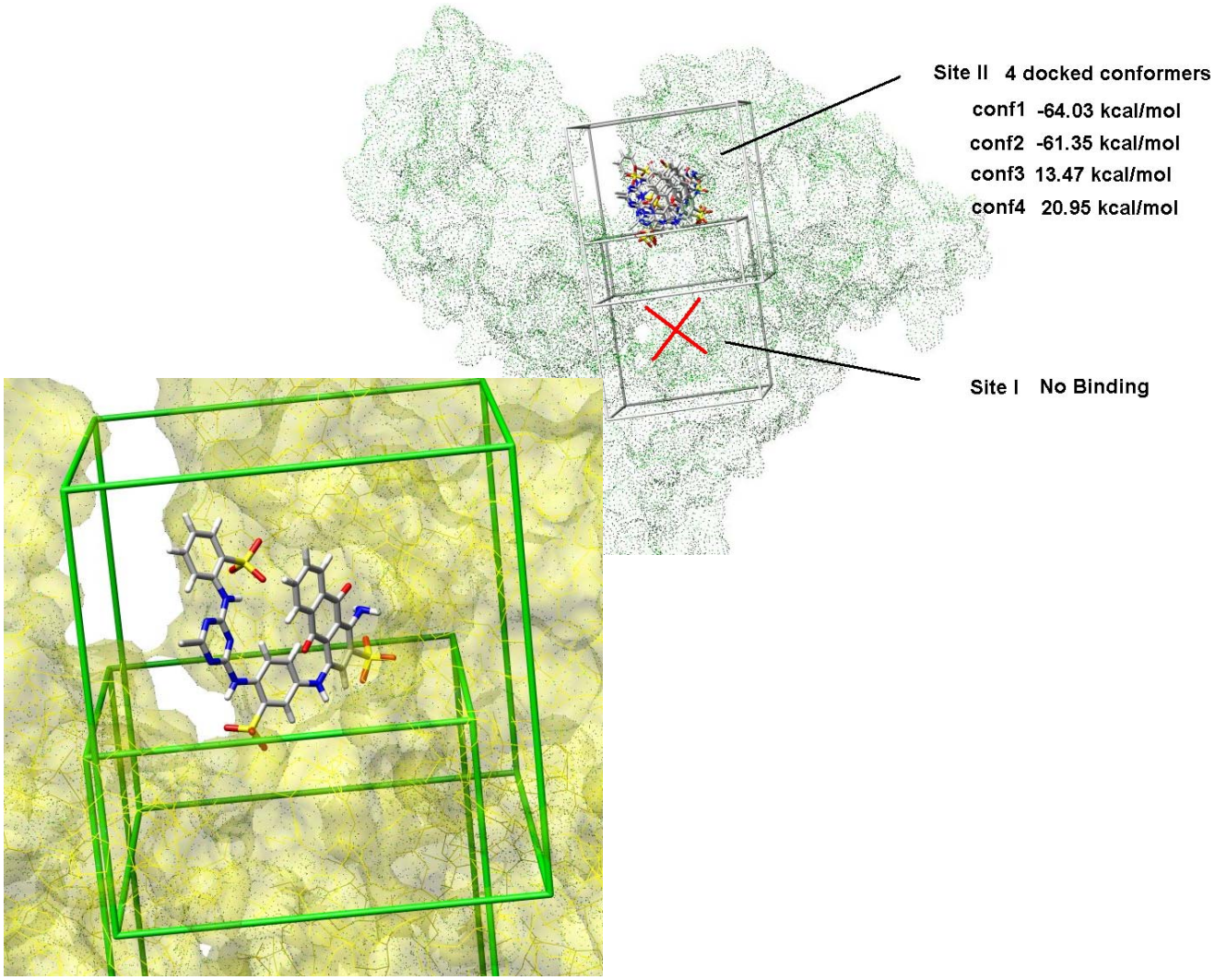

Figure 4.19. 4 different conformers of CB docked into binding site II of HSA (top). Conformer 1 of CB in binding site II of HSA (below).

Molecular dynamics (MD) and thermodynamic computations were implemented by AMBER v10 (Assisted Model Building with Energy Refinement) suite of programs (Case, 2008) running mainly under a 64 bit parallel Linux-PC system. In order to illuminate the binding properties of CB in complex with HSA, 10 ns of MD was applied by AMBER v10 (Case, 2008) using the x-ray coordinates of HSA (PDB ID: 2BXQ) including myristate residues and docked coordinates of CB. Figure 4.20 illustrates 10 ns of RMSD (Å) plots for the protein (black) and for the ligand (red), suggesting that both the ligand and receptor have equilibrated over 6000 psec (6 nsec) of MD.

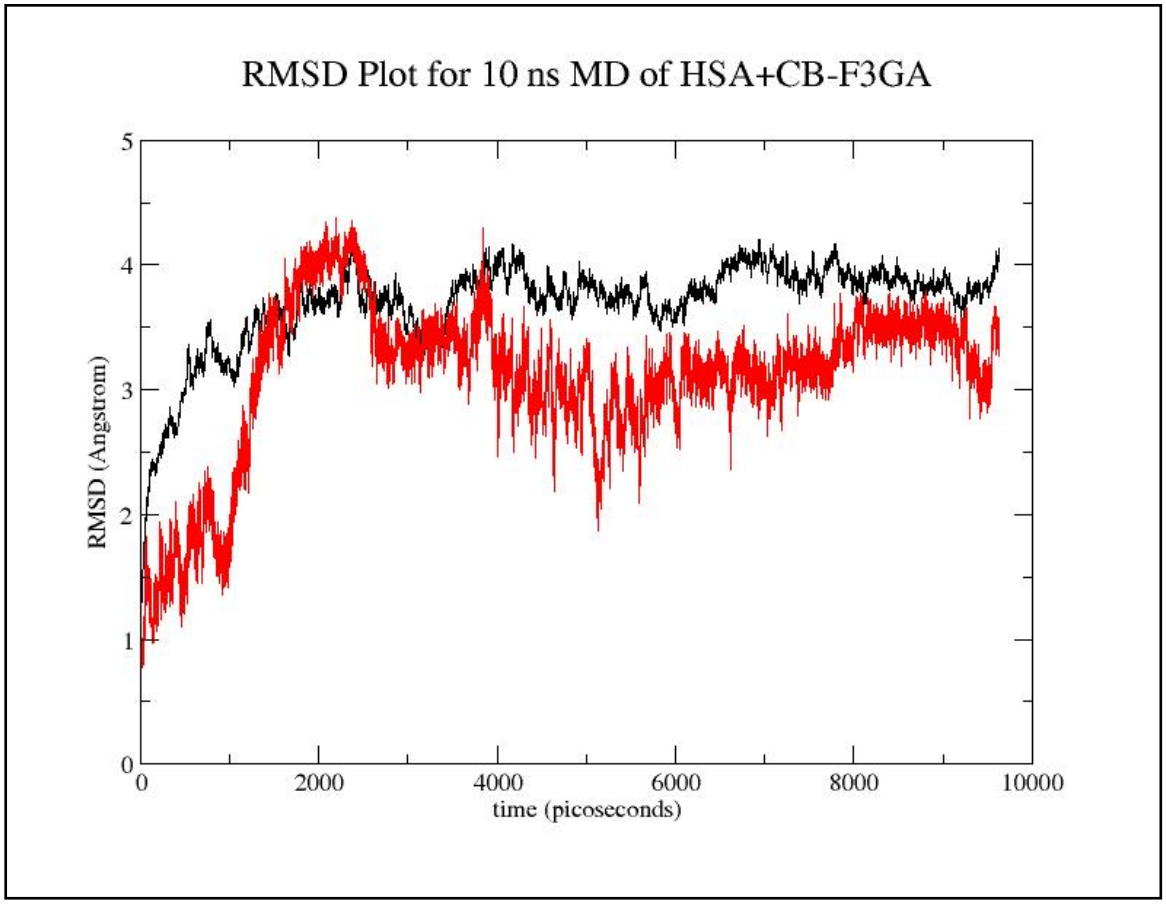

Figure 4.20. Root-mean-square deviations (Å) of CB referenced to docked coordinates (red line) and HSA (black line) for 10000 ps (10 ns) simulation referenced to the X-ray structure coordinates.

Figure 4.21 is a picture of CB in complex with HSA after 10 ns of MD. It was determined that CB snugly fits in the binding site and makes specific H-bonding interactions with the protein. These H-bonding interactions mainly occur between

the sulfonate groups of CB and the guanidino groups of neighboring arginine residues of HSA. The figure also indicates that the chloro-triazine group of CB (marked with asterisks in the figure) sticks out the binding site making CB a strong candidate for immobilization onto solid supports for application in depletion of HSA from human serum.

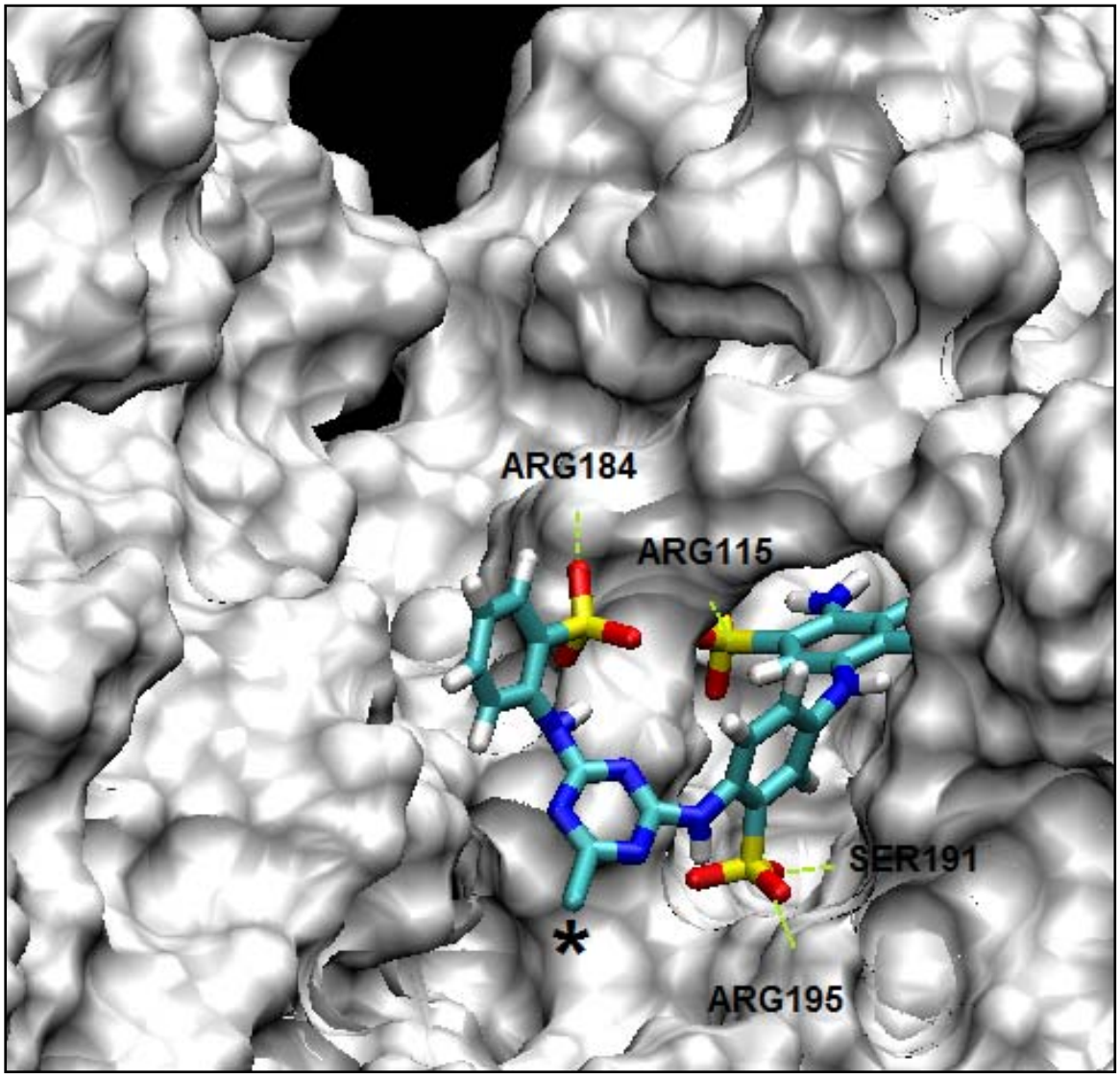

Figure 4.21. A picture of CB in complex with HSA at 10 ns of MD. Green lines indicate strong H-bonding interactions. (*) chloro-triazine group of CB.

To analyze thermodynamic properties of CB in complex with HSA, MM-PBSA (Molecular Mechanics-Poisson Boltzmann/Surface Area) technique of AMBER v10 (Case, 2008) was applied on a single trajectory of the complex. 100 snapshots

between 9 and 10 ns of trajectory were extracted to average out MM-PBSA binding energies listed in Table 4.6.

Table 4.6. MM-PBSA binding energy results.

ΔH_{gas}			ΔG_{solv}		
ΔE_{el}	ΔE_{vdw}	ΔE_{int}	ΔG_{el}	ΔG_{nonel}	$(\Delta H_{gas} + \Delta G_{solv})$
-146.74±99.33	-51.25±32.04	0.82±56.88	131.14±92.95	-7.80±1.57	-42.63±55.57

$T.\Delta S_{trans}$	$T.\Delta S_{rot}$	$T.\Delta S_{vib}$	$T.\Delta S_{tot}$	ΔH_{tot}	$\Delta G_{binding} = \Delta H_{tot} - T.\Delta S_{tot}$
-13.72	-12.19	4.63	-21.28	-42.63	- 21.25

The enthalpy term is dissected into subenergy terms as in;

$$H_{tot} = H_{gas} + H_{tans/rot} + G_{solv} \quad (4.10)$$

where H_{gas} is the potential energy of the solute which is determined as a sum of van der Waals (E_{vdw}), electrostatic (E_{el}) and internal energies (E_{int}) in gas phase by *sander* using the molecular mechanics algorithm in Cornell et. al (1995) force field (Cornell, 1995), $H_{tans/rot}$ is due to six translational and rotational degrees of freedom (6*1/2RT) and is equal to 1.79 kcal/mol at 300 K, and G_{solv} is the solvation free energy for transferring the solute from vacuum into solvent and is a sum of electrostatic (G_{el}) and non-electrostatic (hydrophobic) contributions (G_{nonel}). ΔG_{el} and ΔG_{nonel} represent electrostatic and nonelectrostatic, respectively, contributions to the solvation free energy (ΔG_{solv}). ΔH_{tot} is the enthalpy of binding and is equal to [ΔH_{gas} + ΔG_{solv}]. ΔS_{tot} is the entropy of binding and is a product of translational (ΔS_{trans}), rotational (ΔS_{rot}) and vibrational (ΔS_{vib}) entropy changes. $\Delta G_{binding}$ is the binding free energy and is equal to [$\Delta G_{binding} = \Delta H - T.\Delta S_{tot}$] (Andaç, 2007).

The electrostatic interaction energy in gas phase (ΔE_{el}) between the receptor and CB is favorable by –146.74 ± 99.33 kcal/mol. On the other hand, electrostatic contributions to the solvation energy ($\Delta G_{\mathbf{el}}$) is disfavorable by 131.14 ± 92.95 kcal/mol, which altogether sum to a favorable electrostatic contribution ($\Delta E_{\mathbf{el}}$ + $\Delta G_{\mathbf{el}}$) to the enthalpy of binding by 15.6 kcal/mol, suggesting that the binding of CB is enhanced by residual water molecules at the binding interface. The van der Waals (vdW) interaction energy in gas phase (ΔE_{vdw}= -51.25 ± 32.04 kcal/mol) associated with nonpolar contributions to the solvation energy (ΔG_{nonel}= -7.80 ± 1.57 kcal/mol) seems to favorably contribute to the binding process, yielding a total vdW/hydrophobic energy (ΔE_{vdw} + ΔG_{nonel}) of -59.05 kcal/mol. Therefore, it was determined that both vdW/hydrophobic and electrostatic energies make favorable contribution to the enthalpy of binding (ΔH_{tot}= -42.63 kcal/mol). The entropic term of the binding energy is disfavorable (-T.ΔS_{tot} = -21.28 kcal/mol), which is compensated by a favorable enthalpy term (ΔH_{tot}) to yield a favorable binding energy of -21.25 kcal/mol ($\Delta G_{binding}$ = ΔH_{tot} - T.ΔS_{tot}) suggesting that CB-possesses a very high binding affinity towards HSA.

4.3. HSA imprinted PHEMAPA (PHEMAPA-HSA) cryogel

N-methacryloyl-L-phenylalanine (MAPA) was synthesized as a functional ligand for the interaction with HSA via phenyl and carboxyl group prior to polymerization. Recently, our laboratory developed MAPA ligand for hydrophobic interaction chromatography of proteins by introducing functional groups into polymer structure without any leakage (Öncel, 2005; Öztürk, 2007). The preparation of HSA imprinted cryogel was organized in three main parts.

In the first part; MAPA was synthesized by reacting methacryloyl chloride with L-phenylalanine. MAPA was then complexed with HSA. In the second part; PHEMAPA-HSA cryogel was prepared in the presence of MAPA-HSA complex by free radical polymerization below 0°C. In the third part; HSA was removed by a convenient desorption agent to have imprinted cavities for molecular recognition of HSA (Figure 4.22).

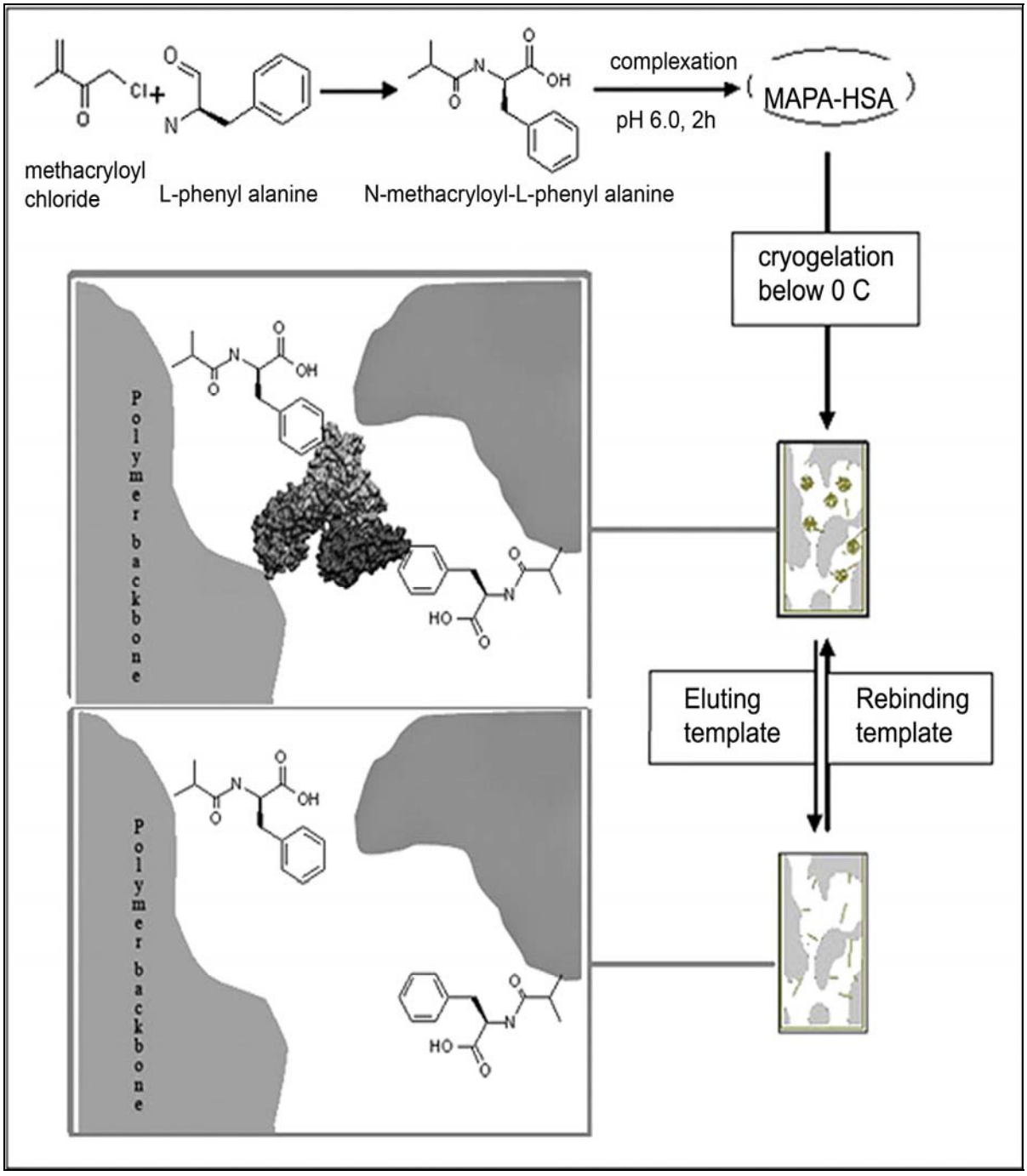

Figure 4.22. Schematic illustration of preparation of PHEMAPA-HSA cryogel.

^{1}H-NMR was used to determine the synthesis of MAPA structure. Figure 4.23 shows the ^{1}H-NMR spectrum of MAPA. ^{1}H-NMR spectrum is shown to indicate the characteristic peaks from the groups in MAPA monomer. These characteristic peaks are as flows: ^{1}H-NMR ($CDCl_3$) 2.84 (t; 3H, J=7.06 Hz, CH_3), 3.05–3.19 (m; 2H, CH_2), 4.80–4.85 (m; 1 H, methin), 5.24 (s; 1H, vinyl H), 5.56 (s; 1H, vinyl); 6.24 (d; 1H, J=7.4 Hz, NH), 7.04–7.20 (m; 5H, aromatic), 10.07 (s; 1H, OH).

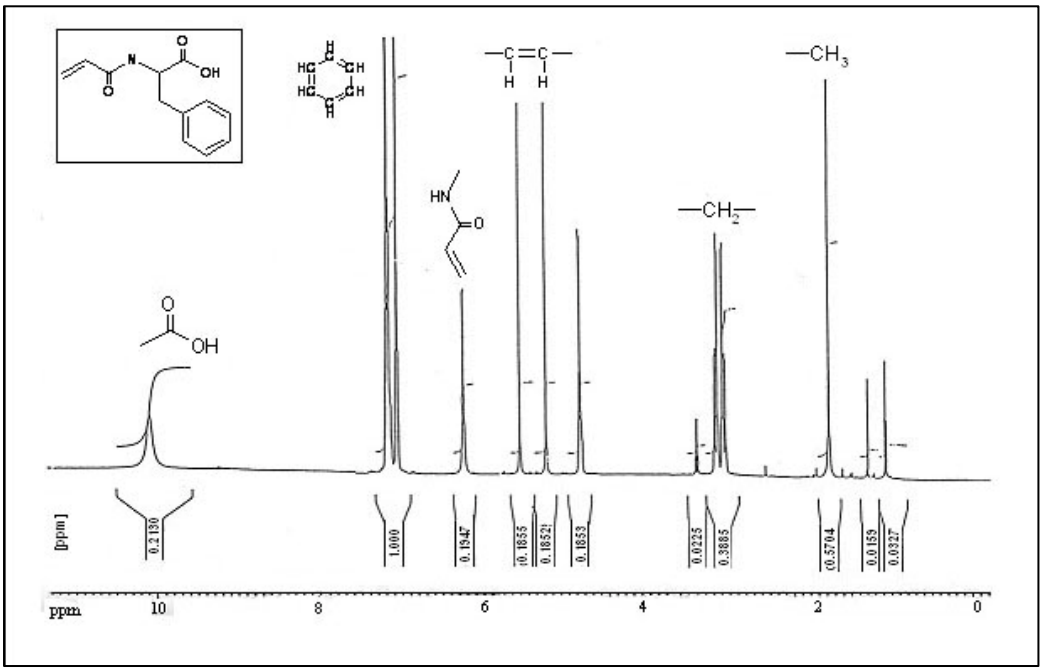

Figure 4.23. ^{1}H-NMR spectrum of MAPA monomer.

FTIR spectra of MAPA having the characteristic bands at 3396 cm^{-1} and 1735 cm^{-1} due to NH asymmetric stretching and COO- stretching confirmed the existence of amino group (Figure 4.24A). The band at 3030 cm^{-1} established the presence of CH group. The strong band at 2952 cm^{-1} established the presence of CH_2 asymmetric stretching. The presence of the band at 1736 cm^{-1} indicated the presence of C–O stretching vibrations. It was observed that MAPA have the characteristic stretching vibration band amide I and amide II absorption bands at 1658 cm^{-1} and 1455 cm^{-1}. The bands at 1524 cm^{-1} and 1440 cm^{-1} established the presence of C=O anti symmetric and symmetric stretching. The band at 1029 cm^{-1} established the presence of C-N stretching. The bands at 1081 cm^{-1} and 745 cm^{-1} established the presence of benzene ring. The bands at 829 cm^{-1} and 695 cm^{-1} established the presence of substituted ring 1,4 distribution. The changes in MAPA-HSA complex indicated the interaction between monomer and protein template. C-O stretching bands of MAPA monomer was shifted to higher frequencies with an intensity decrease, while an intensity decrease and shifting to lower frequencies was observed in benzene ring band. The characteristic broad peak at around 3473 cm^{-1} indicates the O–H stretching vibrations for MAPA-HSA complex (Figure 4.24A). It was observed that both electrostatic and hydrophobic interactions were taken in place during complex formation.

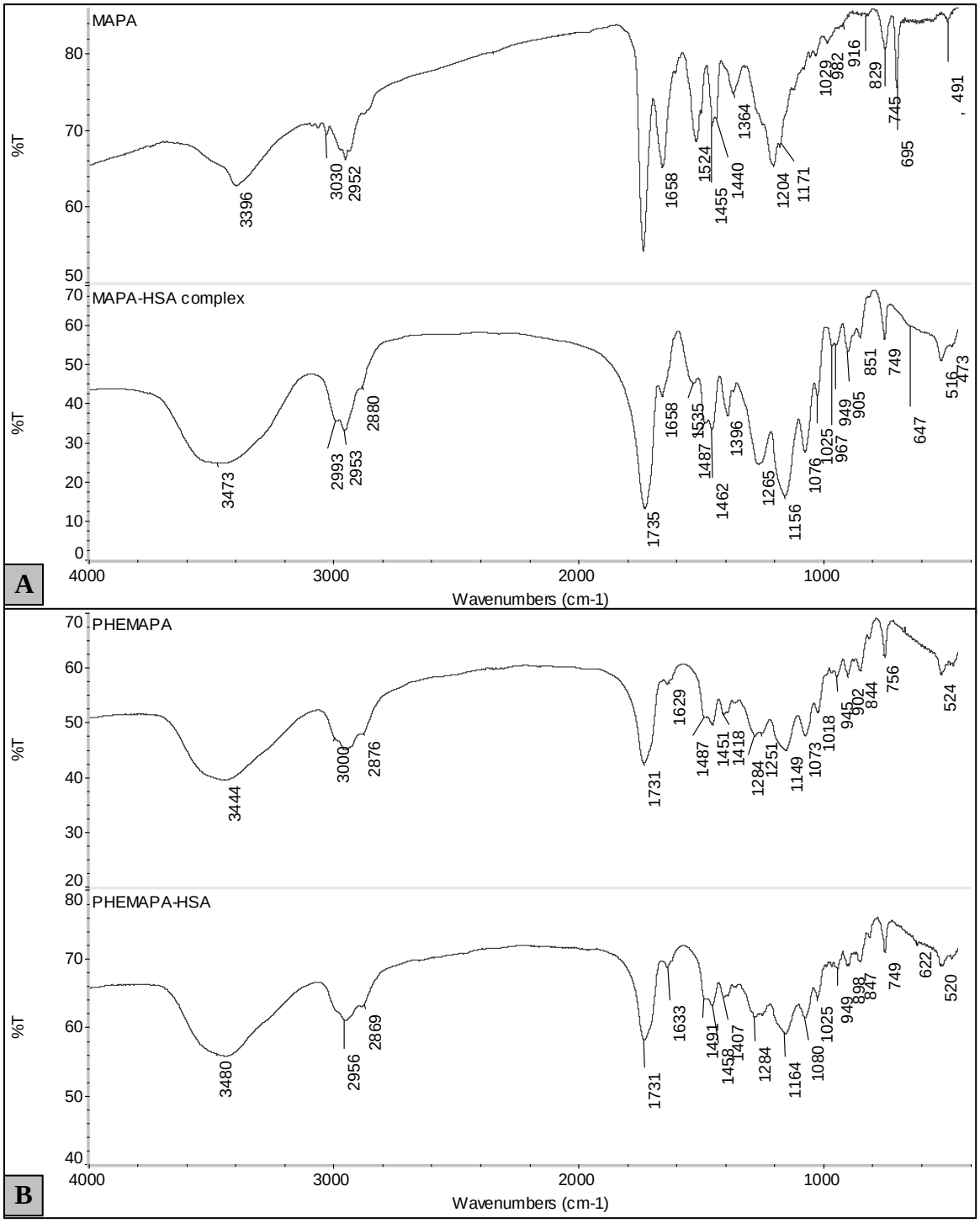

Figure 4.24. FTIR spectra of A) MAPA and MAPA-HSA complex and B) PHEMAPA and PHEMAPA-HSA cryogel.

FTIR spectra for both PHEMAPA-HSA and PHEMAPA cryogel have the characteristic broad peak at around 3400 cm^{-1}, which indicates the O–H stretching vibrations (Figure 4.24B). The bands at about 2950 cm^{-1} and 2880 cm^{-1} were assigned to asymmetric and symmetric C–H stretching vibrations. The presence of

the band of medium intensity at 1731 cm^{-1} indicated the presence of C–O stretching vibrations. The amides were characterized by the absorption bands due to N–H and C–O stretching vibrations, and N–H deformation due to a certain mixed vibration (amide bands). The appearance of strong bands at around frequencies of 1633 cm^{-1} (C–O, amide I) and 1458 cm^{-1} (N–H bending, amide II) indicates the incorporation of MAPA monomer into the polymer structure. Moreover, the bands at 1080 cm^{-1} and 749 cm^{-1} established the presence of benzene ring of MAPA monomer.

The pore morphologies for both PHEMAPA and PHEMAPA-HSA cryogel were exemplified by the scanning electron micrographs in Figure 4.25. As clearly seen from Figure 4.25, the both PHEMAPA and PHEMAPA-HSA cryogel have macropores which formed during the polymerization procedure under semi-frozen conditions. The cryogels produced have large continuous interconnected pores (10–100 μm in diameter, supermacroporous) that provide channels for the mobile phase to flow through. By this way, it can be used for samples with high viscosity, such as, body fluids and serum.

4.3.1. Adsorption Studies of PHEMAPA–HSA Cryogel

4.3.1.1. Adsorption from Aqueous Solutions

4.3.1.1.1. Effect of pH

Figure 4.26 shows HSA adsorption in phosphate buffer at different pH values. In this pH range, maximum adsorption amount was observed at pH 6.0 as 20.6 mg HSA/g dry gel. Maximum adsorption capacity decreased significantly in more acidic and in more alkaline pH regions. Probably, the reason for this behavior is the pH memory as MAPA-HSA complex used to synthesize PHEMAPA-HSA cryogel was produced at pH 6.0 phosphate buffers, in which MAPA monomer was in zwitter ionic form (pI of MAPA: 5.9). HSA is slightly anionic at pH 6.0 which is above of pI for HSA (pI of HSA: 4.9). In molecularly imprinted polymers (MIPs), the protonation pattern of the polymer could also play in a role for this behavior.

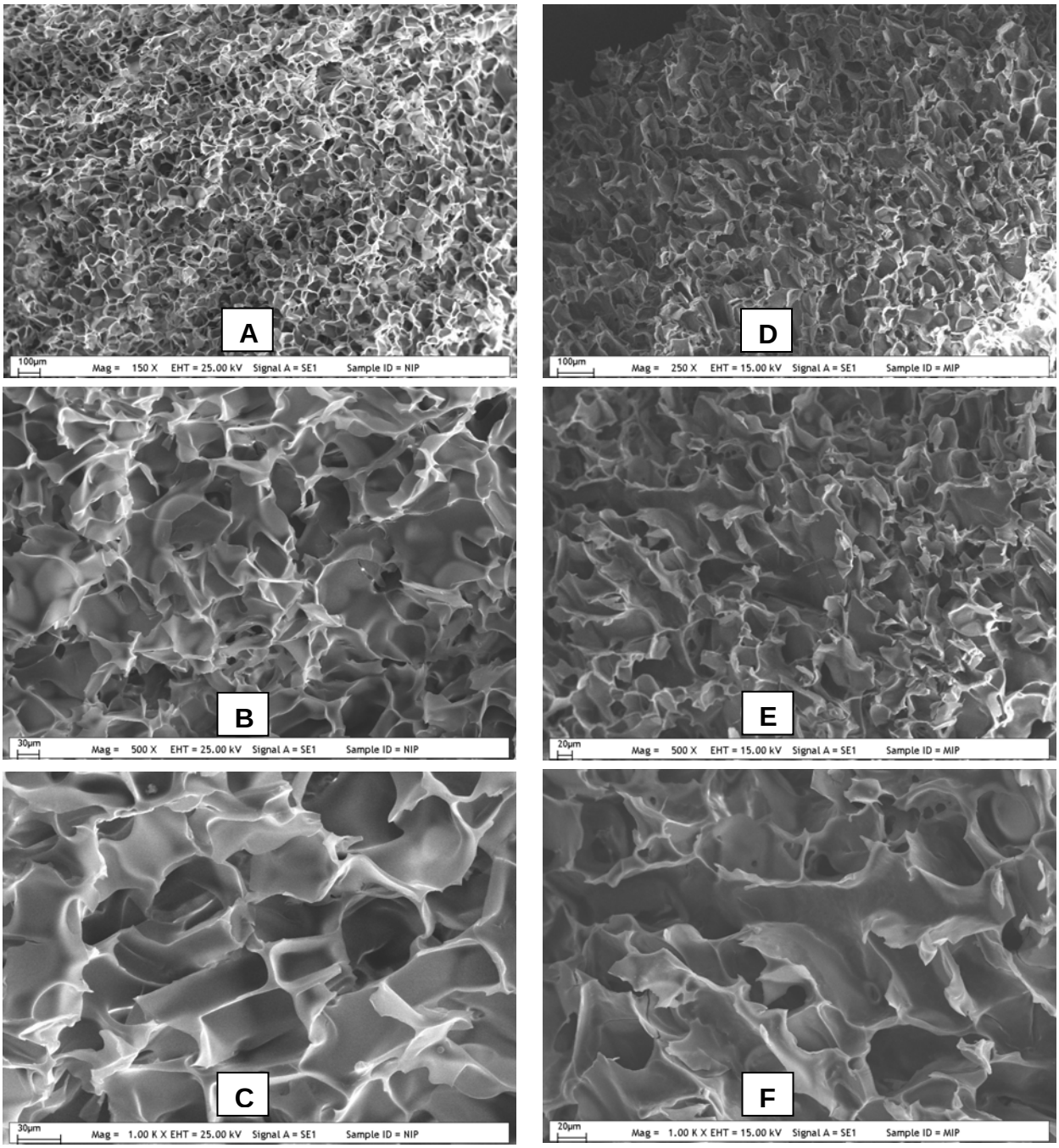

Figure 4.25. SEM photographs of PHEMAPA and PHEMAPA-HSA cryogel with different magnifications. A:150, B:500 and C:1000 times magnified for PHEMAPA and D: 250, E: 500, F: 1000 times magnified for PHEMAPA-HSA cryogel.

4.3.1.1.1. Effect of Flow Rate

The HSA adsorption of the PHEMAPA-HSA decreased drastically from 20.6 mg/g to 7.2 mg/g as the flow rate was increased from 0.5 mL/min to 4.0 mL/min, respectively (Figure 4.27).

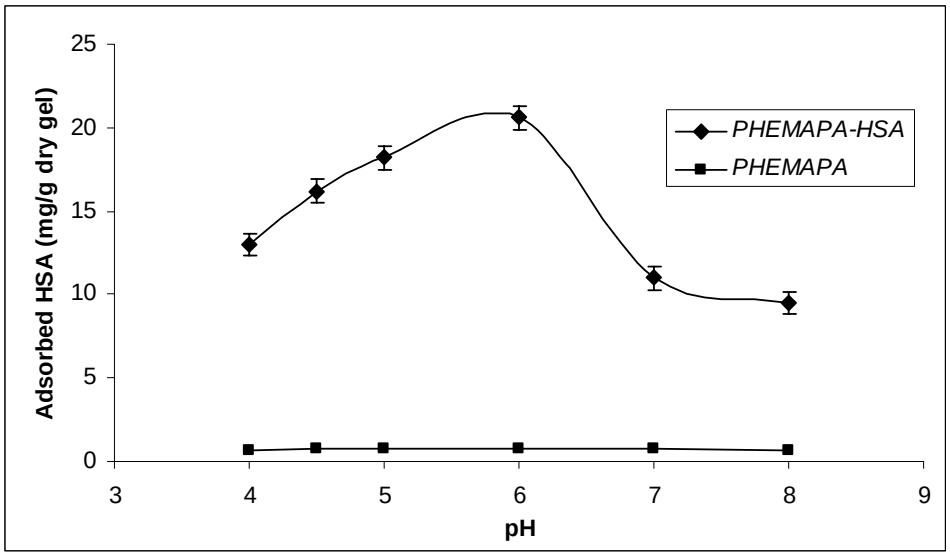

Figure 4.26. Effect of pH on HSA adsorption onto PHEMAPA-HSA cryogel. Experimental conditions: running buffer: 50 mM phosphate buffer, T: 20ºC, flow rate: 0.5 mL/min, HSA concentration: 2 mg/mL, $m_{dry\ cryogel}$: 0.4 g.

Ideally, HSA molecules would have more time to diffuse properly into the pores of cryogel and bind to binding sites at lower flow rates, and hence a better adsorption amount is achieved at a flow rate of 0.5 mL/min. Pores into cryogel are very large, so probably the limiting stage is not diffusion into pores, but rather the time needed for binding. Binding to some poorly exposed sites could be less favorable and hence take more time, than binding to easily available sites.

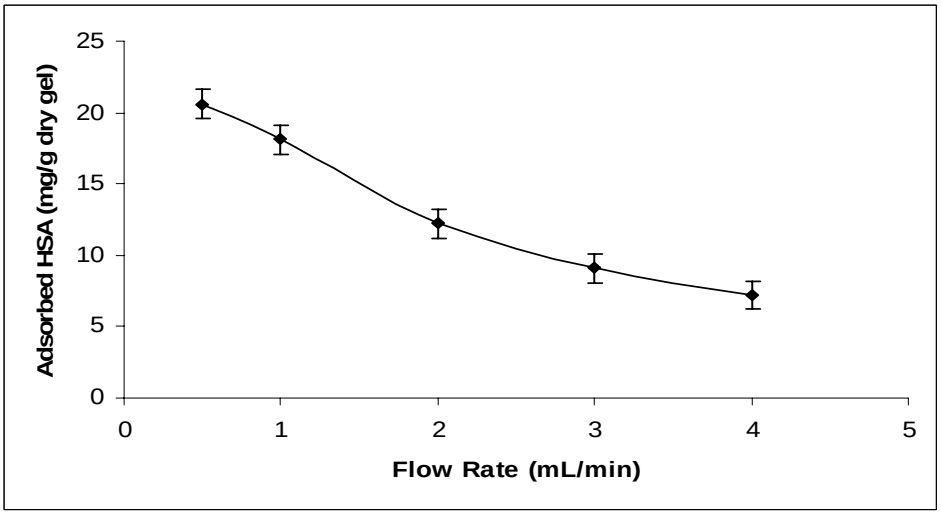

Figure 4.27. Effect of flow rate on HSA adsorption onto PHEMAPA-HSA cryogel. Experimental conditions: running buffer: 50 mM phosphate buffer, pH 6.0, T: 20ºC, HSA concentration: 2 mg/mL, $m_{dry\ cryogel}$: 0.4 g.

4.3.1.1.3. Effect of Initial Concentration

The equilibrium adsorption of HSA increased with increasing HSA concentration in buffer solution and the column was saturated at HSA concentrations above 3.5 mg/mL. The maximum HSA adsorption capacity by the PHEMAPA-HSA column was found to be 25.9 mg/g polymer on the average (Figure 4.28), which represents the saturation of the active binding sites of PHEMAPA-HSA column. It should be noted that the HSA adsorption onto PHEMAPA cryogel was 35-fold lower (about 0.75 mg/g) at the same conditions. The reactive binding groups onto PHEMA cryogel may interact with HSA molecules via nonspecific interactions. For the PHEMAPA-HSA cryogel, the self assembly process between MAPA and HSA results in the existence of complementary cavities in which MAPA and HSA have multiple point interactions after polymerization and removal of HSA. Non specific adsorption is dominant for the PHEMAPA cryogel due to lack of the self-assembly process. In the absence of the imprinting process, the functional groups in MAPA are distributed randomly in the gel network and are isolated from each other, so the multiple-point interactions are much less, which leads to weak interactions and reduced HSA adsorption.

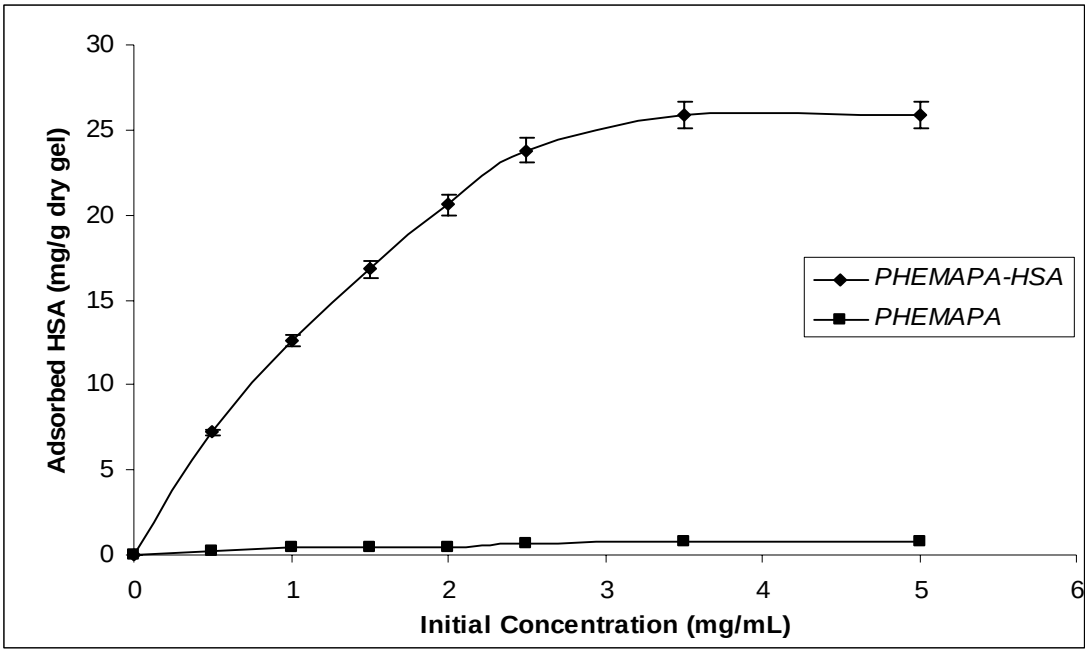

Figure 4.28. Effect of initial concentration on HSA adsorption onto PHEMAPA-HSA cryogel. Experimental conditions: running buffer: 50 mM phosphate buffer, pH 6.0, T: 20ºC, flow rate: 0.5 mL/min, $V_{solution:}$ 10 mL, $m_{dry\ cryogel}$: 0.4 g.

The experimental data tend to be better fitted with Langmuir rather than Freundlich isotherm, since the correlation coefficient (R^2) was high (0.97) (Table 4.7). The maximum amount of adsorption (25.9 mg/g) obtained from experimental results is also very close to the calculated Langmuir adsorption capacity (31.0 mg/g). The Langmuir and Freundlich constants with the correlation coefficients are given in Table 4.7. In Figure 4.29, the experimental adsorption behavior was compared with Langmuir and Freundlich adsorption isotherms. It can be concluded that the adsorption of HSA onto PHEMAPA-HSA cryogel is a monolayer adsorption.

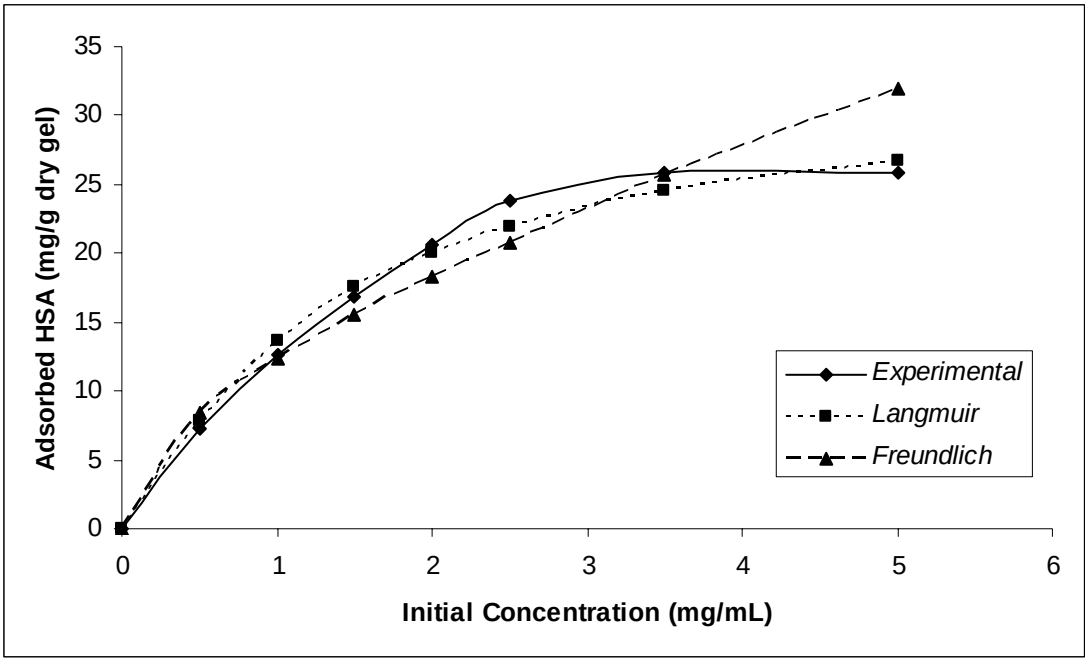

Figure 4.29. Experimental data for HSA adsorption on PHEMAPA-HSA cryogel fitted to Langmuir and Freundlich isotherms, respectively. Experimental conditions: running buffer: 50 mM phosphate buffer, pH 6.0, T: 20ºC, flow rate: 0.5 mL/min, $m_{dry\ cryogel}$: 0.4 g.

Table 4.7. Langmuir and Freundlich isotherm constants for PHEMAPA-HSA cryogel.

Notation for cryogel	Experimental	Langmuir constants				Freundlich constants		
	Q_e (mg/g)	Q_{max} (mg/g)	b (mg/mL)	R_L	R^2	Q_F (mg/g)	n	R^2
PHEMAPA-HSA	25.9	31.0	1.54	0.15	0.97	16.86	2.17	0.91

In order to examine the controlling mechanism of adsorption process such as mass transfer and chemical reaction, kinetic models were used to test experimental data. The kinetic models (Pseudo-first and second-order equations) can be used in this case assuming that the measured concentrations are equal to adsorbent surface concentrations.

Table 4.8. The first and second order kinetic constants for PHEMAPA-HSA cryogel.

Equilibrium	Experimental	First-order kinetic			Second-order kinetic		
Conc. (mg/mL)	Q_e (mg/g)	k_1 (1/min)	Q_e (mg/g)	R^2	k_2 (g/mg.min)	Q_e (mg/g)	R^2
3.5	25.9	0.011	6.05	0.90	$1.03x10^{-3}$	33.55	0.98

A comparison of the experimental adsorption capacity and the theoretical values are presented in Table 4.8. The correlation coefficient for the linear plot of log (Q_e-q_t) vs. t for the pseudo-first order equation is lower than the correlation coefficient for the pseudo-second order equation. These values show that this adsorbent system is not so well described by pseudo-first-order kinetic model. Moreover, the rate constant for second-order kinetic (k_2) is lower than first-order rate constant (k_1), which denotes the adsorption rate was controlled by second-order kinetic. By these results, it is suggested that the pseudo-second order adsorption mechanism is predominant and that the overall rate of the HSA adsorption process appeared to be controlled by chemical process.

4.3.1.1.4. Effect of Ionic Strength

The effect of NaCl concentration on the HSA adsorption amount was also investigated. High ionic strengths weakened the binding as shown in binding experiments when increasing amounts of NaCl were added to the adsorption solution (Figure 4.30). HSA adsorption amount decreased from 20.6 to 5.5 mg/g with the increasing NaCl concentration. Thus, ionic interactions gave an essential contribution to the recognition and binding process. A possible explanation to this phenomenon could be in two ways: (i) the counter salt ions interact with the HSA

molecules via charge–charge interactions and mask the binding sites and (ii) the decrease in the adsorption amount as the ionic strength increases can be attributed to the repulsive electrostatic forces between the PHEMAPA-HSA cryogel and HSA molecules. It should be also noted that a significant decrease of HSA adsorption onto PHEMAPA cryogel was not observed. The non-specific interactions between HSA and PHEMAPA cryogel may result from the cooperative effect of different mechanisms such as electrostatic interactions. It has been reported that the situation is particularly anxious when electrostatic and hydrophobic interactions occur at the same time, since an increase in the ionic strength of the solution decreases the former type of interaction.

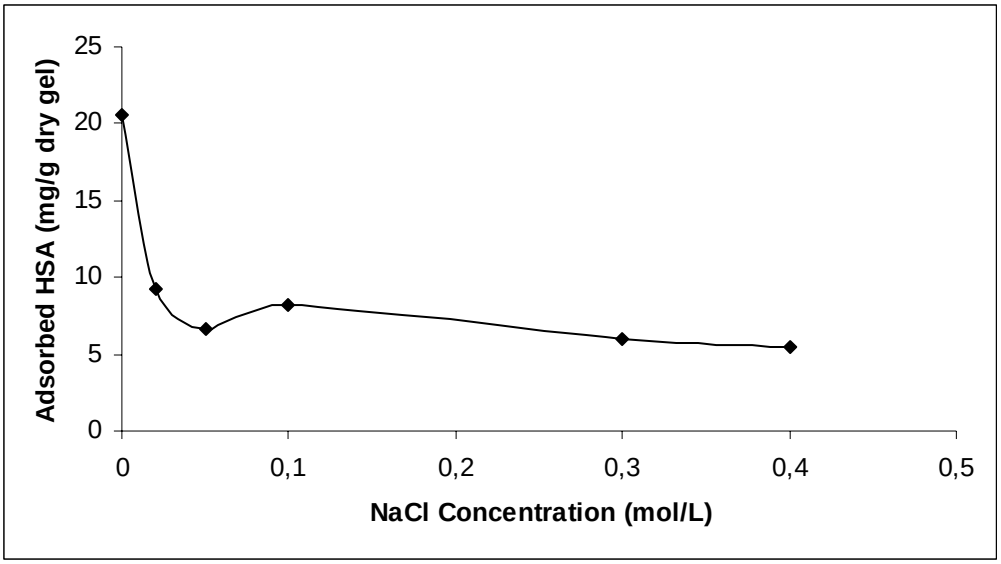

Figure 4.30. Effect of ionic strength on HSA adsorption onto PHEMAPA-HSA cryogel. Experimental conditions; running buffer: 50 mM phosphate buffer (pH 6.0), T: 20ºC, flow rate: 0.5 mL/min, HSA concentration: 2 mg/mL, $V_{solution:}$10 mL, $m_{dry\ cryogel}$: 0.4 g.

4.3.1.1.5. Effect of Temperature

The increased temperature enhances protein retention and the lowered temperature generally promotes the protein elution. Effect of temperature on the adsorption of HSA on PHEMAPA-HSA cryogel was presented in Figure 4.31. As shown in the Figure 4.31, adsorption of HSA on the PHEMAPA-HSA cryogel slightly increased with increasing temperature. The benzene ring of MAPA can interact with HSA molecule via hydrophobic interactions. As the temperature

increases, the hydrophobic groups of HSA come out to interact with PHEMAPA-HSA cryogel.

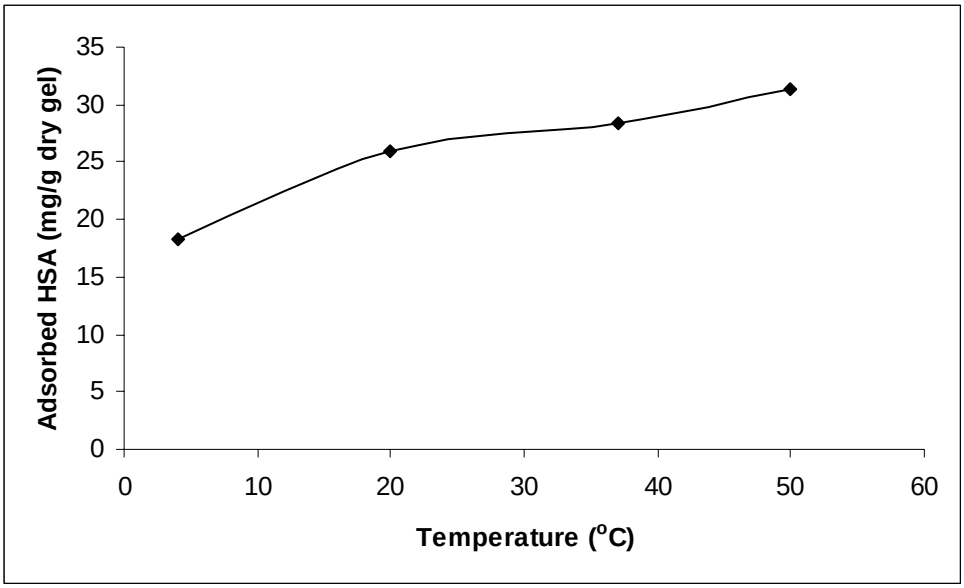

Figure 4.31. Effect of temperature on HSA adsorption onto PHEMAPA-HSA cryogel. Experimental conditions; running buffer: 50 mM phosphate buffer (pH 6.0), flow rate: 0.5 mL/min, HSA concentration: 2 mg/mL, $V_{solution}$: 10 mL, $m_{dry\ cryogel}$: 0.4 g.

4.3.2. Selectivity Studies

Molecular recognition selectivity is the most important parameter in characterizing MIPs because molecular recognition is the essential character of MIPs. The selectivity of PHEMAPA-HSA towards HSA binding was investigated by competitive adsorption of MYB and HTR in phosphate buffer (50 mM, pH 6.0). The competitive protein HTR which has approximately the same pI to HSA and MYB as a representative basic protein (pI: 7.2) were chosen for comparison of selectivity. The selectivity of the PHEMAPA-HSA cryogel for HSA (Mw: 67.0 kDa, pI: 4.9) with the competitive proteins HTR (Mw: 80.0 kDa, pI: 5.2) and MYB (Mw: 17.0 kDa, pI: 6.8-7.2) was evaluated in a circulating system with 0.40 g of the MIP cryogel, using a peristaltic pump for 2 h. The protein mixture was directly applied to PHEMAPA-HSA column, and then, the supernatant solution was analyzed by HPLC as described in section 3.8. Table 4.9 summarizes K_d, and k, values of HTR and MYB with respect to HSA. A comparison of the K_d values for PHEMAPA-HSA

with that for the PHEMAPA showed an increase in K_d for HSA while K_d decreased for HTR and MYB, respectively. The relative selectivity coefficient is an indicator of specificity of recognition sites of PHEMAPA-HSA cryogel (Odabaşı, 2007; Baydemir, 2009). The selectivity coefficients of PHEMAPA-HSA for HSA/HTR and HSA/MYB pairs were 56 and 18 times greater than that for PHEMAPA, respectively. The molecular weight of HSA (67.0 kDa) is larger than that of MYB (17.0 kDa). Although smaller molecules were expected to more easily gain access to the inside of imprint cavities, HSA was selectively adsorbed to the PHEMAPA-HSA cryogel. It can be concluded that the selectivity is dependent on the shape and size of the imprinted cavities. On the other hand, binding preference of HSA with respect to HTR, which have similar pI, was approximately 56 times greater than PHEMAPA cryogel. In addition of these results, Figure 4.32 illustrates the adsorbed template and competitive molecules for both PHEMAPA-HSA and PHEMAPA cryogel in mg/dL of protein. As clearly seen here, the competitive adsorption amount for HSA in PHEMAPA-HSA cryogel is 101.2 mg/dL dry gel in the presence of competitive proteins (HTR and MYB).

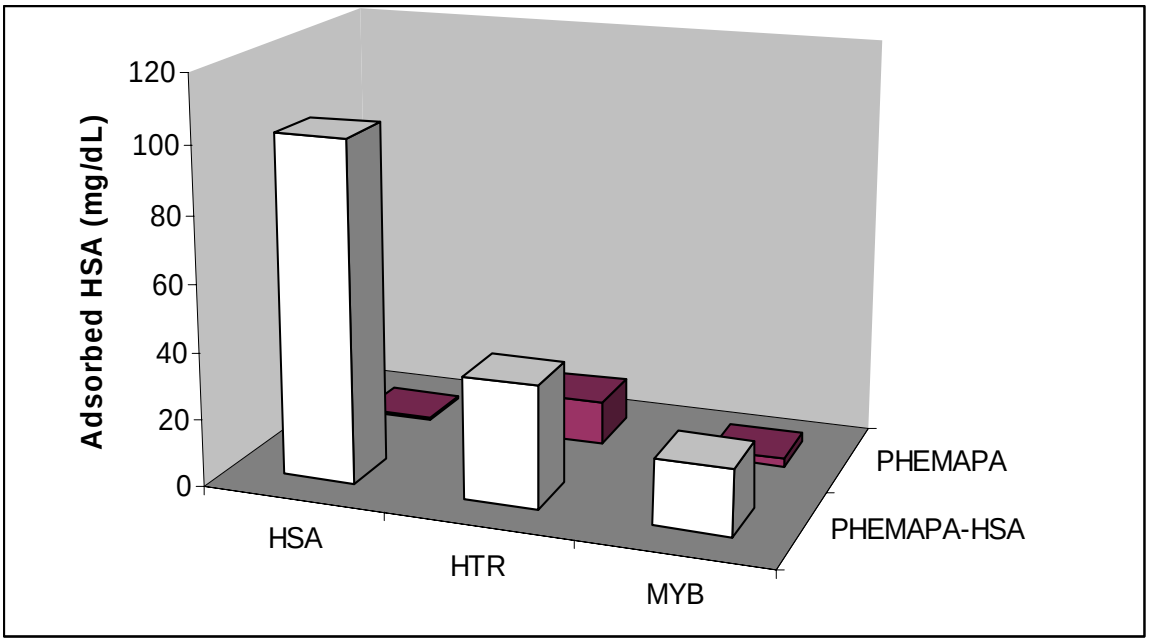

Figure 4.32. Adsorbed template (HSA) and competitive proteins (HTR and MYB) both in PHEMAPA-HSA and PHEMAPA cryogels. Experimental conditions; running buffer: phosphate (50 mM, pH 6.0), flow rate:0.5 mL/min; protein concentration: 3.5 mg/mL; $V_{solution}$:10 mL, $m_{dry\ cryogel}$: 0.4 g; T: 20 °C.

Table 4.9. K_d, k and k' values of HTR and MYB with respect to HSA.

Protein	PHEMAPA		PHEMAPA-HSA		
	K_d (mL/g)	k	K_d (mL/g)	k	k'
HSA	0.06	-	10.28	-	-
HTR	0.94	0.062	2.92	3.51	56.6
MYB	0.16	0.366	1.51	6.78	18.5

4.3.3. Adsorption of HSA from Human Serum

Figure 4.33 shows the depletion efficiency of HSA from human serum with different serum dilution ratios. PBS was used for dilution of human serum by 1/2, 1/5, 1/10 ratios. The maximum adsorption capacity for PHEMAPA-HSA cryogel column was obtained as 390.2 mg/g cryogel for non-diluted serum. The adsorption capacity was decreased with increasing dilution ratios while the depletion ratio of HSA was remained as 35 % in serum sample. The elution of bound HSA to PHEMAPA-HSA column was obtained by 0.1 M acetate buffer containing %10 ethylene glycol (pH 4.0) solution. Desorption ratio was achieved as 96 % in elution buffer. It should be noted that the decrease in desorption ratio with repeated 10 adsorption-desorption cycles is negligible.

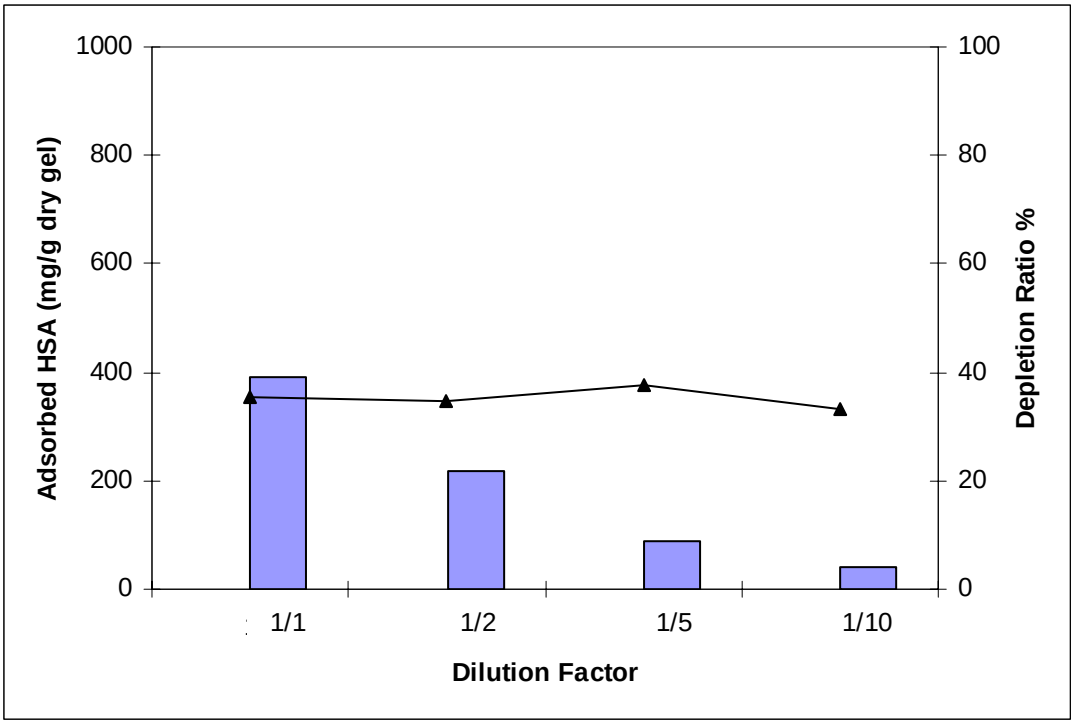

Figure 4.33. Depletion efficiency of HSA with different dilution ratios of human serum in PHEMAPA-HSA column. ∏ Adsorbed HSA (mg/g dry cryogel). ▲Depletion ratio (%) of HSA in human serum. Experimental conditions; dilution buffer: 50 mM of PBS (pH 7.4), flow rate: 0.5 mL/min, HSA initial concentration: 45 mg/mL, $V_{solution}$: 10 mL, $m_{dry\ cryogel}$: 0.40 g.

The FPLC step focused on the rapid removal of the high abundant proteins from the human serum. PHEMAPA-HSA cryogel column with a high binding capacity, well suited for depletion, was optimized for FPLC application. As shown in Figure 4.34, optimization of the depletion step allowed the use of a step elution at high flow rate (3 mL/min) to speed up the purification. This was particularly advantageous when working with this potentially unstable sample.

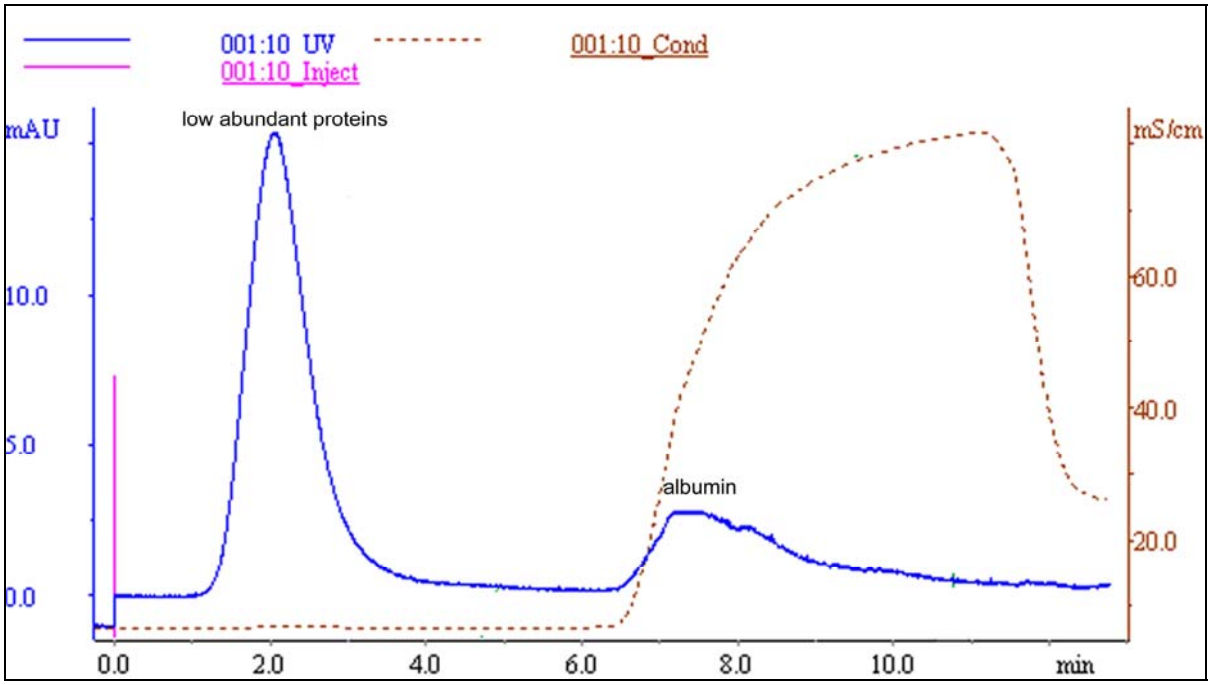

Figure 4.34. Separation of serum proteins via PHEMAPA-HSA column with FPLC. Experimental conditions; sample volume: 2 mL, mobile phase A: 50 mM phosphate buffer (pH 7.0), mobile phase B: 0.1 M acetate buffer containing %10 ethylene glycol (pH 4.0), flow rate: 3 mL/min, column volume: 8 mL, back pressure: 0.25 mPa, λ: 280 nm.

In Figure 4.34, high abundant proteins such as HSA were eluted from human serum by linear gradient of two mobile phases A and B. After a 9.0 min starting period with 100% mobile phase A, a linear gradient started from 0% B to 100% B

in 3.0 min, continued with 4.0 min 100% eluent B and finished last 4 min 100% buffer A.

Figure 4.35 shows the SDS-PAGE analysis of human serum before and after treatment with PHEMAPA-HSA cryogel column. Lane 1 corresponds to the molecular weight marker (Da). In Lane 2, it was observed that the high abundant protein albumin masked the low abundant proteins in human serum. After treatment with PHEMAPA-HSA cryogel column, the decrease in HSA concentration was clearly seen in Lane 3. Even though, the depletion ratio was relatively low (35%), the selectivity of PHEMAPA-HSA cryogel column was obviously high. The number of bands increased as observed on the right side of Figure 4.35. It was monitored serum proteins increased 2-fold in Lane 3. The elution of HSA was placed in Lane 4. PHEMAPA-HSA cryogel column was successfully applied in selective depletion of HSA in human serum.

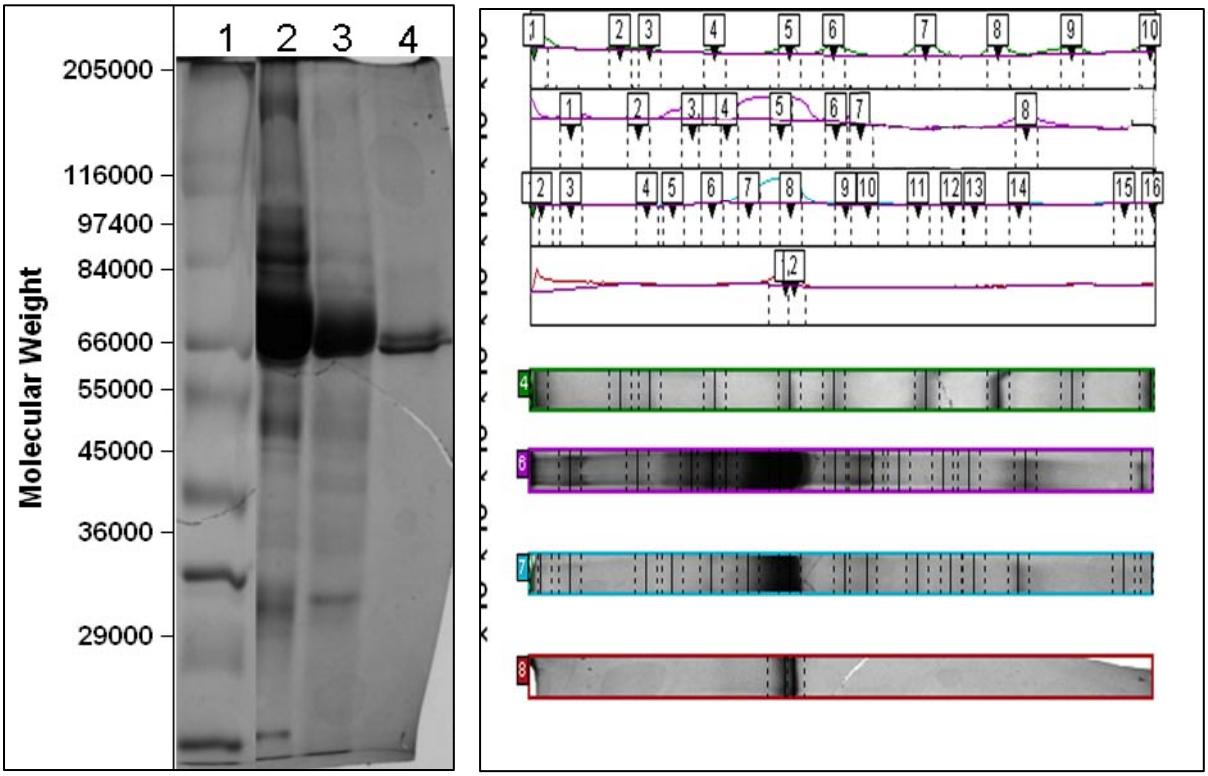

Figure 4.35. SDS-PAGE analysis of human serum before and after treatment with PHEMAPA-HSA cryogel column. 5–12% SDS-PAGE, Lane 1: Wide range Sigma Marker (Molecular Weight, Da) Lane 2: untreated human serum, Lane 3: human serum after treatment with cryogel column, Lane 4: the elution from the cryogel column.

4.3.4. Desorption and Reusability

The regeneration molecularly imprinted affinity column is a crucial step to render these columns more affordable for laboratory and commercial applications. Desorption ratios as high as 95% have been achieved and after 10 adsorption-desorption cycles, the PHEMAPA-HSA cryogel column maintained of about 90% of initial binding capacity (Figure 4.36).

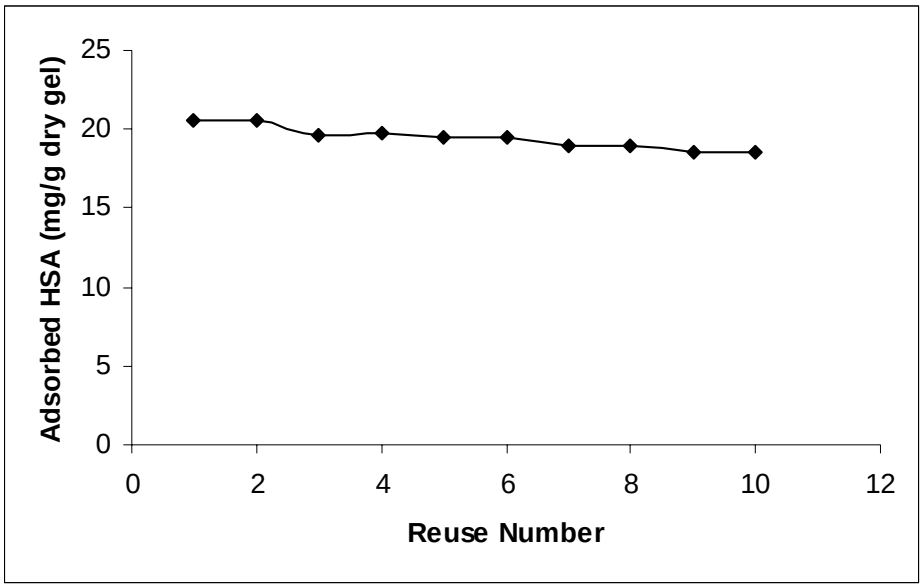

Figure 4.36. Adsorption-desorption cycle showing the reusability potential of PHEMAPA-HSA cryogel column. Desorption buffer: 0.1 M acetate buffer containing %10 ethylene glycol (pH 4.0); HSA concentration: 2 mg/mL, flow rate: 0.5 mL/min, T: 20ºC, $V_{solution}$: 10 mL, $m_{dry\ cryogel}$: 0.4 g.

4.4. HSA Surface-Imprinted (PGMA-HSA/PHEMA) Composite Cryogel

As mentioned in previous section, the disadvantage of the cryogels, on the other hand, is their low surface area and thus low adsorption capacity (Savina, 2005). Actually, bioseparation processes, it is a great importance to increase the adsorption capacity of supermacroporous cryogel. Therefore, bead embedding would be a useful improvement mode to use in the preparation of novel composite cryogels for increasing both surface area and adsorption capacity (Baydemir, 2009). HSA surface-imprinted (PGMA-HSA/PHEMA) composite cryogel was

prepared to increase the depletion capacity of HSA in human serum with high selectivity. The surface imprinting of template (HSA) was obtained by immobilization at the surface of the PGMA beads (Figure 4.37), with an approach modified from Tan et al. in which surface imprinting was achieved by minidispersion polymerization (Tan, 2008). Hence, the size and shape recognition was maintained for HSA molecules.

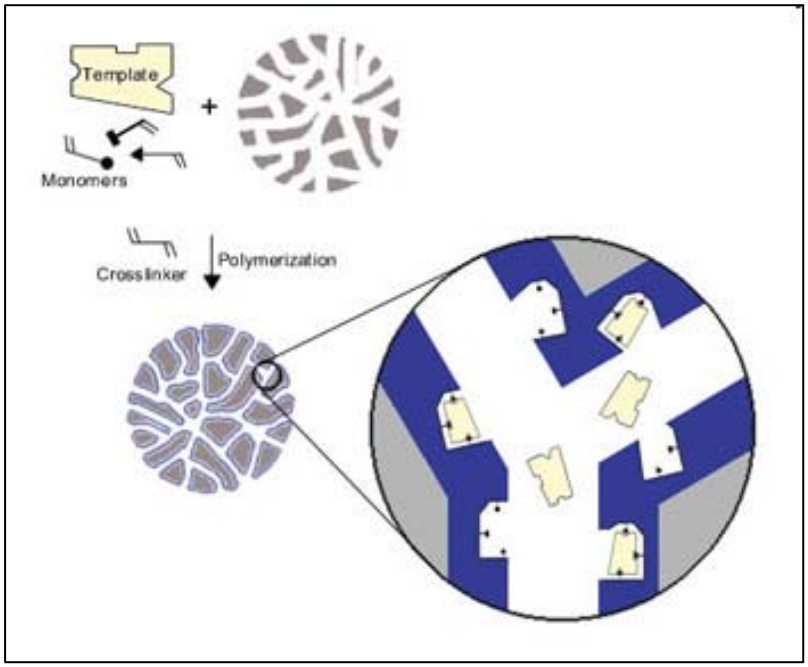

Figure 4.37. Schematic presentation of surface imprinting of template (HSA) at the surface of PGMA beads.

As seen in SEM photographs of HSA imprinted-PGMA beads (Figure 4.38), the particles were in spherical shape with sizes in the range of 1–10 μm. The presence of pores within the bead interior is clearly seen in this photograph. It can be concluded that the HSA imprinted-PGMA beads have a porous interior surrounded by a reasonably rough surface, in the dry state. The roughness of the surface should be considered as a factor providing an increase in the surface area. In addition, these pores reduce diffusional resistance and facilitate mass transfer because of high internal surface area. This also provides higher protein adsorption capacity.

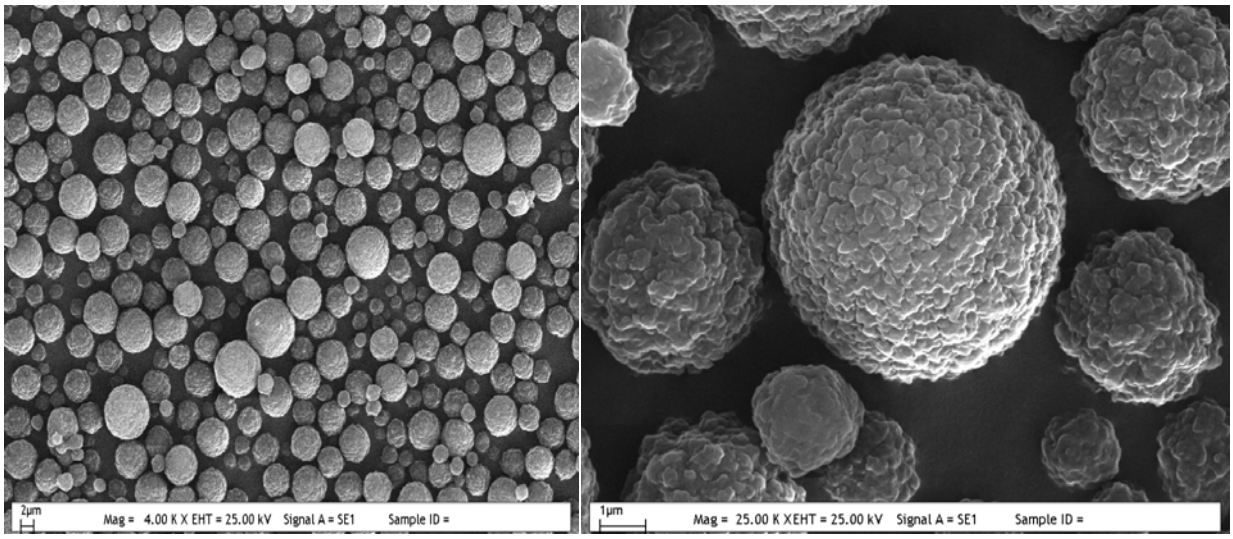

Figure 4.38. SEM photographs of HSA imprinted-PGMA beads with 4000 times (on the right side) and 25000 times magnified.

The HSA imprinted-PGMA beads and extracted beads (after HSA removal) showed different water uptake behaviour. The water absorption of a polymer is generally determined by the balance of ions, the affinity between the polymer and water (i.e., hydrophilicity of the matrix) and the rubbery elasticity (i.e., degree of cross-linking). In the HSA imprinted-PGMA beads, the interaction moieties of protein-matrix (i.e., template cavities) are empty, and therefore occupied by more water molecules (78%) than beads with HSA (65%).

Effect of embedding particle amount was studied by Baydemir et al. and was found that adsorption capacity of the PHEMA/MIP composite cryogel was improved significantly due to the embedded MIP particles amount up to 200 mg (Baydemir, 2009). Then, it reached a saturation level. The HSA imprinted-PGMA beads were embedded in PHEMA cryogel with 150 mg bead of loading ratio per mL of cryogel.

Specific surface area, total pore volume and average pore diameter of PGMA-HSA/PHEMA composite cryogel are compared in Table 4.10. The specific surface areas of PGMA-HSA/PHEMA composite cryogel were determined by a multipoint BET apparatus to be 232.0 m^2/g cryogel in average, which was approximately 10-

fold larger than conventional PHEMA cryogel. The sizes of the pores on PGMA-HSA/PHEMA composite cryogel were determined via a BJH instrument to average out to 76 Å in diameter, in which the pore diameters range from 20 Å to 245 Å, suggesting the presence of macropores on the surface of PGMA-HSA/PHEMA composite cryogel. This pore diameter is convenient for convection of high viscosity fluids such as human serum.

Table 4.10. Physical properties of PHEMA cryogel and PGMA-HSA/PHEMA composite cryogel.

Notation for Cryogels	Surface Area[a] (m^2/g)	Total Pore Volume[b] (ml/g)	Average Pore Diameter[c] (Å)
PHEMA	25.2	0.038	74.0
PGMA-HSA/PHEMA	232	0.25	76.0

a. Determined using multipoint BET method.

b. BJH cumulative desorption pore volume of pores between 20 and 245 Å.

c. BJH desorption average pore diameter of pores between 20 and 245 Å.

The SEM images of the internal structures of the PGMA-HSA/PHEMA and PGMA/PHEMA composite cryogel are shown in Figure 4.39. The PGMA-HSA/PHEMA composite cryogel was produced in such a way have porous and thin polymer walls, large continuous interconnected pores (10–100 μm in diameter) that provide channels for the mobile phase to flow through. SEM images showed that the HSA imprinted-PGMA beads were uniformly distributed into the PHEMA cryogel network. Pore size of the matrix is much larger than the size of the HSA molecules, allowing them to enter easily through the pores. As a result of the convective flow of the human serum through the pores, the mass transfer resistance is practically negligible. PGMA-HSA/PHEMA composite cryogel is opaque, sponge like and elastic. This cryogel can be easily compressed by hand to remove water accumulated inside the pores. When the compressed piece of

cryogel was submerged in water, it soaked in water and within 1–2 s restored its original size and shape due to its shape memory.

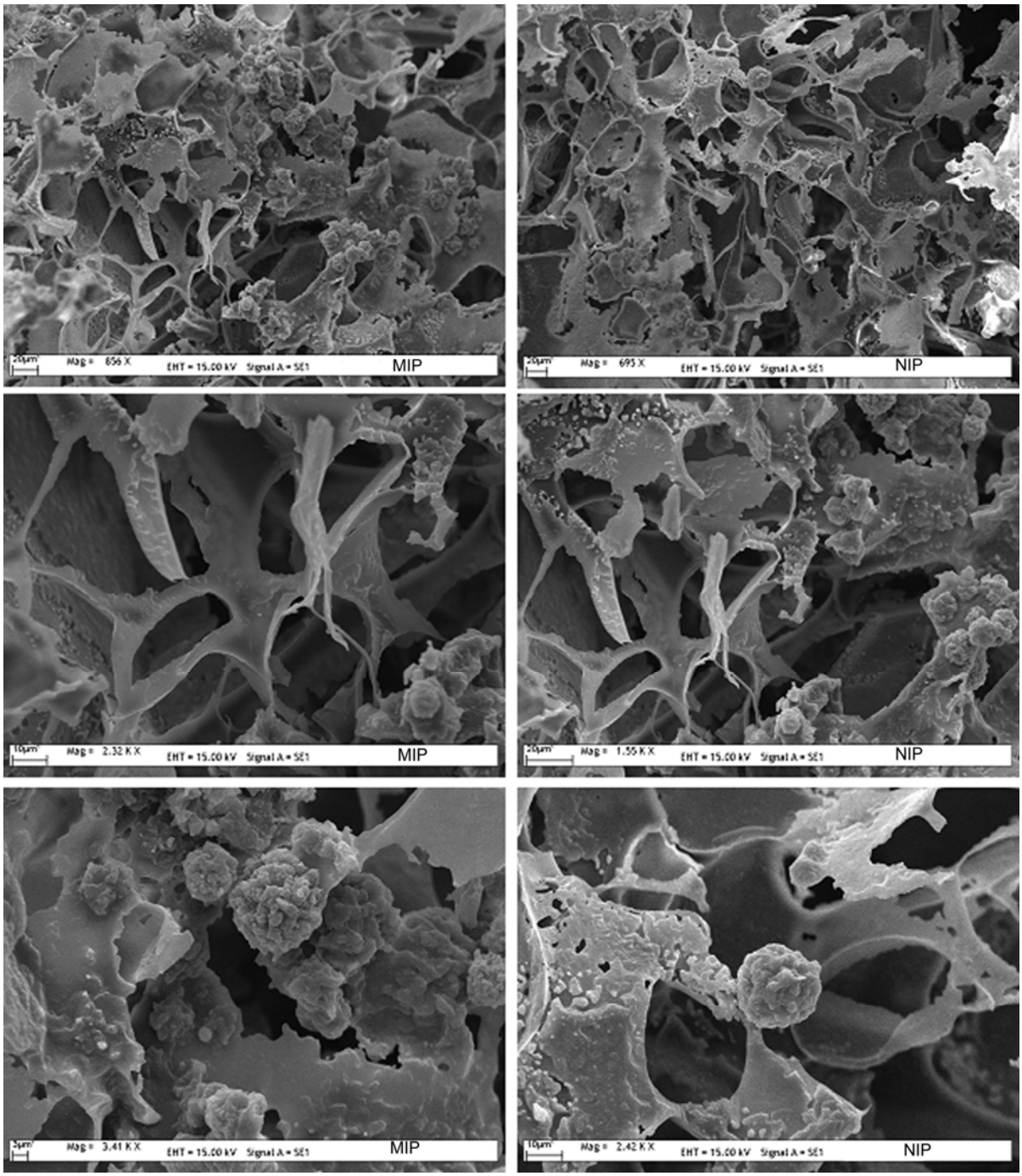

Figure 4.39. SEM photographs of PGMA-HSA/PHEMA (on the left side) and PGMA/PHEMA (on the right side) composite cryogels with different magnification levels.

FTIR spectra of both PGMA-HSA/PHEMA and PGMA/PHEMA cryogel have the characteristic broad peak at around 3400 cm^{-1}, which indicates the O–H stretching vibrations (Figure 4.40). The bands at about 2950 cm^{-1} and 2883 cm^{-1} were assigned to asymmetric and symmetric C–H stretching vibrations. The presence of the band of medium intensity at 1721 cm^{-1} indicated the presence of C–O stretching vibrations.

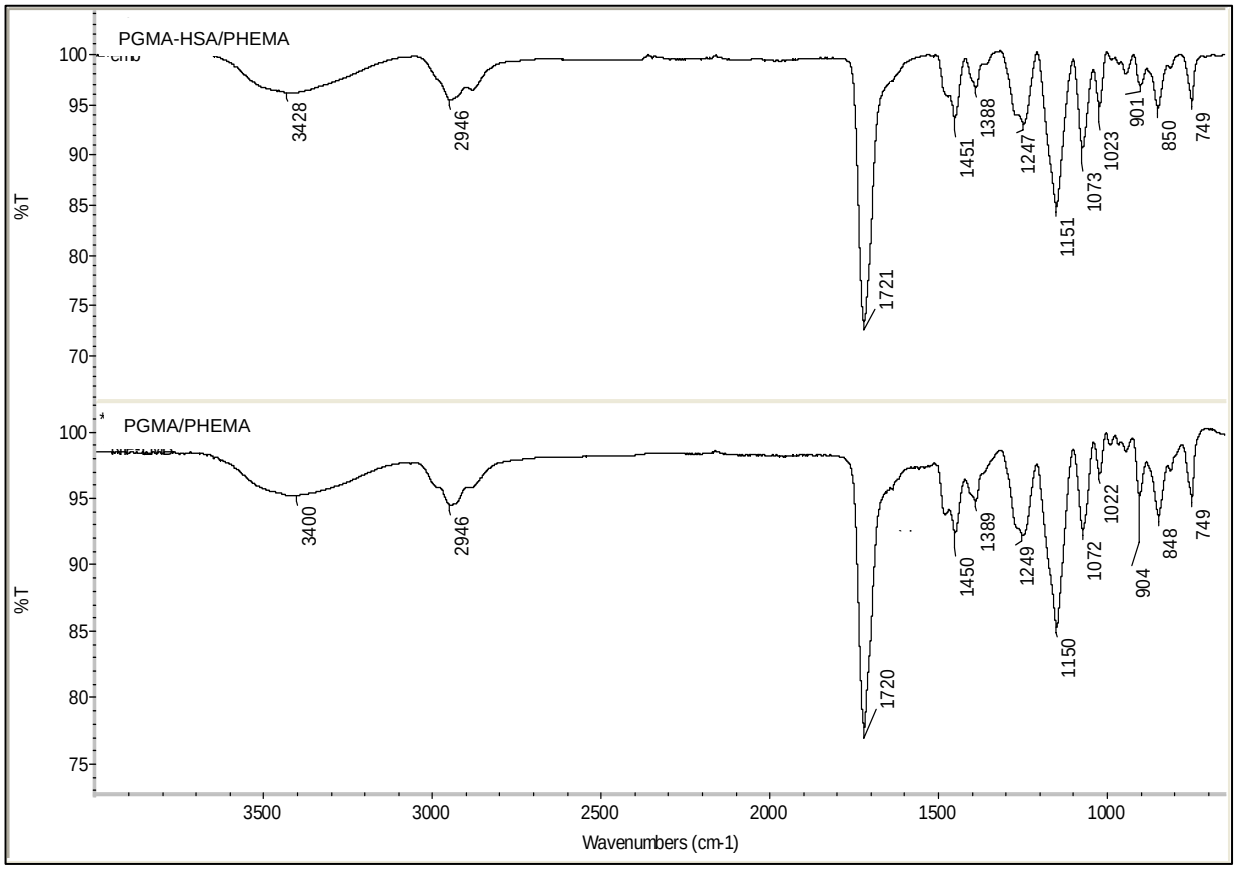

Figure 4.40. FTIR spectra of PGMA-HSA/PHEMA and PGMA/PHEMA composite cryogel.

4.4.1. Adsorption Studies of PGMA-HSA/PHEMA Composite Cryogel

4.4.1.1. Adsorption from Aqueous Solutions

4.4.1.1.1. Effect of pH

The adsorption capacity of molecularly imprinted polymers (MIPs) was highly dependent on the pH of medium. Figure 4.41 illustrates HSA adsorption in phosphate buffer at different pH values. In this pH range, maximum adsorption amount was observed at pH 5.0 as 98.2 mg HSA/g dry gel. Maximum adsorption

capacity was decreased significantly in more acidic and in more alkaline pH regions. Probably, the reason for this behavior is the protonation manner of the HSA, in which pI for HSA is (4.9). In MIPs, the protonation pattern of the polymer could also play in a role for this behavior.

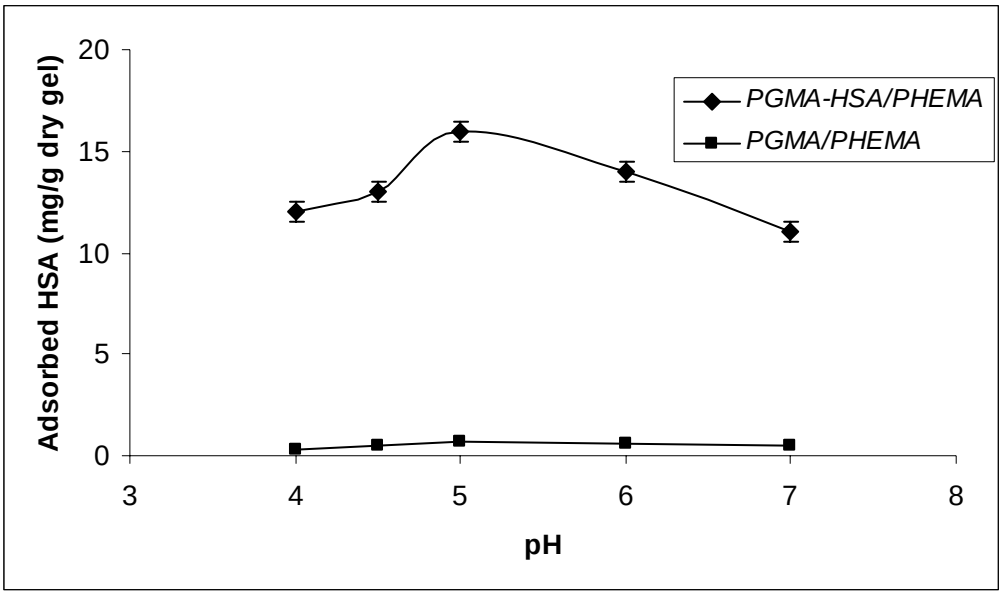

Figure 4.41. Effect of pH on HSA adsorption onto PGMA-HSA/PHEMA composite cryogel. Experimental conditions: running buffer: 50 mM acetate buffer and phosphate buffer, T: 20ºC, flow rate: 0.5 mL/min, HSA concentration: 2 mg/mL, $m_{dry\ cryogel}$: 0.8 g.

4.4.1.1.2. Effect of Flow Rate

Results show that the HSA adsorption capacity onto the PGMA-HSA/PHEMA composite cryogel decreased when the flow-rate through the column increased. The HSA adsorption of the PGMA-HSA/PHEMA decreased drastically from 16.3 mg/g to 10.2 mg/g as the flow rate was increased from 0.5 mL/min to 3.0 mL/min, respectively (Figure 4.42). The maximum adsorption amount was achieved at a flow rate of 0.5 mL/min. This is due to decrease in contact time between the HSA molecules and the composite cryogel at higher flow rates. When the flow-rate decreases the contact time in the column is longer. Thus, HSA has more time to recognize to the HSA molecular cavities in embedded MIP beads in the PHEMA cryogel structure and to enter to the molecular cavities, hence a higher adsorption amount is obtained.

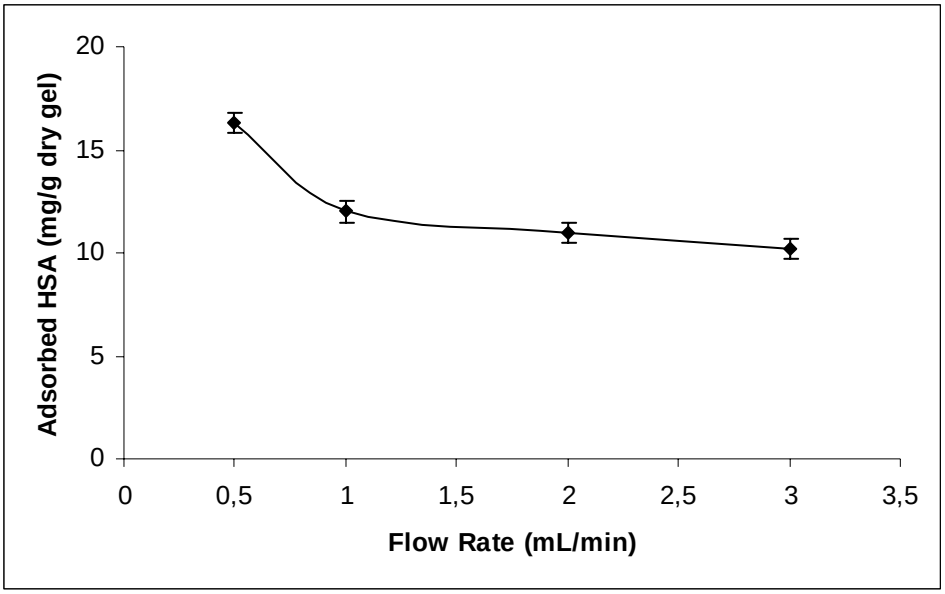

Figure 4.42. Effect of flow rate on HSA adsorption onto PGMA-HSA/PHEMA composite cryogel. Experimental conditions: running buffer: 50 mM acetate buffer, pH 5.0, T: 20ºC, HSA concentration: 2 mg/mL, $V_{solution}$: 10 mL, $m_{dry\ cryogel}$: 0.8 g.

4.4.1.1.3. Effect of Initial Concentration

The equilibrium adsorption of HSA increased with increasing HSA concentration in buffer solution and the column was saturated at HSA concentrations above 40 mg/mL. The maximum HSA adsorption capacity by the PGMA-HSA/PHEMA composite cryogel column was found to be 98.2 mg/g polymer on the average (Figure 4.43), which represents the saturation of the active binding sites of MIP column. It is obviously seen that the HSA adsorption capacity increased with increasing surface area. It should be noted that the HSA adsorption onto PGMA/PHEMA composite cryogel was 28-fold lower (about 3.6 mg/g) at the same conditions. The nonspecific interactions may contribute to HSA adsorption onto the embedded PGMA beads in PHEMA cryogel. These nonspecific adsorption may be due to diffusion of HSA molecules into the swollen cryogel and weak interactions (van der Waals interaction and hydrogen binding) between HSA and PGMA surface of cryogel.

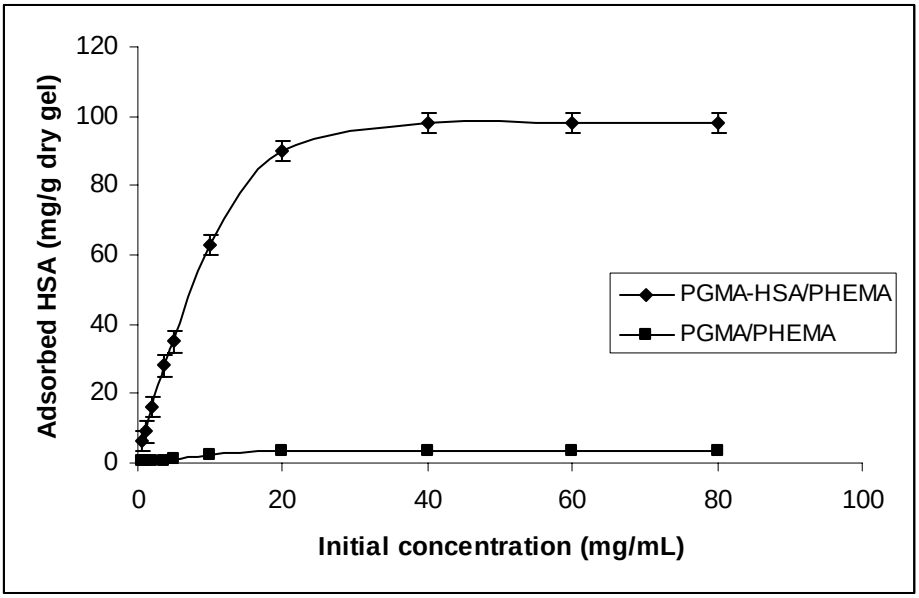

Figure 4.43. Effect of initial concentration on HSA adsorption onto PGMA-HSA/PHEMA composite cryogel. Experimental conditions: running buffer: 50 mM acetate buffer, pH 5.0, T: 20ºC, flow-rate: 0.5 mL/min, $V_{solution:}$ 10 mL, $m_{dry\ cryogel}$: 0.8 g.

The experimental data tend to be better fitted with Langmuir rather than Freundlich isotherm, since the correlation coefficient (R^2) was high (0.99) (Table 4.11). The maximum amount of adsorption (98.2 mg/g) obtained from experimental results is also very close to the calculated Langmuir adsorption capacity (103.10 mg/g). The Langmuir and Freundlich constants with the correlation coefficients are given in Table 4.11. In Figure 4.44, the experimental adsorption behavior was compared with Langmuir and Freundlich adsorption isotherms. It can be concluded that the adsorption of HSA onto PGMA-HSA/PHEMA composite cryogel is a monolayer adsorption.

Table 4.11. Langmuir and Freundlich isotherm constants for PGMA-HSA/PHEMA composite cryogel.

Notation for cryogel	Experimental	Langmuir constants				Freundlich constants		
	Q_e (mg/g)	Q_{max} (mg/g)	b (mg/mL)	R_L	R^2	Q_F (mg/g)	n	R^2
PGMA-HSA/PHEMA	98.2	103.10	0.35	0.066	0.99	23.75	2.58	0.92

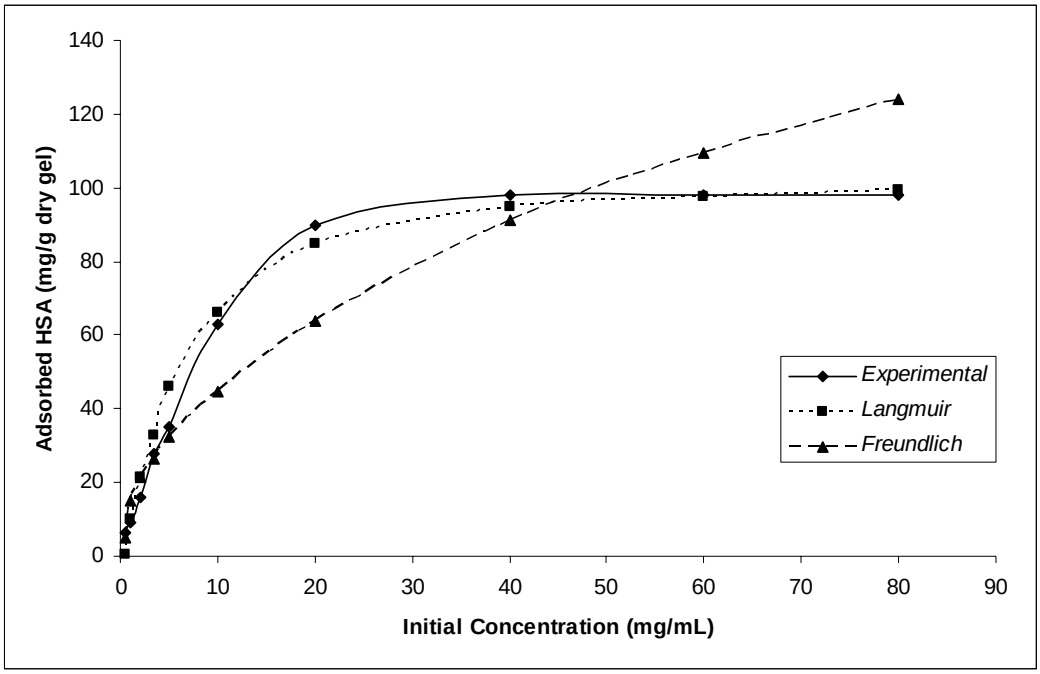

Figure 4.44. Experimental data for HSA absorption on PGMA-HSA/PHEMA composite cryogel fitted to Langmuir and Freundlich isotherms, respectively. Experimental conditions: running buffer: 50 mM acetate buffer, pH 5.0, T: 20ºC, flow rate: 0.5 mL/min, $m_{dry\ cryogel}$: 0.8 g.

In order to examine the controlling mechanism of adsorption process such as mass transfer and chemical reaction, kinetic models were used to test experimental data. The kinetic models (Pseudo-first and second-order equations) can be used in this case assuming that the measured concentrations are equal to adsorbent surface concentrations.

Table 4.12. The first and second order kinetic constants for PGMA-HSA/PHEMA composite cryogel.

Equilibrium	Experimental	First-order kinetic			Second-order kinetic		
Conc. (mg/mL)	Q_e (mg/g)	k_1 (1/min)	Q_e (mg/g)	R^2	k_2 (g/mg.min)	Q_e (mg/g)	R^2
40	98.2	$2.97x10^{-4}$	16.50	0.94	0.25	147.06	0.87

A comparison of the experimental adsorption capacity and the theoretical values are presented in Table 4.12. The correlation coefficient for the linear plot of log (Q_e-q_t) vs. t for the pseudo-second order equation is lower than the correlation

coefficient for the pseudo-first order equation. These values show that this adsorbent system is not so well described by pseudo-second order kinetic model. Moreover, the rate constant for first-order kinetic (k_2) is lower than second-order rate constant (k_1), which denotes the adsorption rate was controlled by first-order kinetic. By these results, it is suggested that the pseudo-first order adsorption mechanism is predominant and that the overall rate of the HSA adsorption process appeared to be controlled by diffusion.

4.4.2. Selectivity Studies

Molecular recognition selectivity is the most important parameter in characterizing MIPs because molecular recognition is the essential character of MIPs. The selectivity of PGMA-HSA/PHEMA towards HSA binding was investigated by competitive adsorption of MYB and HTR in acetate buffer (50 mM, pH 5.0). The competitive protein HTR which has higher molecular weight than HSA and MYB as a representative basic protein (pI: 7.2), which was lower molecular weight than HSA, were chosen as model proteins. The selectivity of the PGMA-HSA/PHEMA composite cryogel for HSA (Mw: 67.0 kDa, pI: 4.9) with the competitive proteins HTR (Mw: 80.0 kDa, pI: 5.2) and MYB (Mw: 17.0 kDa, pI: 6.8-7.2) was evaluated in a circulating system with 0.40 g of the MIP/composite cryogel, using a peristaltic pump for 2 h. The protein mixture was directly applied to PGMA-HSA/PHEMA composite cryogel column, and then, the supernatant solution was analyzed by HPLC as described in section 3.8. Table 4.13 summarizes K_d, and k, values of HTR and MYB with respect to HSA. A comparison of the K_d values for PGMA-HSA/PHEMA composite cryogel with that for the PGMA/PHEMA composite cryogel showed an increase in K_d for HSA while K_d decreased for HTR and MYB, respectively. The relative selectivity coefficient is an indicator of specificity of recognition sites of PGMA-HSA/PHEMA composite cryogel (Baydemir, 2009). The selectivity coefficients of PGMA-HSA/PHEMA for HSA/HTR and HSA/MYB pairs were 7 and 22 times greater than that for PGMA/PHEMA, respectively. The molecular weight of HSA (67.0 kDa) is larger than that of MYB (17.0 kDa). Although smaller molecules were expected to more easily gain access to the inside of imprint cavities, HSA was selectively adsorbed to the PGMA-HSA/PHEMA cryogel. It can be concluded that the selectivity is dependent on the

shape and size of the imprinted cavities. On the other hand, binding preference of HSA with respect to HTR, which has higher molecular weight, was approximately 7 times greater than PGMA/PHEMA cryogel. In addition of these results, Figure 4.45 illustrates the adsorbed template and competitive molecules for both PGMA-HSA/PHEMA and PGMA/PHEMA composite cryogel in mg/dL of protein. As clearly seen here, the competitive adsorption amount for HSA in PGMA-HSA/PHEMA composite cryogel is 722.1 mg/dL dry gel in the presence of competitive proteins (HTR and MYB).

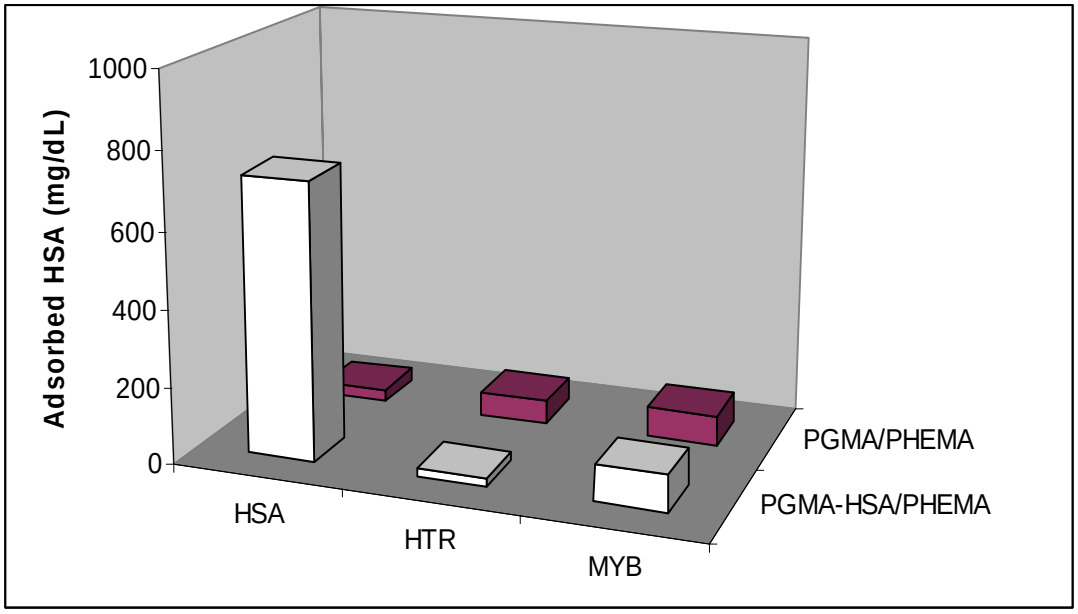

Figure 4.45. Adsorbed template (HSA) and competitive proteins (HTR and MYB) both in PGMA-HSA/PHEMA and PGMA/PHEMA cryogels. Experimental conditions; running buffer: acetate (50 mM, pH 5.0), flow rate: 0.5 mL/min; protein concentration: 40 mg/mL; $V_{solution}$: 10 mL; $m_{dry\ cryogel}$: 0.8 g; T: 20 °C.

Table 4.13. K_d, k and k' values of HTR and MYB with respect to HSA.

Protein	PGMA/PHEMA		PGMA-HSA/PHEMA		k'
	K_d (mL/g)	k	K_d (mL/g)	k	
HSA	2.11	-	5.47	-	-
HTR	0.38	5.56	0.14	40.46	7.27
MYB	3.67	0.57	0.42	12.9	22.44

4.4.1.2. Adsorption of HSA from Human Serum

Figure 4.46 shows the depletion efficiency of HSA from human serum with different serum dilution ratios. PBS was used for dilution of human serum by 1/2, 1/5, 1/10 ratios. The maximum adsorption capacity for PGMA-HSA/PHEMA cryogel column was obtained as 683.3 mg/g cryogel for non-diluted serum. The adsorption capacity was decreased with increasing dilution ratios while the depletion ratio of HSA was remained as 85% in serum sample. The elution of bound HSA to PGMA-HSA/PHEMA column was obtained by a solution of SDS and acetic acid (10% w/v; 10% v/v). Desorption ratio was achieved as 97% in this elution buffer. It should be noted that the decrease in desorption ratio with repeated 10 adsorption-desorption cycles is negligible.

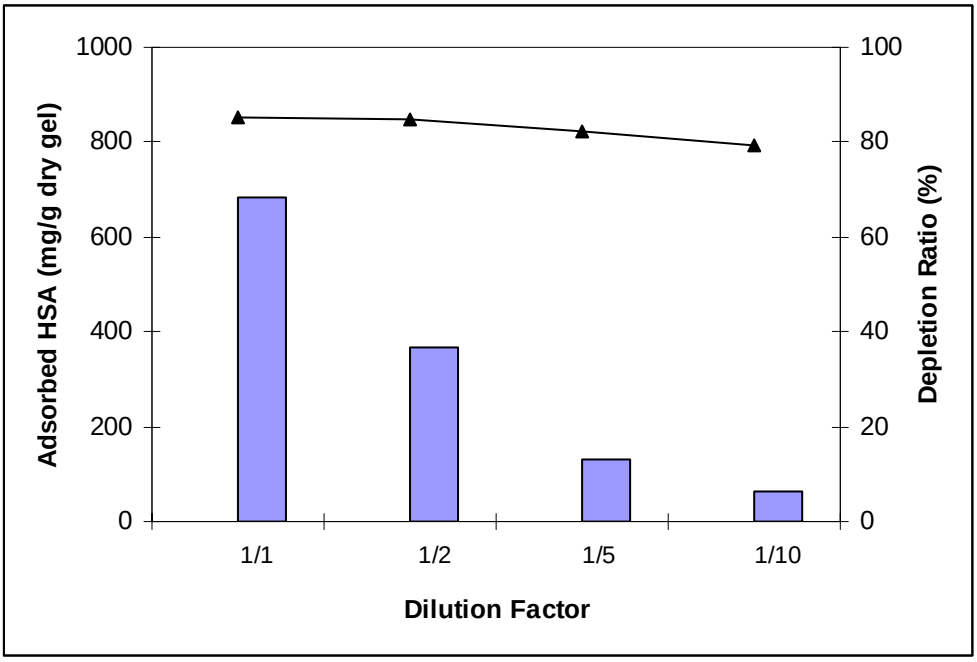

Figure 4.46. Depletion efficiency of HSA with different dilution ratios of human serum in PGMA-HSA/PHEMA column. ∏ Adsorbed HSA (mg/g dry cryogel). ▲Depletion ratio (%) of HSA in human serum. Experimental conditions; dilution buffer: 50 mM of PBS (pH 7.4), flow rate: 0.5 mL/min, HSA initial concentration: 48 mg/mL, $V_{solution}$: 10 mL, $m_{dry\ cryogel}$: 0.8 g.

The FPLC step focused on the rapid removal of the high abundant proteins from the human serum. PGMA-HSA/PHEMA cryogel column with a high binding capacity, well suited for depletion, was optimized for FPLC application. As shown

in Figure 4.47, optimization of the depletion step allowed the use of a step elution at moderately low flow rate (1 mL/min) due to the embedded PGMA beads in cryogel column. However, the disadvantage of high back pressure (0.25 mPa) with low flow rate potentially increases the adsorption capacity of PGMA-HSA/PHEMA cryogel column in FLPC application.

In Figure 4.47, high abundant proteins such as HSA were eluted from human serum by linear gradient of two mobile phases A and B. After a 10.0 min starting period with 100% mobile phase A, a linear gradient started from 0% B to 100% B in 5.0 min, continued with 5.0 min 100% eluent B and finished last 5 min 100% buffer A.

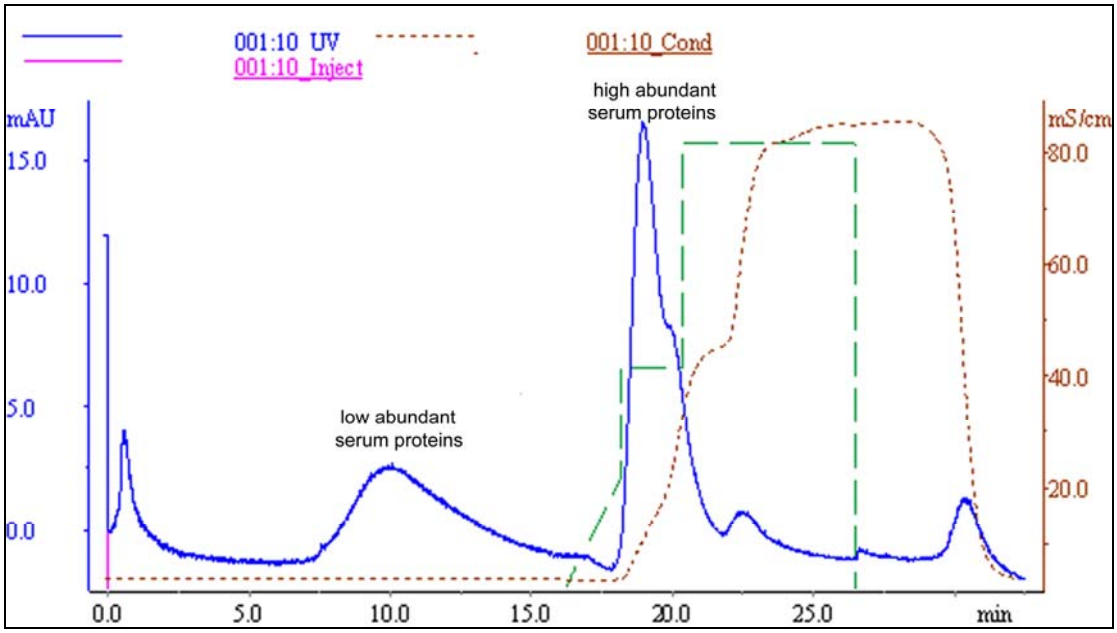

Figure 4.47. Separation of serum proteins via PGMA-HSA/PHEMA column with FPLC. Experimental conditions; sample volume: 2 mL, mobile phase A: 50 mM phosphate buffer (pH 7.0), mobile phase B: SDS and acetic acid (10% w/v; 10% v/v), flow rate: 1 mL/min, column volume: 8 mL, back pressure: 0.25 mPa, λ: 280 nm.

Figure 4.48 shows the SDS-PAGE analysis of human serum before and after treatment with PGMA-HSA/PHEMA cryogel column. Lane 1 corresponds to the molecular weight marker (Da). In Lane 2, it was observed that the high abundant protein albumin masked the low abundant proteins in human serum. After treatment with PGMA-HSA/PHEMA cryogel column, the decrease in HSA

concentration reveals bands (Lane 3). The depletion ratio was highly increased by embedding beads into cryogel column (85%), Furthermore; the selectivity of PGMA-HSA/PHEMA cryogel column was obviously high. However, the presence of additional bands may be a consequence of non-specific retention of proteins on the PGMA-HSA/PHEMA cryogel column during adsorption.The number of bands increased as observed on right side of Figure 4.48. It was monitored serum proteins increased 2-fold in Lane 2. The elution of HSA was placed in Lane 4. The elution ratio was obtained as 97% by this HSA-surface imprinted cryogel column. PGMA-HSA/PHEMA cryogel column was successfully applied in selective depletion of HSA in human serum.

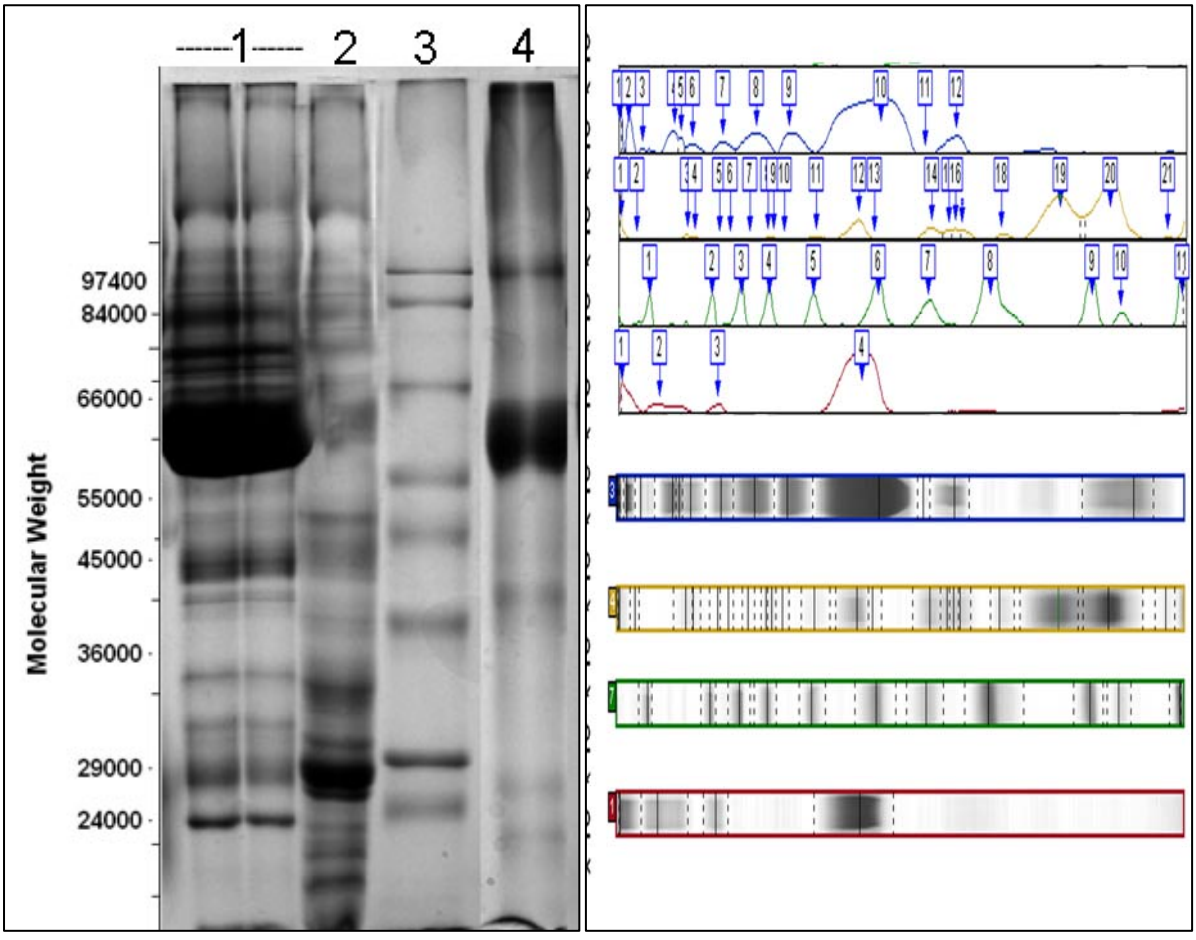

Figure 4.48. SDS-PAGE analysis of human serum before and after treatment with PGMA-HSA/PHEMA composite cryogel column. 5–12% SDS-PAGE, Lane 1: untreated human serum, Lane 2: human serum after treatment with cryogel column, Lane 3: Wide range Sigma Marker (Molecular Weight, Da), Lane 4: the elution from the cryogel column.

4.3.4. Desorption and Reusability

The regeneration molecularly imprinted affinity column is a crucial step to render these columns more affordable for laboratory and commercial applications. Desorption ratios as high as 95% have been achieved and after 10 adsorption-desorption cycles, the PGMA-HSA/PHEMA composite cryogel column maintained of about 97% of initial binding capacity (Figure 4.49).

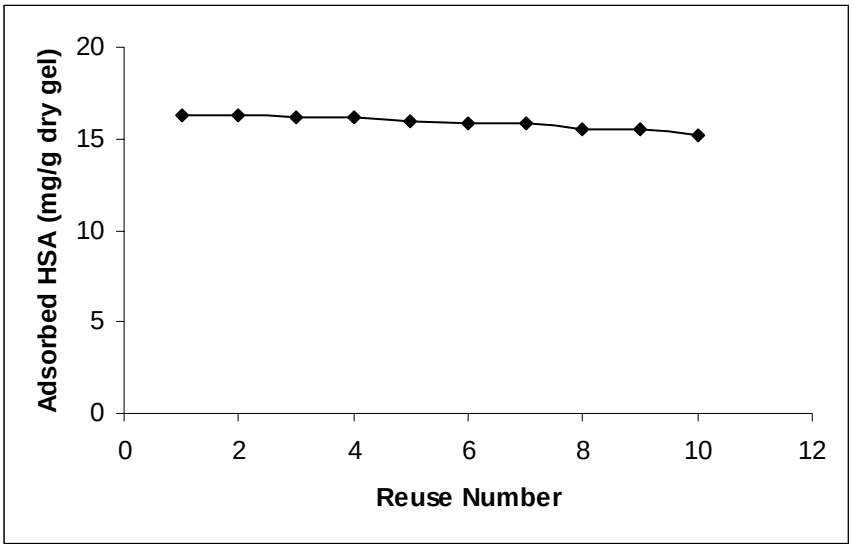

Figure 4.49. Adsorption-desorption cycle showing the reusability potential of PGMA-HSA/PHEMA composite cryogel column. Desorption buffer: SDS and acetic acid (10% w/v; 10% v/v); HSA concentration: 2 mg/mL, flow rate: 0.5 mL/min, T: 20ºC, $m_{dry\ cryogel}$: 0.80 g.

4.5. Comparison with Literature

Different support systems have been used for HSA adsorption/purification from various sources including human serum. Nigel et al. used dye-incorporated Sepharose CL-6B–200 and they reported bovine serum albumin (BSA) adsorption capacities around 1–3 mg/g moist gel (Nigel, 1989) Denizli et al. used dye affinity supports including monosize PGMA and poly(methyl methacrylate-hydroxyethyl methacrylate) beads, polyamide hollow fibers, PHEMA and magnetic PHEMA macrobeads, poly(ethylene glycol dimethacrylate- glycidyl methacrylate) monolith, and they obtained 35–220 mg/g polymer for HSA (Altıntas and Denizli, 2006;

Kassab, 2000; Denizli, 1997; Odabası, 2004; Uzun, 2004; Denizli, 1999). Nash and Chase used poly(vinyl alcohol) modified poly(styrene-divinyl benzene) beads carring different dye ligands (Nash and Chase, 1997). They presented adsorption capacities of 11.7–27 mg HSA/g. Boyer and Hsu used Sepharose beads carrying different amounts of Cibacron Blue F3GA (2–25 mmol/mL) and reported adsorption values up to 55.9 mg/g (BSA) polymer (Boyer and Hsu, 1992). Zeng and Ruckenstein reported 10.2 mg HSA/g adsorption capacity with Cibacron Blue F3GA-attachedpolyethersulfone supported chitosan supports (Zeng and Ruckenstein, 1996). Li and Spencer used Cibacron Blue F3GA-attached polyethylene imine coated titania and achieved 4.4 mg HSA/g (Li and Spencer, 1994). Chase reached 14 mg BSA/g with Cibacron Blue F3GA attached Sepharose CL-6B (Chase, 1984). Tuncel et al. reported 60 mg BSA/g adsorption capacity with Cibacron Blue F3GA-attached poly(vinyl alcohol)-coated monosize polystyrene beads (Tuncel, 1993). Muller-Shulte et al. used several polymeric carriers made of different polymers, and Cibacron Blue F3GA as the dye-ligand (Muller-Shulte, 1991). Their albumin adsorption values were in the range of 0.19–0.81 mg HSA/mL support. McCreath et al. developed liquid pefluorocarbon chromatographic supports carrying Reactive Blue 4 and the maximum capacity of the flocculated emulsion for HSA was found to be 1.81 mg/mL (McCreath, 1993). Gu et al. employed Cibacron Blue F3GA attached microporous poly(tetrafluoroethylene) capillary membrane and they achieved 198.5 mg/g albumin adsorption capacity (Gu, 2007). Zhang et al. used a series of aminated chitosan microspheres carrying Cibacron Blue F3GA and they obtained maximum adsorption capacity as 108.7 mg albumin per gram support (Zhang,2006). Ma et al. prepared nonporous micrometer sized magnetic poly(styrene-divinyl benzene-glycidyl methacrylate) having CB-F3GA and they showed that the magnetic microspheres had high adsorption capacity of albumin (80.2 mg/g) (Ma, 2006). Demiryas et al prepared CB-F3GA attached Poly(acrylamide-allyl glycidyl ether) [poly-(AAm-AGE)] cryogel adsorption/desorption of HSA from aqueous solutions and human plasma. They obtained maximum amount of HSA adsorption from aqueous solution as 27 mg/g at pH 5.0 and higher HSA adsorption value from human plasma (up to 74.2 mg/g) (Demiryas, 2007).

Björhal et al used five different commercially available depletion columns including Aurum Serum Protein Minikit (Bio-Rad, Hercules, CA, USA), ProteoExtract HSAumin/IgG Removal kit (Merck, Darmstadt, Germany), Multiple Affinity Removal Column (Agilent Technologies, San Diego, CA, USA), POROS Affinity Depletion Cartridges (Applied Biosystems, Framingham, MA, USA) and HSA-IgG Removal Kit (Amersham Biosciences, Uppsala, Sweden) (Björhal, 2005). It should be noted that Aurum Serum Protein Minikit (Bio-Rad, USA) and ProteoExtract HSA/IgG Removal kit contained protein A as ligand, Multiple Affinity Removal Column and HSA-IgG Removal Kit contained polyclonal antibodies as ligand. POROS Affinity Depletion Cartridges contained protein G. The depletion efficiency was above 90%, but due to the high dilution factor after the depletion procedure as compared crude serum. Altıntas and Denizli reached 99.3% HSA depletion efficiency with Cibacron Blue F3GA loaded poly(GMA) beads (Altıntaş and Denizli, 2006). Soskic et al. prepared hexadecanedioic acid immobilized Sepharose 4B for HSA removal and obtained 41.9% depletion efficiency (Soskic, 2006). Bonini et.al., prepared HSA imprinted poly-aminophenylboronic acid beads for specific removal of HSA and reached 58% removal efficiency from serum (Bonini, 2007). Jmeian and El Rassi has been presented an integral microcolumn-based fluidic platform for the simultaneous depletion of high-abundance proteins and the subsequent on-line concentration and capture of medium- and low-abundance proteins from human serum. They depleted 8 most abundant serum proteins (HSA, IgG, IgA, IgM, transferring, 1-antityripsin, haptoglobin and 2-macroglobulin) which representing the 85% of total protein mass (Jmeian and El Rassi, 2008). Kumar et al. generated a systematic library of 96 affinity resins was generated using novel analogs of Cibacron Blue 3GA and tested in a batch binding and elution mode using seven different proteins –four Aspergillus enzymes namely, NADP-glutamate dehydrogenase, laccase, glutamine synthetase and arginase, bovine pancreatic trypsin and the two serum proteins, HSA and immunoglobulin G. Binding capacity o the 96 affinity resins was obtained up to 50 mg/mL HSA (Kumar, 2009). Steel et al. used CB-based and immunoaffinity resin to remove albumin and IgG from human serum samples in order to simplify the serum proteome in a single step (Steel, 2003). Chromy et al prepared antibody based resin to remove high abundant proteins in human serum and obtained 76% increase in protein spot detection by 2D-PAGE (Chromy, 2004). Zhou et al

combined immunoprecipitation with microcapillary reversed-phase liquid chromatography (µRPLC) to investigate the low molecular weight proteins by removing high abundant proteins. They achieved 73% increase in spot analysis (Zhou, 2004). Colantonio and co workers reported CB based extraction method for the effective and specific removal of albumin from serum with increased detection of low abundant proteins in electrophoresis (Colantonio, 2005). Greenough and co workers reported the specific removal of 98% of albumin and 80% of immunoglobulin heavy chain from human plasma by affinity chromatography, and the subsequent improvement in the number of spots detected and their resolution following two-dimensional gel electrophoresis (Greenough, 2004).

Methacrylic acid based gel beads were imprinted with bovine serum albumin (BSA) by Pang, using an inverse-phase suspension method (Pang, 2006). They obtained good quality spherical beads exhibiting excellent macroporous structure, which is important in facilitating the movement of proteins through the material. The produced beads demonstrated higher adsorption over their non-imprinted counterparts, and more importantly, a relatively high separation factor (k': 4.71) was obtained between the BSA (MW 67 kD, pI 4.8) and a challenging protein (ovalbumin, MW 44 kD, pI 4.5). The authors attributed this success to steric factors and multiple point electrostatic interactions.

Similarly, the group of Hjerten polymerized acrylamide and mBAAm in the presence of protein to form a gel (Hjerten, 1997; Liao, 1996; Tong, 2001). The gel was pressed through a sieve, and the resultant particles were packed into a column for chromatography. The protein was removed from the gel using a solution of acetic acid (HOAc) and sodium dodecyl sulfate (SDS). When a variety of proteins including the template were run on the column, the template was selectively adsorbed. This technique was demonstrated for bovine hemoglobin (Hb), cytochrome C (CyC), and transferrin (Tf) (Liao, 1996) and later for human growth hormone (HgH), RNase, and horse myoglobin (Mb) (Hjerten, 1997). It was hypothesized that a large number of weak electrostatic bonds formed between the gel and the protein, giving an overall strong interaction and hence the success of the imprint. This is in opposition to traditional imprinting theory that suggests that fewer strong bonds are better than numerous weak ones.

5. CONCLUSIONS

In this thesis, 3 different affinity columns (Figure 5.1) were prepared for depletion of HSA from human serum. Characteristic properties, binding affinities, depletion efficiencies and selectivities of these systems were discussed.

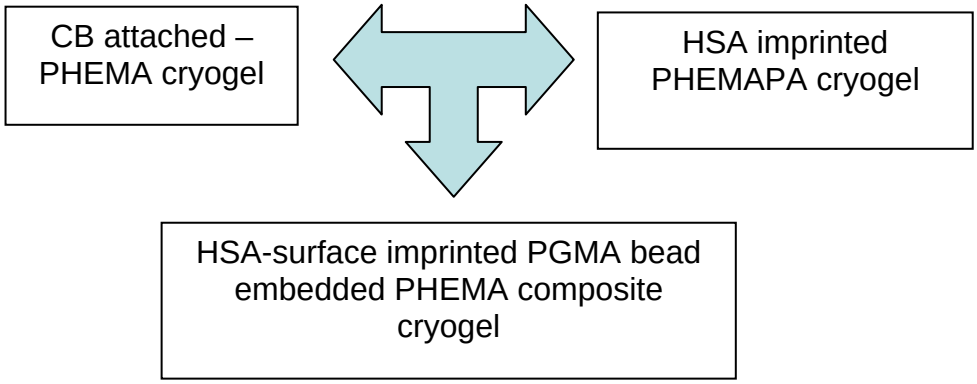

Figure 5.1. Schematic representaiton of 3 different affinity column systems for depletion of HSA from human serum.

Cryogels are very good alternatives of matrices for protein purification with the advantages of large pores, short diffusion path, low pressure drop and very short residence time for both adsorption and elution. They are also cheap materials and they can be used as disposable avoiding cross-contamination between batches. Removal of albumin from serum samples is problematic because of its extremely high concentration. A high specificity and high capacity resin is required. While Cibacron Blue and related dyes have been shown to bind albumin with high affinity (Travis and Pannell, 1973), they also bind many other abundant serum proteins (Gianazza and Arnaud, 1982). Dye-based systems that have been optimized for albumin binding are commercially available, but our results suggest that they still lack sufficient specificity. The need to compromise between specificity and capacity may account for the failure of the PHEMA-CB column. By this purpose, HSA imprinted PHEMAPA cryogel was prepared by self-assembling MAPA and HSA prior to polymerization. HSA imprinted PHEMAPA cryogel showed high selectiviy towards HSA molecules but lack of sufficient efficiency (35%). The disadvantage of the cryogels, on the other hand, is their low surface area and thus

low adsorption capacity. Bead loaded matrices aim to combine the advantages of both small beads and convective media without bringing along the disadvantages of a high pressure drop and low capacity (Le Noir,2007; Ciardelli, 2006). Due to the embedded HSA-surface imprinted PGMA beads, the protein adsorption capacity of the composite cryogels was improved compared with cryogels without embedded beads. Because, the MIP particles are located, or close to, the macropore surface, these MIP particles have a good site accessibility toward, the target HSA molecules in human serum. The HSA-surface imprinted PGMA beads can be well dispersed in cryogel structure. Embedding with HSA-surface imprinted PGMA beads increased the surface area of the PHEMA cryogel by 10-fold. Furthermore, the large surface area of the particles results in higher HSA binding capacity of the PGMA-HSA/PHEMA composite cryogel.

This thesis also involves the application of these affinity columns that prepared with different methods to a real biological fluid, human serum to remove the bulk of the HSA. Removal of highly abundant serum proteins improves the detection of less abundant proteins electrophoresis, as well as the display of proteins that comigrate and are otherwise obscured by HSA or IgG. The removal of the large and poorly resolved bands created by these highly abundant proteins, and the numerous smaller bands that represent albumin fragments, also helps in computer-assisted gel analysis. We expect that many of the new technologies being developed for protein profiling will benefit in similar ways by the improvements in sensitivity and reduction of background that result from the removal of a small number of very abundant proteins from samples prior to analysis.

In the light of the above discussion we believe that PHEMA based cryogels offer promising approach with good depletion efficiency of HSA from human serum.

6. REFERENCES

Adkins, J. N., Varnum, S. M., Auberry, K. J., Moore, R. J., Angell, N. H., Smith, R. D., Springer, D. L., Pounds, J. G., **2002**. Mol. Cell. Proteomics, 1, 947.

Ahmed, N., Barker, G., Oliva, K., Garfin, D., Rice, G., **2003**. Proteomics, 3, 1980.

Alberghina, G., Fisichella, S., Renda, E., **1999**. J. Chromatogr. A, 840, 51.

Alderton, W. K., Thatcher, D., Lowe, C. R., **1995**. Eur. J. Biochem. 233, 880.

Allary, M., Saint-Blancard, J., Boschetti, E., Girot, P., **1991**. Bioseparation, 2, 167.
Altıntas, E. B., Denizli, A., **2006**. J. Chromatogr. B, 832, 216.

Andaç, C., Andaç, M., Denizli, A., **2007**. Inter. J. Biol. Macromol., 41, 430.

Anderson, L., **2005**. J. Physiol., 563, 23.

Andersson, H. S., **1999**. Towards the rational design of molecular imprinted polymers, Department of Pure and Applied Biochemistry, Doctoral Thesis, University of Lund, ISBN: 91–7874–011–8.

Andersson, L. I., Muller, R., Vlatakis, G., Mosbach, K., **1995.** Proc. Natl. Acad. Sci. USA, 92, 4788.

Andersson, L. I., Schweitz, L., **2003**. Handb. Anal., 4, 45.

Andersson, N. L., Anderson N. G., **2002**. Mol. Cell. Proteomics, 11, 845.

Arica, M. Y., Testereci, H. N., Denizli, A., **1998**. J. Chromatogr. A, 799, 83.

Arshady, R., Mosbach, K., **1981**. Macromol. Chem. Phys., 182 (2), 687.

Arvidsson, P., Plieva, F. M., Lozinsky, V. I., Galaev, I. Y., Mattiasson, B., **2003.** J. Chromatogr. A*,* 986, 275.

Arvidsson, P., Plieva, F. M., Savina, I. N., Lozinsky V. I., Fexby, S., Bülow, L., Galaev, I. Y., Mattiasson, B., **2002**. J. Chromatogr. A, 977, 27.

Asanuma, H., Akiyama, T., Kajiya, K., Hishiya, T., Komiyama, M., **2001**. Anal. Chim. Acta, 435 (1), 25.

Babaç, C., Yavuz, H., Galaev, I. Y., Pişkin, E., Denizli, A., **2006**. React. Funct. Polym., 66, 1263.

Bacheva, A. V., Plieva, F. M., Lysogorsky, E. N., Filippova, I. Y., Lozinsky, V. I., **2001**. Bioorg. Med. Chem. Lett., 11, 1005.

Badock, V., Steinhusen, U., Bommert, K., Otto, A., **2001**. Electrophoresis, 22, 2856.

Baggiani, C., Giraudi, G., Giovannoli, C., Trotta, F., Vanni, A., **2000**. J. Chromatogr. A, 883 (1-2), 119.

Bartels, H., **1967**. J. Chromatogr., 30 (1), 113.

Baydemir G., Bereli, N., Andaç, M., Say, R., Galaev, I. Y., Denizli, A., **2009.** Colloids and Surfaces B*,* 68, 33.

Baydemir, G., Bereli, N., Andaç, M., Say, R., Galaev, I. Y., Denizli, A., **2009**. React. Funct. Polym., 69, 36.

Beach, J. V., Shea, K. J., **1994**. J. Am. Chem. Soc., 116 (1), 379.

Beckett, A. H., Youssef, H. Z., **1963**. J. Pharm. Pharmacol., 15, T253.

Belmont, A. S., **2006**. Molecularly imprinted polymers at the nanometric scale: Synthetic receptros for chemical sensors, Doctoral Thesis, University of Lund, ISBN: 91-7422-134-5.

Belokon, Y. N., Kochetkov, K. A., Plieva, F. M., Ikonnikov, N. S., Maleev, V. I., Parmar, V. S., Kumar, R., Lozinsky, V. I., **2000**. Appl. Biochem. Biotechnol., 88, 97.

Benoy, I., Salgado, R., Colpaert, C., Weytjens, R., Vermeulen, P. B., Dirix, L. Y., **2002**. Clin. Breast Cancer, 2, 311.

Biellmann, J. F., Samama, J. P., Braden, C., Eklund, H., **1979**. Eur. J. Biochem., 102, 107.

Bioseparation (1999) 8, No. 1/5 special issue of on Expanded Bed Chromatography.

Björhall, K., Miliotis, T., Davidsson, P., **2005**. Proteomics, 5, 307.

Bogan, M. J., Agnes, G. R., **2004**. J. Am. Soc. Mass Spectrom., 15, 486.

Bonini, F., Piletsky, S., Turner, A. P. F., Speghini, A., Bossi, A., **2007**. Biosens. Bioelectron., 22, 2322.

Bossi, A., Piletsky, S. A., Piletska, E. V., Righetti P. G., Turner A. P. F., **2001**. Anal. Chem., 73, 5281.

Boyer, P. M., Hsu, J. T., **1992**. Chem. Eng. J., 47, 241.

Brown, R. A., Combridge, B. S., **1986**. J. Virol. Methods, 14, 267.

Burnouf, T., Radosevich, M., **2001**. J. Biochem. Biophys. Methods, 49, 575.

Burow, M., Minoura, N., **1996**. Biochem. Biophys. Res. Commun., 227, 419.

Case D. A., T.A. Darden, T.E. Cheatham, III, C.L. Simmerling, J. Wang, R.E. Duke, R. Luo, M. Crowley, Ross C. Walker,W. Zhang, K.M. Merz, B.Wang, S. Hayik, A. Roitberg, G. Seabra, I. Kolossváry, K.F.Wong, F. Paesani, J. Vanicek, X.Wu, S.R. Brozell, T. Steinbrecher, H. Gohlke, L. Yang, C. Tan, J. Mongan, V. Hornak, G. Cui, D.H. Mathews, M.G. Seetin, C. Sagui, V. Babin, and P.A. Kollman (**2008**), AMBER 10, University of California, San Francisco.

Caspi, S., Halimi, M., Yanai, A., Sasson, S. B., Taraboulos, A., Gabizon, R., **1998**. J. Biol. Chem., 273, 3484.

Chan, K. C., Lucas, D. A., Schaefer, C. F., Xiao, Z., Janini, G. M., Buetow, K. H., Issaq, H. J., Veenstra, T. D., Conrads, T. P., **2004**. Clin. Prot., 1, 101.

Chase, H. A., **1984**. J. Chromatogr., 297, 179.

Chen, J-P., **2002.** Enzymes immobilized in smart hydrogels. In Smart Polymers for Bioseparation and Bioprocessing (Galaev, Yu.I. and Mattiasson, B., eds), pp. 230–256, Taylor & Francis.Y.

Cheung, C. W., Porter, J. F., Mckay, G., **2001**. Char Pergamon, 35, 3, 605.

Chianella, I., Piletsky, S. A., Tothill, I. E., Chen, B., Turner A. P. F., **2003**. Biosens. Bioelectron., 18, 119.

Cho, W. C., **2007**. Am. J. Chin. Med., 35, 6, 911.

Cho, W. C., **2007**. Mol. Cancer, 6, 25.

Cho, W. C., Cheng, C. H., **2007**. Expert Rev. Proteomics, 4, 401.

Chromy, B. A., Gonzales, A. D., Perkins, J., Choi, M. W., Corzett, M. H., Chang, B. C., Corzett, C. H., Maloney, S. L., **2004**. Journal of Proteome Research, 3, 1120.

Ciardelli, G., Borrelli, C., Silvestri, D., Crisallini, C., Barbani, N., Giusti, P., **2006**. Biosens. Bioelectron., 21, 2329.

Clonis, Y. D., Labrou, N. E., Kotsira, V., Mazitsos, K., Melissis, S., Gogolas, G., **2000**. J. Chromatogr. A, 891, 33.

Colantonio, D. A., Chan, D. W., **2005**. Clin. Chim. Acta, 357, 151.

Colantonio, D. A., Dunkinson, C., Bovenkamp, D. E., Van Eyk. J. E., **2005**. Proteomics, 5, 3831.

Cornell, W. D., Cieplak, P., Bayly, C.I., Gould, I. R., Merz, Jr., K. M., Ferguson, D. M., Spellmeyer, D. C., Fox, T., Caldwell, J. W., Kollman, P. A., **1995**. *JACS*, **117**, 5179.

Dai, S., Shin, Y. S., Barnes, C. E., **1997**. Chem. Mater., 9 (11), 2521.

Darde, V. M., Barderas, M. G., Vivanco, F., **2007**. Methods Mol. Biol., 357, 351.

Demiryas, N., Tuzmen, N., Galaev, I. Y., Piskin, E., Denizli, A., **2007**. J. Appl. Polym. Sci., 105, 1808.

Denizli, A., Kocakulak, M., Piskin, E., **1998**. J. Chromatogr. B, 707, 25.

Denizli, A., Kokturk, G., Salih, B., Kozluca, A., Piskin, E., **1997**. J. Appl. Polym. Sci., 63, 27.

Denizli, A., Kokturk, G., Yavuz, H., Piskin, E., **1999**. J. Appl. Polym. Sci., 74, 2803.

Denizli, A., Piskin, E., **2001**. J. Biochem. Biophys. Methods, 49, 391.

Denizli, A., Pişkin, E., **2001**. J. Biochem. Biophys. Methods, 49, 391.

Denizli, A., Salih, B., Kavakli, C., Piskin, E., **1997**. J. Chromatogr. B, 698, 89.

Denizli, A., Salih, B., Piskin, E., **1998**. J. Biomater. Sci. Polym. Ed., 9, 175.

Denizli, A., Salih, B., Senel, S., Arica, M. Y., **1998**. J. Appl. Polym. Sci., 68, 657.

Denizli, A., Say, R., Piskin, E., **2003.** React. Funct. Polym., 55, 99.

Denizli, A., Yavuz, H., **2000**. Colloids & Surfaces A, 174, 147.

Dhal, P. K, Arnold, F. H., **1992**. Macromol., 25 (25), 7051.

Dhal, P. K., Arnold, F. H., **1991**. J. Am. Chem. Soc.113 (19), 7417.

Dickert, F. L., Hayden, O., **2002**. Anal. Chem., 74, 1302.

Dickey, F. H., **1955**. J. Phys. Chem., 59(8), 695.

Engle, W. A., Schreiner, R. L., Baehner, R. L., **1983**. Semin. Perinatol., 7, 184.

Filippova, I. Y., **2001**. Russ. Chem. Bull., 10, 1886.

Finette, G. M. S., Qui-Ming, M., Hearn, M. T. W., **1997**. J. Chromatogr. A., 763, 71.

Firer, M. A., **2001**. J. Biochem. Biophys. Methods, 49, 433.

Fraser, C. G., Biological variation: from principles to practice. AACC Press; 2001.

Friess, S. D., Zenobi, R., **2001**. J. Am. Soc. Mass Spectrom., 12, 810.

Fujii, K., Nakano, T., Kawamura, T., Usui, F., Bando, Y., Wang, R., Nishimura, T. J., **2004**. Proteome Res., 3, 712.

Fujii, Y., Matsutani, K., Kikuchi, K., **1985**. J. Chem. Soc., Chem. Commun., 7, 415.

Galaev, I. Y., Mattiasson, B., **1999**. Trends Biotechnol., 17, 335.

Gamez, P., Dunjic, B., Pinel, C., Lemaire, M., **1995**, Tetrahedron Lett., 36 (48), 8779.

Garber, K., **2001.** Nat. Biotechnol., 19, 184.

Garcia-Calzon, J. A., Diaz-Garcia, M. E., **2007**. Sensors and Actuators B: Chemical, 123 (2), 1180.

Garg, N., Galaev, I. Y., Mattiasson, B., **1996**. Bioseparation, 6, 193.

Garipcan B., Denizli, A., **2002.** Macromol. Biosci*., 2*, 135.

Georgiou, H. M., Rice, G. E., Baker, M. S., **2001**. Proteomics, 1, 1503.

Ghuman J., Zunszain, P. A., Petitas, I., Bhattacharya, A. A., Otagiri, M., Curry, S., **2005**. J. Mol. Biol. 353, 38.

Gianazza, E., Arnaud, P. A., **1982**. J. Biochem., 201, 129.

Gianazza, E., Arnaud, P. A., **1982**. J. Biochem., 203, 637.

Ginsburg, G. S., McCarthy, J. J., **2001**. Trends Biotechnol., 19, 491.

Glad, M., Norrlow, O., Sellergren, B., **1985**. J. Liq. Chromatogr., 347 (1), 11.

Gong, Y., Li, X., Yang, B., Ying, W., Li, D., Zhang, Y., Dai, S., Cai, Y., Wang, J., He, F., Qian, X., **2006**. J. Proteome Res., 5, 1379.

Govoroum, M. S., Huet, J. C., Pernollet, J. C., Breton, B., **1997**. J. Chromatogr. B, 698, 35.

Gu, J., Lei, Z., Qizhi, Y., **2007**. J. Membr. Sci., 287, 271.

Gundry, R. L., Fu, Q., Jelinek, C. A., Van Eyk, J. E., Cotter, R. **2007**. J. Proteomics Clin. Appl., 1, 73.

Guo, T. Y., Xia, Y. Q., Hao, G. J., Song, M. D., Zhang, B. H., **2004**. Biomaterials, 25, 5905.

Haeckel, R., Hess, B., Lauterborn, W., Wurster, K. H., Hoppe-Seyler's, Z., **1968**. Physiol. Chem., 349, 699.

Haginaka, J., **2001**. Bioseparation, 10 (6), 337.

Haginaka, J., Sanbe, H., **2003**. J. Pharm. Biomed. Anal., 30 (6), 1835.

Hassan, C. M., Peppas, N. A., **2000**. Adv. Polym. Sci., 153, 37.

Hattori, T., Zhang, X., Weiss, C., Xu, Y., Kubo, T., Sato, Y., Nishikawa, S., Sakaida, H., Uchiyama, T., **1997**. Microbiol. Immunol., 41, 717.

Haupt, K., Mosbach, K., **2000**. Chem. Rev., 100, 2495.

Hayashi, T., Hyon, S.-H., Cha, W.-I., Ikada, Y., **1993**. J. Appl. Polym. Sci., 49, 2121.

Hedborg, E., Winquist, F., Lundstrom, I., **1993**. Sens. Actuators A, 37, 796.

Herbert, B., Righetti, P. G., **2000**. Electrophoresis, 21, 3639.

Hjerten, S.; Liao, J. L.; Nakazato, K.; Wang, Y.; Zamaratskaia, G.; Zhang, H. X. **1997.** Chromatographia, 44, 227.

Hwang, C. C., Lee, W. C., **2002**. J. Chromatogr. A, 962 (1-2), 69.

Ichinose, I., Kikuchi, T., Lee, S. W., Kunitake, T., **2002**. Chem. Lett., 1, 104.

Issaq, H. J., Xiao, Z., Veenstra, T. D., **2007**. Chem. Rev., 107, 3601.

Jacobs, J. M., Adkins, J. N., Qian, W, Liu, T., Shen, Y., Camp, D. G., Smith, R., **2005**. J. Proteome Res., 4, 1073.

Jenkins, A. L., Uy, O. M., Murray, G. M., **1997**. Anal. Commun., 34 (8), 221.

Jin, W. H., Dai, J., Li, S. J., Xia, Q. C., **2005**. J. Proteome Res., 4, 613 .

Jmeian, Y., El Rassi, Z., **2008**. Electrophoresis, 29, 2801.

Johnston, K. A., **2001.** PharmaGenomics, Oct/Nov, 28.

Josic, D., Buchacher, A., Jungbauer, A., **2001**. J. Chromatogr. B Biomed. Sci. Appl., 752, 191.

Kaetsu, I., **1993**. Adv. Polym. Sci., 105, 81.

Kassab, A., Yavuz, H., Odabası, M., Denizli, A., **2000**. J. Chromatogr. B, 746, 123.

Katz, A., Davis M. E., **2000**. Nature, 403 (6767), 286.

Kempe, M., Glad, M., Mosbach, K., **1995**. J. Mol. Recognit., 8, 35.

Kempe, M., Mosbach, K., **1994**. J. Chromatogr. A, 664 (2), 276.

Kim, W. K., Henschel, A., Winter, C., Schroeder, M., **2006**. PLoS Comput. Biol., 2, e124.

Kobayashi, T., Reddy, P. S., Ohta, M., Abe, M., Fujii, N., **2002**. Chem. Mater., 14 (6), 2499.

Koch, C., Borg, L., Skjodt, K., Houen, G., **1998**. J. Chromatogr. B, 718, 41.

Kodadek, T., **2001**. Chem. Biol., 8, 105.

Kokufuta, E., Jinbo, E., **1992**. Macromol., 25, 3549.

Komiyama, M., Takeuchi, T., Mukawa, T., Asanuma, H., **2003**. Molecular imprinting: From fundamentals to applications, Wiley-VCH. 12.

Kopperschlager, G., Bohme, H. J., Hofmann, E., **1982**. Adv. Biochem. Eng., 25, 101.

Kosak, S. T., Groudine, M., **2004**. Science, 306, 644.

Kumakura, M., **1997**. Process Biochem., 32, 555.

Kumakura, M., **2001**. Polym. Adv. Technol., 12, 415.

Kumar, S., Dalvi, D. B., Moorthy, M., Korde, S. S., Fondekar, K. P., Sahasrabudhe, S. D., Schacht, H. T., Ekkundi, V. S., Halik, C., Choudhury, R., Kumar, A., Punekar, N. S., **2009**. J. Chromatogr. B, 877, 3610.

Labrou, N. E., **2000.** Dye-ligand affinity chromatography for protein separation and purification, in Methods in Molecular Biology, Affinity Chromatography: Methods and Protocols, Walker, J. M., Ed., Humana Press, Totowa, NJ, pp. 129.

Labrou, N. E., Clonis, Y. D., **1994**. J. Biotechnol., 36, 95.

Labrou, N. E., Clonis, Y. D., **2002.** Immobilised synthetic dyes in affinity chromatography, in Theory and Practice of Biochromatography, Vijayalakshmi, M. A., Ed., Taylor & Francis, London, , pp. 335.

Labrou, N. E., Karagouni, A., Clonis, Y. D., **1995**. Biotech. Bioeng., 48, 278.

Laemmli, U. K., **1970**. Nature, 227, 680.

Lai, J. P., He, X.W., Chen, F., Analyt. Bioanalyt. Chem., 377 (1) **2003**, 208.

Lai, J. P., Lu, C. Y., He, X. W., **2002**. Chinese J. Chem., 20 (10), 1012.

Lali, A., Balan, S., John, R., D'Souza, F., **1999**. Bioseparation, 7, 195.

Lanza, F., Sellergren, B., **2001**. Adv. Chromatogr., 3, 41137.

Le Noir, M., Guieysse, B., Mattiasson, B., **2006**. Water Sci. Technol., 53 (11), 205.

Le Noir, M., Lepeuple, A. S., Guieysse, B., Mattiasson, B., **2007**. Water Research, 41, 2825.

Le Noir, M., Plieva, F., Hey, T., Guieysse, B., Mattiasson, B., **2007**. J. Chromatogr. A, 1154, 158.

Le Noir, M., Plieva, F., Hey, T., Mattasson, B., **2007**. J. Chromatogr. A, 1154 (1-2), 158.

Leatherbarrowand, R. L, Dean, P. D. G., **1980**. Biochem. J., 189, 27.

Lee, S. W., Ichinose, I., Kunitake, T., **1998**. Langmuir, 14 (10), 2857.

Li, R., Bianchet, M. A., Talalay, P., Amzel, L. M., **1995**. Proc. Natl. Acad. Sci., 92, 8846.

Li, Y., Spencer, H. G., **1994.** In: Polymers of Biological and Biomedical Significance; Shalaby, W. Ed.; ACS: Washington DC, p 297.

Liao, J. L.; Wang, Y.; Hjerten, S. **1996**. Chromatographia, 42, 259.

Lolo, B. A., Harvey,, S., Liao J., Stevens, A. C., Wagenknecht, R., Sayen, R., Whaley, J., Sajjadi, F. G., **1999**. Electrophoresis, 20, 854.

Lowe, C. R., **2001**. Curr. Opin. Chem. Biol., 5, 248.

Lowe, C. R., Burton, S. J., Burton, N. P., Alderton, W. K., Pitts, J. M., Thomas, J. A., **1992**. Trends Biotechnol., 10, 442.

Lowe, C. R., Burton, S. J., Pearson, J., Clonis, Y. D., Stead, C. V., **1986**. J. Chromatogr., 376, 121.

Lozinsky, V. I., **1995**. Biotechnologiya, 32.

Lozinsky, V. I., **1997**. Polym., 39A, 1300.

Lozinsky, V. I., **1998**. Russ. Chem. Rev., 67, 573.

Lozinsky, V. I., **2002**. Russ. Chem. Rev., 71, 489.

Lozinsky, V. I., Galaev, I. Y., Plieva, F. M., Savina, I. N., Jungvid, H., Mattiasson, B., **2003**. Trends in Biotechnol., 21, 445.

Lozinsky, V. I., Plieva, F. M, Galaev, I. Y., Mattiasson, B., **2002**. Bioseparation, 10, 163.

Lozinsky, V. I., Plieva, F. M., **1998**. Enzyme Microb. Technol., 23, 227.

Lozinsky, V. I., Plieva, F.M., Galaev, I. Y., Mattiasson, B., **2002.** Bioseparation, 10, 163.

Lum, G., Gambino, S. R., **1974**. Am. J. Clin. Pathol., 61, 108.

Ma, Z. Y., Guan, Y. P., Liu, H. Z., **2006**. React. Funct. Polym., 66, 618.

Makote, R, Collinson, M. M., **1998**. Chem. Commun., 3, 425.

Mallik, S., Johnson, R. D., Arnold, F. H., **1994**. J. Am. Chem. Soc., 116 (20), 8902.

Marshall, J., Kupchak, P., Zhu, W., Yantha, J., Vrees, T., Furesz, S., **2003**. J. Proteome Res. 2 (4), 361.

Martin-Esteban, A., Fresenius, **2001**. J. Anal. Chem., 370 (7), 795.

Matsui, J., Doblhoffdier, O., Takeuchi, T., **1995**. Chem. Lett., 6, 489.

Matsui, J., Fujiwara, K., Takeuchi, T., **2000**. Anal. Chem., 72 (8), 1810.

Matsui, J., Nicholls, I. A., Karube, I., Mosbach, K., **1996**. J. Org. Chem., 61 (16), 5414.

Mattiasson, B., Galaev, Y.I., Garg, N., **1996**. J. Mol. Recognit., 9, 509.

McCormack, A. L., Schieltz, D. M., Goode, B., Yang, S., Barnes, G., Drubin, D., Yates, J. R., **1997**. Anal. Chem., 69, 767.

McCoy, M., Kalghatgi, K., Regnier, F. E., Afeyan, N., **1996**. J. Chromatogr. A, 743, 221.

McCreath, G. E., Chase, H. A., Purvis, D. R., Lowe, C. R., **1993**. J. Chromatogr., 629, 201.

Minoura, N., Rachkov A., **2000**. J. Chromatogr. A, 889, 111.

Moore, L. G., Ng-Chie, W., Lun, S., Lawrence, S. B., Young, W., McNatty, K. P., **1997**. Gen. Comp. Endocrinol., 106, 30.

Mosbach, K., **1994**. Trends Biochem. Sci., 19, 9.

Mosbach, K., Ramstrom, O., **1996**. Biotechnology, 14, 163.

Muller-Schulte, D., Manjini, S., Vijayalakshmi, M. A., **1991**. J. Chromatogr., 539, 307.

Mullett, W. M., Lai, E. P. C., **1998**. Anal. Chem., 70 (17), 3636.

Nambu, M., **1990**. Kobunshi Ronbunshu, 47, 695.

Nash, D. C., Chase, H. A., **1997**. J. Chromatogr. A, 776, 55.

Nigel, M., Lindner, R., Jeffcoat, R., Lowe, C. R., **1989**. J. Chromatogr., 473, 227.

Njayou, M., Quash, G., **1991**. J. Virol. Methods, 32, 67.

Noppe, W., Plieva, F. M., Vanhoorelbeke, K., Deckmey, H., Tuncel, M., Tuncel, A., Galaev, I. Y., Mattiasson, B., **2007**. J. Biotechnol., 131, 293.

Norrlow, O., Glad, M., Mosbach, K., **1984**. J. Chromatogr., 299 (1), 29.

Oakley, A. J., Lo Bello, M., Nuccetelli, M., Mazzetti, A. P., Parker, M. W., **1999**. J. Mol. Biol., 291, 913.

Odabaşı, M., Denizli, A., **2004**. Polym. Int., 53, 332.

Odabaşı, M., Say, R., Denizli, A., **2007.** Mater. Sci. Eng. C., 27, 90.

Öncel, Ş., Uzun Öncel, Ş., Uzun, L., Garipcan, B., Denizli, A., **2005.** Ind. Eng. Chem. Res. 44, 7049.

Özcan A. A., Say, R., Denizli, A., Ersoz, A., **2006.** Anal. Chem., 78, 7253.

Özkara, S., Garipcan, B., Pişkin, E., Denizli, A., **2003**. J. Biomater. Sci. Polym. Ed., 14, 761.

Özturk, N., Akgol, S., Arısoy, M., Denizli, A., **2007**. Sep. Pur. Technol., 58, 83.

Pang, X., Cheng, G., Lu, S., Tang, E., **2006**. Anal. Bioanal. Chem., 384, 225.

Pauling, L., Campbell, D. H., **1942**. J. Exp. Med., 76 (2), 211.

Peng, Z. G., Hidajat, K., Udin, M. S., **2004**. Colloids and Surfaces B, 33, 15.

Plieva, F. M., Kochetkov, K. A., Singh, I., Parmar, V. S., Belokon', Yu. N., Lozinsky, V. I., **2000**. Biotechnol. Lett., 22, 551.

Polyakov, M. V., **1931**. Zhur. Fiz. Khim., 2, 799.

Rachkov, A. E., Cheong, S.-H., El'skaya, A. V., Yano, K., Karube, I., **1998**. Polym. Adv. Technol., 9 (8), 511.

Ramstrom, O., Skudar, K., Haines, J., Patel, P., Bruggemann O., **2001**. J. Agric. Food Chem., 49, 2105.

Rodrigues, A. E., **1997**. J. Chromatogr. B Biomed. Sci. Appl., 699, 47.

Rothemund, D. L., Locke, V. L., Liew, A., Thomas T. M., **2003**. Proteomics, 3, 279.

Salih, B., Zenobi, R., **1998**. Anal. Chem., 70, 1536.

Sato, A. K., Sexton, D. J., Morganelli, L. A., Cohen, E. H., Wu, Q. L., Conley, G. P., Streltsova, Z., Lee, S. W., Devlin, M., De Oliveira, D. B., Enright, J., Kent, R. B., Wescott, C. R., Ransohoff, T. C., Ley, A. C., Ladner, R. C., **2002**. Biotechnol. Prog., 18, 182.

Savina, I. N., Galaev, I. Y., Mattiasson, B., **2005**. J. Chromatogr. A, 1092, 199.

Savina, I. N., Hanora, A., Plieva, F. M., Galaev, I. Y., Mattiasson, B., Lozinsky, V. I., **2005**. J. Appl. Polym. Sci., 95, 529.

Sellergren, B., **1989**. Macromol. Chem. Phys., 190 (11), 2703.

Sellergren, B., **1994**. Polymer. Anal. Chem. 66 (9), 1578.

Sellergren, B., **2001a**. Techniques and Instrumentation in Analytical Chemistry, vol. 23. Elsevier, Amsterdam.

Sellergren, B., **2001b** In: Subramanian G. (Ed.), Chiral Separation Techniques, 2nd ed. Wiley-VCH, Weinheim, pp. 153.

Shea, K. J., Thompson, E .A., Pandey, S. D., Beauchamp, P. S., **1980**. J. Am. Chem. Soc., 102 (9), 3149.

Shen, Y., Kim, J., Strittmatter, E. F., Jacobs, J. M., Camp, D. G., Fang, R., Tolic, N., Moore, R. J., Smith, R. D. **2005**. Proteomics, 5, 4034.

Shi, H. Q., Tsa, W. B. I., Garrison, M. D., Ferrari, S., Ratner, B. D., **1999**. Nature, 398, 593.

Shi, Y., Zhang, J. H., Shi, D., Jiang, M., Zhu, Y. X., Mei, S. R. **2006**. Journal of Pharmaceutical and Biomedical Analysis, 42, 549.

Shiomi, T., Matsui, M., Mizukami, F., Sakaguchi, K., **2005**. Biomaterials, 27, 5564.

Sitnikov, D., Chan, D., Thibaudeau, E., Pinard, M., Hunter, J. M., **2006**. J. Chromatogr. B, 832, 41.

Soskic, V., Schwall, G., Nyakatura, E., Poznanovic, S., Stegmann, W., Schrattenholz, A., **2006**. J. Proteome Res. 5, 3453.

Spence, G. M., Graham, A. N., Mulholland, K., Maxwell, P., McCluggage, W. G., Sloan, J. M., McGuigan, J. A. **2002**. Int. J. Biol. Markers 17, 119.

Sreenivasan, K., **2001**. J. Appl. Polym. Sci., 80 (14), 2795.

Sreenivasan, K., Sivakumar, R., **2003**. Adsorpt. Sci. Technol., 21 (3), 261.

Staal, G., Koster, J., Kamp, H., Van Milligen-Boersma, L., Veeger, C., **1971**. Biochem. Biophys. Acta 227, 86.

Steel, L. F., Trotter, M. G., Nakajima, P. B., Mattu, T. S., Gonye, G., Block, T., **2003**. Mol. Cell Proteomics, 2, 262.

Steel, L., Trotter, M.G., Nakajima, P. B., Mattu, T. S., Gonye, G., Block. T., **2003**. Molecular & Cellular Proteomics, 2, 262.

Suarez-Rodriguez, J. L., Diaz-Garcia, M. E., **2001**. Biosens. Bioelectron., 16, 9-12, 955.

Sun, Y., Ichikawa, S., Sugiura, S., Furusaki, S., **1998**. Biotechnol. Bioeng., 58, 58.

Surugiu, I., Danielsson, B., Ye, L., Mosbach, K. and Haupt, K., **2001**. Anal. Chem., 73 (3), 487.

Sutania, K., Kaetsua, I., Uchidab, K., **2001**. Radiat. Phys. Chem., 61, 49.

Suzuki, M., Hirasa, O., **1993**. Adv. Polym. Sci., 110, 241.

Swaminathan, S., Khanna, N., **1999**. Protein Exp. Purif., 15, 236.

Szafranski, C., Bailey, J., Christoph, W. T., Martosella, J., Zolotarjova, N., **2004**. Pharma Genomics, 40.

Takagishi, T., Klotz, I. M., **1972**. Biopolymers, 11 (2), 483.

Tennikova, T. B., Freitag, R., **2000**. J. High Resolut. Chromotogr. Commun., 23, 27.

Theodoridis, G., Manesiotis, P., **2002**. J. Chromatogr. A, 948 (1-2), 163.

Thomas, R., **2001**. Trends Biotechnol., 19, 496.

Tirumalai, R. S., Chan, K. C., Prieto, D. A., Issaq, H. J., Conrads, T. P., Veenstra, T. D., **2003**. Mol. Cell. Proteomics, 2, 1096.

Tong, D.; Hetenyi, C.; Bikadi, Z.; Gao, J. P.; Hjerten, S. **2001**. Chromatographia, 54, 7.

Travis, J., Pannell, R., **1973**. Clin. Chim. Acta, 49**,** 49.

Tuncel, A., Denizli, A., Purvis, D., Lowe, C. R., Piskin, E. **1993**. J. Chromatogr., 634, 161.

Ulbricht, M., Malaisamy, R., **2005**. J. Mater. Chem., 15 (14), 1487.

Umpleby, R. J., Baxter, S. C., Chen, Y., Shah, R. N., Shimizu, K. D., **2001**. Anal. Chem., 73, 4584.

Uygun, D. A., Karagözler, A. A., Akgöl, S., Denizli A., **2009**. Mater. Sci. Eng. C, 29, 2165.

Uzun, L., Yavuz, H., Say, R., Ersoz, A., Denizli, A., **2004**. Ind. Eng. Chem. Res., 43, 6507.

Vlatakis, G., Andersson, L. I., Muller, R., Mosbach, K., **1993**. Nature, 361 (6413), 645.

Wan Ngah, W. S, Endud, C. S, Mayanar, R., **2002**. React. Funct. Polym., 50, 181.

Wang, Y. Y., Cheng, P., Chan, D. W., **2003**. Proteomics, 3, 243.

Wehr, T., **2001**. LC-GC 19, 702.

Westermeier, R. 1997. Electrophoresis in Practice 2nd ed. VCH, Weinheim, Germany, 1.

Whitcombe, M. J., Alexander, C., Vulfson, E. N., **1997**. Trends Food Sci. Technol., 8, 140.

Whitcombe, M. J., Rodriguez, M. E., Villar, P. and Vulfson, E. N., **1995**. J. Am. Chem. Soc., 117 (27), 7105.

Whiteaker, J. R., Zhang, H., Eng, J. K., Fang, R., Piening, B. D., Feng, L. C., Lorentzen, T. D., Schoenherr, R. M., Keane, J. F., Holzman, T., Fitzgibbon, M., Lin, C., Zhang, H., Cooke, K., Liu, T., Camp, D. G., Anderson, L., Watts, J., Smith, R. D., McIntosh, M. W., Paulovich, A. G., **2007**. J. Proteome Res. 6, 828.

Wulff, G., **1993**. Trends Biotechnol., 11, 85.

Wulff, G., **1995**. Angew. Chem. Int. Ed., 34 (17), 1812.

Wulff, G., Sarhan, A., **1972**. Angew. Chem. Int. Ed., 11(4), 341.

Xie, J. C., Zhu, L. L., Xu, X. **2002**. J., Anal. Chem., 74 (10), 2352.

Yao, K. J., Yun, J. X., Shen, S. C., Wang, L. H., He, X. J., Yu, X. M., **2006**. J. Chromatogr. A, 1109, 103.

Ye, L., Ramstrom, O., Ansell, R. J., Mansson, M. O., Mosbach, K., **1999**. Biotechnol. Bioeng., 64 (6), 650.

Ye, L., Yu, Y. H., Mosbach, K., **2001**. Analyst, 126 (6), 760.

Yilmaz, E., Haup, K., Mosbach, K., **2000**. Angew Chem. Int. Ed., 39, 2115.

Zeng, X., Ruckenstein, E., **1996**. J. Membr. Sci., 117, 271.

Zhang, H., Liu, A. Y., Loriaux, P., Wollshceid, B., Zhou, Y., Watts, J. D., Aebersold, R. A., **2007**. Mol. Cell. Proteomics, 6, 64.

Zhang, J., Zhang, Z., Song, Y., Cai, H., **2006**. React. Funct. Polym., 66, 916.

Zhao, C. S., Yang, K. G., Liu, X. D., Nomizu, M., Nishi, N., **2004**. Desalination, 170 (3), 263.

Zhou, M., Lucas, D. A., Chan, K. C., Issaq, H. J., Petricoin, E. F., Liotta, L. A., Veenstra, T. D., Conrads, T. P., **2004**. Electrophoresis, 25, 1289.

Zijlstra, G. M., Michielsen, M. J., De Gooijer, C. D., Van der Pol, L. A., Tramper, J., **1998**. Bioseparation, 7, 117.

Zolotarjova, N., Martosella, J., Nicol, G., Bailey, J., Boyes, B. E., Barrett, W. C., **2005**. Proteomics, 5, 3304.

Zurutuza, A., Bayoudh, S., Cormack P. A. G., **2005**. Anal. Chim. Acta., 542 (1), 14.